Dual International Master's Degree in Automotive Engineering

Master of Science Thesis

Investigation of 3D Non-Contact Laser-Based Inspection Techniques for Application in Gear Metrology

Student: Antonio Logaldo

University of Windsor:Dr. Alpas

Politecnico di Torino: Prof.ssa Curà

FCA NAFTA: Sue McNally, Joseph Lamanna

CRF (Research Center of FCA): Eva Butano

2018-2019

Abstract

Gear shape accuracy, surface quality and, as a consequence, a proper gear inspection needed to guarantee these features, are critical in order to improve drivetrain efficiency as well as to reduce noise in automotive power transmission systems.

Contact stylus type measuring methods using contact probes are today's dominant industrial solution for gear metrology. Due to the difficulties of further improving those methods, new non-contact measuring systems have been developed in the past few years.

The most promising option that meets the requirements of accuracy, repeatability and high cycle time is the 3D non-contact measurement method based on triangulation laser sensors. These laser scanners have been improved over the last few years both in terms of resolution, optical quality, image processing and data analysis to make them comparable, if not superior, to the traditional contact probe.

This thesis provides an evaluation of the surface profilometer Urano HC-N400, using the contact technology currently employed by Omega gear metrology labs as a benchmark. The measurements obtained with the alternative inspection system indicate that the analyzed non-contact solution is not ready yet for in-line and high volume inspection applications, but is well-suited to research and development purposes.

Omega is also looking for the possible causes of a particular noise problem which is difficult to detect using current technology. One gear that exhibited this phantom phenomenon, also know as the "ghost noise", has been analyzed and compared with another gear identified as the "best of best". During the analysis, undulations have been found in both gears. The combination of those waves through the use of the Ripple Analysis software represents the best solution to discover other gears with the same problem in the early stages of inspection.

Dedication

To my father and my mother

Acknowledgements

It is my pleasure to acknowledge all the individuals who sustained me for the development and completion of my master's thesis.
First of all, I would like to thank Dr. Alpas, supervisor of this thesis, for the help, great knowledge, experience, innovative ideas and availability that he has given me in all this last year. Without his help it would have been impossible to achieve these results.
I would also like to acknowledge Sue McNally and Joseph Lamanna, my industrial advisors, for all the opportunities they have given me. They have been fundamental both for my thesis development and for my professional growth.
I am very grateful to Mohammed Malik and Marie Mills. With all their advice, they lead me always through the right choices along the entire year.
Vorrei anche ringraziare la professoressa Francesca Curà ed Eva Butano per avermi dato le basi necessarie per affrontare questa esperienza e, soprattutto, per essere sempre state disponibili a dare i giusti consigli ogni qual volta ne avessi avuto bisogno.
Grazie ai miei genitori, a mio fratello e a mia sorella, per essermi sempre stati vicini in questo lungo anno, per avermi supportato, motivato in ogni occasione ed essere stati pazienti durante i momenti in cui non ho potuto dedicarli tutto il tempo desiderato.
Un ringraziamento speciale va anche ai miei coinquilini Salvo, Ale e Carlo: ad Ale, per avermi sostenuto nei momenti più bui di quest'anno ricordandomi prontamente quanto sia bella la vita; a Salvo per essere sempre stato fonte di ispirazione in cucina ed avermi indirizzato verso il corretto utilizzo di Latex; e Carlo, per avermi indirizzato verso una dieta più corretta fatta di insalata, insalata e in fine, tanta insalata.
Last but not least, thanks to Dj Mike, our landlord, for stealing all my money with the rent and for lying on that wonderful train, that, every day, make us happy with his horn. I will give my best to forgive you for all the pizza that you bought for us.

Contents

List of Figures

List of Tables

List of Appendices

List of Symbols

α	Pressure angle
λ	Wavelength
φ	Interferometric phase
φ_0	Phase constant offset
C_α	Profile Barelling
C_β	Lead Crown
F_{alpha}	Total Profile Deviation
F_{beta}	Total Lead Deviation
$f_{f\alpha}$	Profile Form Deviation
$f_{f\beta}$	Lead Form Deviation
$f_{h\alpha}$	Profile Slope Deviation
$f_{h\beta}$	Lead Slope Deviation
F_p	Total cumulative pitch
f_p	Single cylindrical pitch
F_r	Adjacent pitch
F_r	Pitch line run-out
h_a	Addendum
h_f	Dedendum
I	Light Intensity
K	Wave number
L	Object Distance

Chapter 1

Introduction

1.1 Motivation

Gears are critical components not only in automotive power transmission systems, but also in other kinds of machines such as industrial equipment, aircraft etc [1]. Currently, it has been observed that car manufactures are pushed by the market to improve the drivetrain efficiency as well as to effectively reduce the noise and emissions standard. As manufacturers design increasingly quieter engines to meet this demand, acoustic disturbances from the gears that otherwise would have been hidden have become more audible. This, in turn, has created its own demand for quieter transmission systems. As a result, the already high demands on shape accuracy and surface quality (roughness, surface layer properties, etc.) of gears are elevated to an even higher level. Because of these requirements, the measurement of gears and gear tools becomes of critical importance for gear production.

The most important features to evaluate the performance of every inspection machine are its accuracy and repeatability. Accuracy, or trueness, of a measurement system is the degree of closeness of sample measurements of a given quantity to that quantity's true value. The evaluation is generally done by measuring a master gear of perfectly known dimensions which are defined by international gear metrology labs [2][3]. The machines should also be able to repeat this measurement several times with as little variation possible. For this reason, the measurements are done several times and the machine performance is defined by a repeatability (or precision) value. The concepts of accuracy and precision are further explained in Figure 1.1.

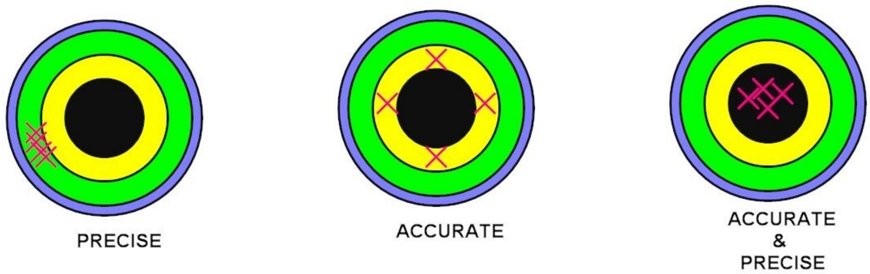

Figure 1.1: Accuracy and Repeatability (Precision) [4]

Once an acceptable inspection quality is obtained, automobile manufacturers then look for the fastest possible measurement speed. This is because the overall number of gears produced is increasing and the time available to perform quality assurance checks is reducing due to market constraints. For this reason, another fundamental parameter that is of concern to the automotive field is the "Cycle Time" which is defined as the total time from the beginning to the end of the process.
Today, profiles of involute gears are measured with contact measuring methods that dominate today's industrial solution for gear inspection [1][5]. While these machines can easily reach an accuracy of around 1 μm with a repeatability of 0.1 μm, they are limited by the fact that they are unable to exceed these specifications to detect smaller geometry deviations that could be the source of noise and vibrations. Furthermore, tactile methods have been found to have a very low data acquisition ratio. Cycle time on standard inspections can range from 4 minutes to 12 minutes. As a result, only about 1 % of the gears produced can be checked. The same results (Table 2.2) have been achieved by the Emera, the metrology system mainly used by Omega.

	Emera		
Acccuracy		μm	1
Repeatability		μm	0.1
Cycle Time	Standard Inspection	min	$4-12$
	2–D / 3–D Contour Map	[-]	Several Hours

Table 1.1: Performance of Emera contact metrology system

However, because these devices suffer from slower measuring speeds with higher densities of measuring points, car manufacturers are investigating new methods to accelerate the inspection process, saving both time and money. The solution that could solve these problems is a 3D non-contact measurement method based on laser inspection [6]. Optical measure-

ment systems collect much more data in the same or less time because of improvements in resolution, optical quality, image processing and data analysis. Due to these qualities, laser line scanning is becoming a more productive substitute for tactile measurement. In addition, this innovative technology improves its accuracy to a level very close to the one of tactile probes and is even superior with perfectly flat surfaces.
Several suppliers have developed non-contact gear metrology systems in the last few years. Among these suppliers, Urano was the first one to arrive on the market. The solution proposed by Urano is the HC-N400, which is able to acquire around 120 000 points per second and to generate a complete 3D countour map of every tooth in just a few minutes. The same operation performed using a contact machine would require hours. Unfortunately, non-contact scanners have the great disadvantage that the reflected light is highly influenced by material properties and surface imperfections. A first comparison between the advantages and disadvantages of the contact and non-contact technologies is shown in Table 1.2.

Table 1.2: Advantages and disadvantages of Contact and Non-Contact Solutions for Gear Metrology

Contact	
Advantages	**Disadvantages**
- Repeatability - Not influenced by surface irregularities - Not influenced by material properties	- Points Acquisition Rate - Technology Peak already reached
Non-Contact	
Advantages	**Disadvantages**
- Accuracy with flat surface - Points Acquisition rate - High development opportunities	- Influenced by surface irregularities - Influenced by material properties

1.2 Objectives

This thesis has two main goals:

- The first is to effectively evaluate the performance that could be achieved using laser inspection relative to a contact measurement and analyze the benefits that are obtained by introducing this new technology to the Omega Gear Metrology lab. The machine studied is the Urano HC-N400. It has been compared with the contact inspection machine used today in Omega Metrology lab, the Emera. The main features considered are the accuracy, repeatability and cycle time needed for a Standard Gear Inspection measurement. In addition, a correlation study between the two outputs obtained by the two technologies will be done.

The desired improvements must be such as to recover the investment needed for the new technology. For this reason, a consideration of:

- environmental conditions needed to guarantee the perfect functioning of the machine;
- daily and long term maintenance;

has been done, as well. This study will conclude with personal recommendations for the best technology;

- The second is to investigate the geometrical causes of a particular noise problem that can be detected only by means of Noise Test on the assembled transmission. This particular noise is also known as "Ghost Noise". One gear, indicated as the cause of this phantom phenomenon, has been analyzed at the University of Windsor Tribology of Material Research Centre by using the Profilometer Zygo New View 100. Thanks to the profilometer, it has been looked for cracks, waves and other possible defects at nanometric level that could be the cause of this phantom noise.
  The ghost noise gear, also defined as "Worst of Worst" (WOW), has been compared with the "Best of Best" (BOB) sample. Also in this case, personal recommendations on the tools needed to easily find out other possible gears that can be the cause of these disturbance, have been given.

1.3 Thesis Organization

In order to facilitate the reader of this thesis, an itinerary of the main contents of each chapter is provided in Table 1.3.

Table 1.3: Chapter Organization

Chapter 2	• General background on gear basics and the gear manufacturing process • Contact inspection methods utilized in the main gear lab and other in-line solutions for fast manufacturing machine set-up • Theory and applications of non-contact metrology systems • Ghost Noise
Chapter 3	• Evaluation of the contact machine used in the main Omega gear metrology lab: Emera • Evaluation of the 3D Non-Contact metrology system developed by Urano
Chapter 4	• Study of the Ghost Noise and "Worst of Worst" gear by means of the Profilometer Zygo. • An overview of the Nital Etch analysis to characterize the possible damage caused by the Grinding process
Chapter 5	• Consideration of the Urano system • Consideration of the results obtained by Zygo and Nital etch Test
Chapter 6	• Thesis Conclusions
Chapter 7	• Possible future research

Chapter 2

Literature Survey

The following chapter gives a brief description of the basic gear concepts such as the terminology used and their application in the automotive field, followed by an overview of the main steps of the gear manufacturing process.
The literature survey then goes into a discussion of the current contact technologies used both in gear labs and as in-line solutions for an initial set-up for the machine used for future production. It then provides a description of the operating principle, parameters and devices that affect the quality of the non-contact systems. Application of these machines are then discussed.
Finally, an introduction to the main sources of vibration on the transmission Gearbox and the Ghost Noise problem is provided.

2.1 Gear Basics

A Gear is a cylinder or a cone having equally spaced teeth around the surface with the goal of transmitting torque and motion from one shaft to the other.
Gears can be divided into three categories:

- Straight Spur Gears
- Helical Gears
- Bevel Gears

(a) Straight Spur Gear

(b) Helical Gear

(c) Spiral Bevel Gear

Figure 2.1: Gears Types [7]

Straight Spur gears (Figure 2.1a) are the simplest form of gear having teeth parallel to the gear axis. The contact of two teeth takes place over the entire width along a line parallel to the axes of rotation. Helical gears (Figure 2.1b) are one type of cylindrical gears with a slanted tooth trace. Compared to spur gears, they have a larger contact ratio and are quieter, have less vibration and are able to transmit larger forces. A spiral bevel gear (Figure 2.1c) is a bevel gear with helical teeth. Bevel gears are characterized by intersecting axes of two shaft and tooth faces that are conically shaped. Their purpose is to transmit torque between non-parallel shafts. Their main application is in a vehicle differential, where the direction of drive from the drive shaft must be turned 90 degrees to drive the wheels.

2.1.1 Gear Terminology

Figure 2.2 represents the main features that characterize a gear tooth. Generally, tooth flanks are designed with a barrel shape such that the load is concentrated on their central portion: the benefits will be a life increase of the parts. Furthermore, chamfers are present in every edge in order to both avoid gear flanks being damaged during the handling and transportation as well as to avoid breaking the hard finishing tools during the material removing processes.

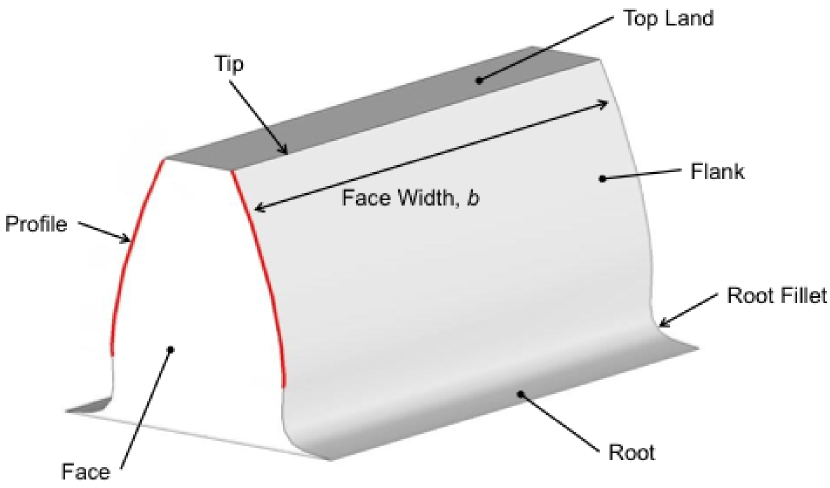

Figure 2.2: Gear Tooth Features [8]

In addition to the above features, other important specifications can be made in order to define the main diameters that are used in Gear Design (Figure 2.3).

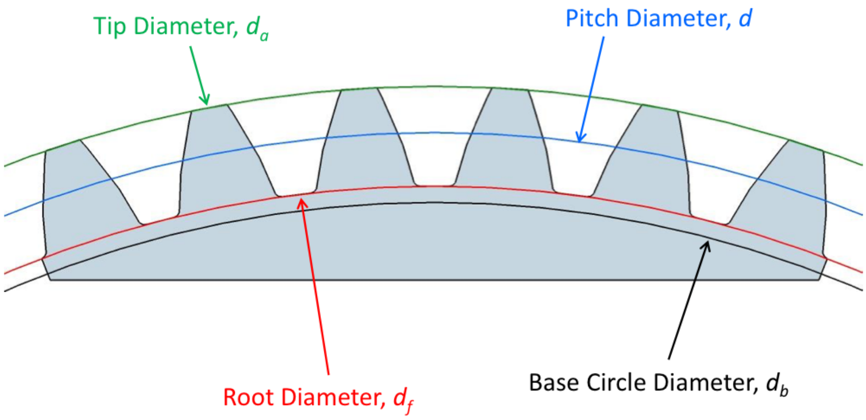

Figure 2.3: Gear Diameters [8]

The pitch diameter is the corresponded diameters of the discs when two gears are visualized as a pair of contacting discs. The root and tip diameters will be defined by the Addendum (h_a) and the Dedendum (h_f) (Figure 2.4). "h_a" is the distance between the pitch diameter and the tooth tip. Both tip and root diameters are reference circles that cannot be seen on a gear, as they are virtual. The dimension of the Addendum and the Dedendum are defined by:

$$h_a = m \tag{2.1}$$

$$h_f = 1.2m \tag{2.2}$$

where "m", the gear module, is one of the most important gear parameters and essential for its design; it is defined as the ratio between the millimeters of pitch diameter and the number of Teeth "z".
In the Figure 2.4, it can be seen that, when two gears mesh with each other, they will not be in contact at the root of the flank but rather only for a limited working depth. The reason is related to the fact that any possible damage of the tip in the contact at the root of the matching gear should be avoided for both better performance and smoothness of the gear mesh.
Another important parameter for every gear is the Pressure Angle "α". It is the leading angle of a gear tooth and it determines the tooth profile (Figure 2.4). Typically, the one indicated in every gear chart is measured at the pitch circle. Today, the pressure angle is usually set to 20 degrees.

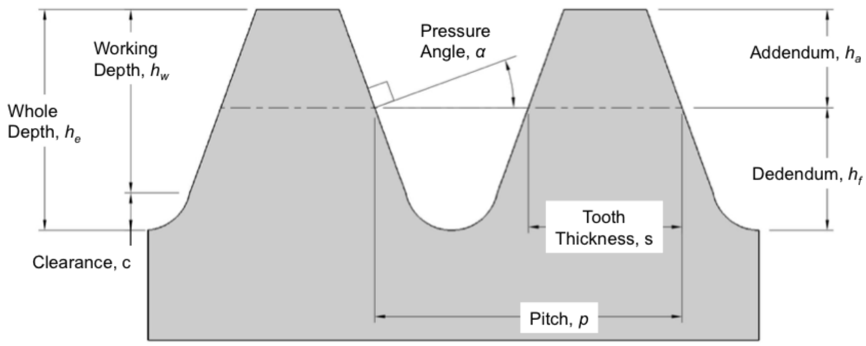

Figure 2.4: Gear Tooth Terminology [8]

In Figure 2.5 it is indicated how the pressure angle will influence the tooth geometry. As it can be seen, the higher the pressure angle, the straighter the tooth profile. This characteristic is related to the manufacturing process itself.

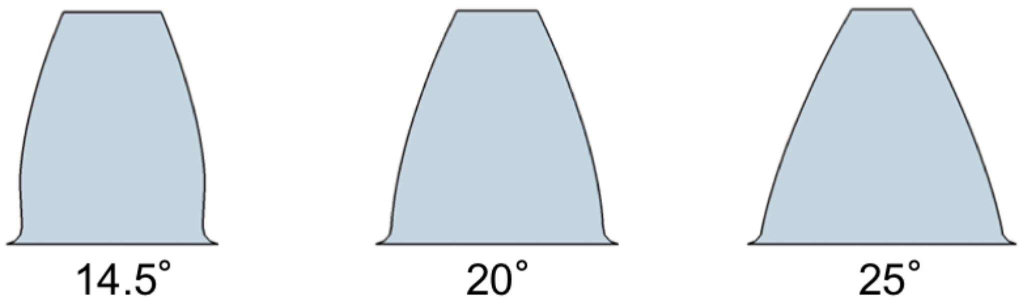

Figure 2.5: Influnce of the Pressure Angle on the Gear tooth geometry [8]

2.1.2 Planetary Gear Set

The main application of gears in the Automotive field is in the Transmission Gear Box. The need for a transmission system in an automobile is a consequence of the characteristics of the internal combustion engine. The engine always provides both its highest torque and power outputs. But, often, the greatest torque is required when the vehicle is moving from rest or traveling slowly while high power is not. Likewise, maximum power is needed at high speeds, but high torque is not. For this reason, a transmission is required to transform the engine's output so that it can supply high torque at low speeds, but also operate at highway speeds with the motor still operating within its limits. In the thesis, the transmission considered is automatic.

Automatic transmissions work following the principle of a planetary gear set. A planetary set (Figure 2.6) is composed of planet gears that rotate around an axes that revolves around a sun gear and the ring gear binds the planets on the outside. Typically, the planet gears are mounted on a movable arm or carrier, which itself may rotate relative to the sun gear. Generally, several gear sets are present in a single transmission. For this reason, the Planetary Set, the pinions, sun and outer ring gear itself will be identified by a number.

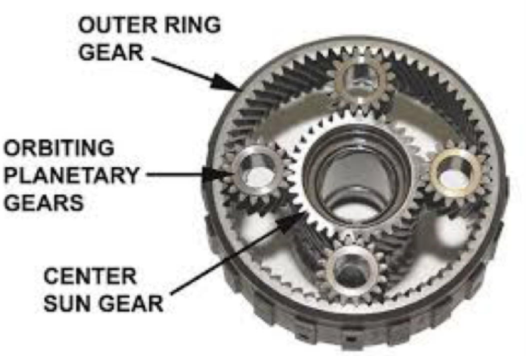

Figure 2.6: Planetary Set of an Automatic Transmission Gearbox [9]

Both for the sun, planets and outer ring, helical gears are used. The reason is due to a higher contact ratio, which results in less noise and less vibration. The contact ratio can be defined as the maximum number of teeth that are in contact at the same time in a gear matching. Helical gears will be the only gears used in the present research.

The gear ratio of an epicyclic gearing system is non-intuitive because there are several ways in which an input rotation can be converted into an output rotation. The overall gear ratio of a simple planetary gear set can be calculated using Equations 2.3 and 2.4 that represent the sun-planet and planet-ring interactions respectively:

$$N_s\omega_s + N_p\omega_p - (N_s + N_p)\omega_c = 0 \tag{2.3}$$

$$N_r\omega_r - N_p\omega_p - (N_r - N_p)\omega_c = 0 \tag{2.4}$$

- where ω_r, ω_s, ω_p, ω_c are the angular velocity of the ring, sun gear, planet gear and carrier respectively.
- N_r, N_s, N_p, N_c are the number of teeth of the ring, sun gear, planet gear and carrier respectively. Equation 2.5 can be deduced.

$$N_s\omega_s + N_r\omega_r = (N_r + N_p)\omega_c \tag{2.5}$$

In the planetary gear systems, one of the three components is held stationary, one is an input, providing power to the system, while the last component is an output, receiving power from the system. The ratio of input rotation to output rotation is dependent upon the number of teeth in each gear, and upon which component is held stationary.

2.1.3 Gear Inspection Parameters

There are a lot of parameters that influence the engagement between teeth and, as a consequence, the stress distribution along the flank of the gear, noise generated during engagement and wear of the teeth themselves. These parameters could be related both to the profile (pressure angle, crowning height, tip or root relief), the helix angle, (crowning, end relief or helix deviation) or to the pitch (distance along a curve from one tooth to next at same pitch diameter) or runnout (radial deviation over a ball occurring once per revolution).

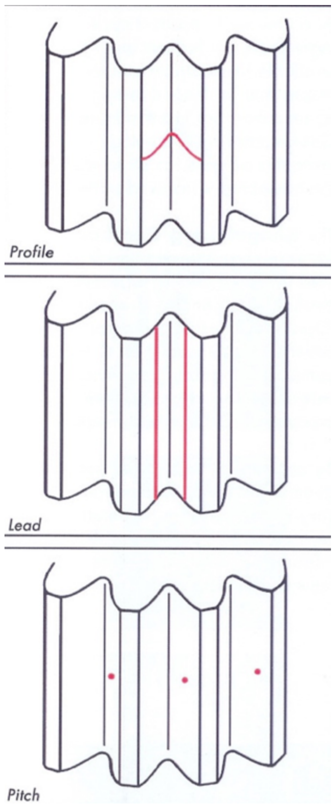

Figure 2.7: Standard Inspection: Profile, Lead and Pitch/Runout [10]

During a standard in-line measuring operation of both profile and lead, only 4 teeth at 90° are analyzed. The measurements occur across the middle of the tooth and a continuous trace is followed. For the first tooth measured, two extra measurements are performed both at the top and root of the profile and at different height than the lead. Those extra measurements are important in order to define particular bias that could be present between the upper and the lower trace. In some cases, tolerances for the maximum admissible bias are established, too. To measure the pitch and runnout deviation, a single point on both the left and the right flank of each tooth at pitch circle height is measured. In Figure 2.7, the path and points measured on a flank for the profile, lead and pitch deviation are indicated. The definition of the different measured parameters are defined by the DIN, ISO, AGMA and JIS standards.
Figure 2.8 gives a graphically representation of how both form and slope deviations (for lead and profile) can be defined on a flank. The view of this representation is shown in Figure 2.7. For the profile and lead deviation both the slope and the form of the traces should fall within certain tolerances. Those tolerances are defined internally by each manufacturer according to the best trade-off between manufacturing costs and quality achieved.

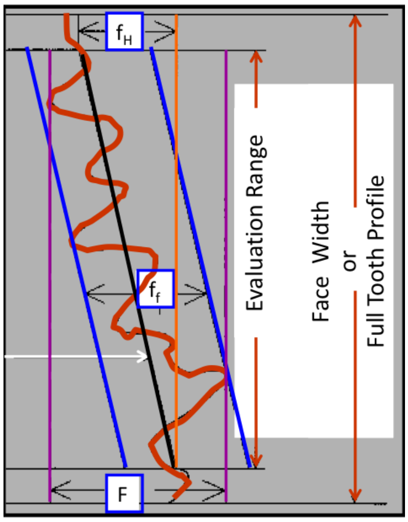

Figure 2.8: Evaluation of Profile and Lead Deviation [10]

For the profile evaluation, the following parameters are used [11][12][13][14]:

- The profile slope deviation "$f_{h\alpha}$" is derived from the deviation of the actual slope of the involute of a tooth flank and the nominal slope without the influence of the form deviations. It is the distance between the nominal profiles and the fitting line that intersects the average profile at start and end points of the profile range;
- The profile form deviation "$f_{f\alpha}$" is derived from the deviation of the actual to the nominal form without the angular influence. It indicates the distance between two involutes of the actual involute profile within the profile inspection range;
- The total profile deviation "F_{α}" is derived from the superposition of the profile slope deviation and the profile form deviation. The deviation will be the distance between two nominal profiles enclosed within the profile test range.

Generally, a table below each chart is reported. In this table, the maximum deviation measured is indicated. Naturally, this number should be lower than the specified tolerance in order to accept the gear. Sometimes, mean values of the measured deviation for every tooth are indicated as well. This is the only value considered during the inspection of gears in the intermediate manufacturing process steps.

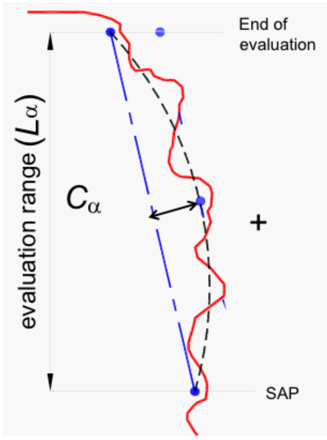

Figure 2.9: Profile Barelling C_α [10]

Another parameter, also known as Profile Barelling "C_α", is used to further describe the Profile deviation (Figure 2.9).

- Profile barreling is the distance from the best fit curve to the slope deviation line. This is sometimes called "involute crown".

A typical profile evaluation for both right and left tooth flanks is shown in Figure 2.10. The ideal profile results in a straight line in a chart and the evaluations are performed from the start of the active profile until the minimum chamfer line.

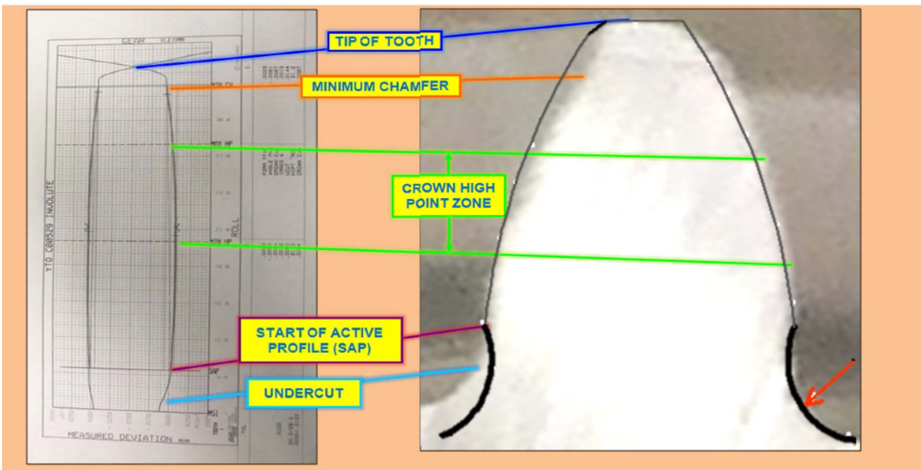

Figure 2.10: Profile Measuring Region [10]

As it can be seen, the tip of the tooth falls after the minimum chamfer line. In the case in which this line falls too soon, it means that an improper cut or bur on the hob is present. The same definitions can be applied for the lead evaluation. The only change will be present in the nomenclature. In fact, instead of having "$f_{h\alpha}$", "$f_{f\alpha}$", "F_α" and "C_α", it will be "$f_{h\beta}$",

"$f_{f\beta}$", "F_β" and "C_β". Figure 2.11 shows a schematic of a lead measurement (Figure 2.7) is presented on the chart. The lead or helix trace will appear straight if no deviations are present. Furthermore, deviation on the left or right side will mean the absence or material or the presence of additional material according to whether the right or left profile has been evaluated.

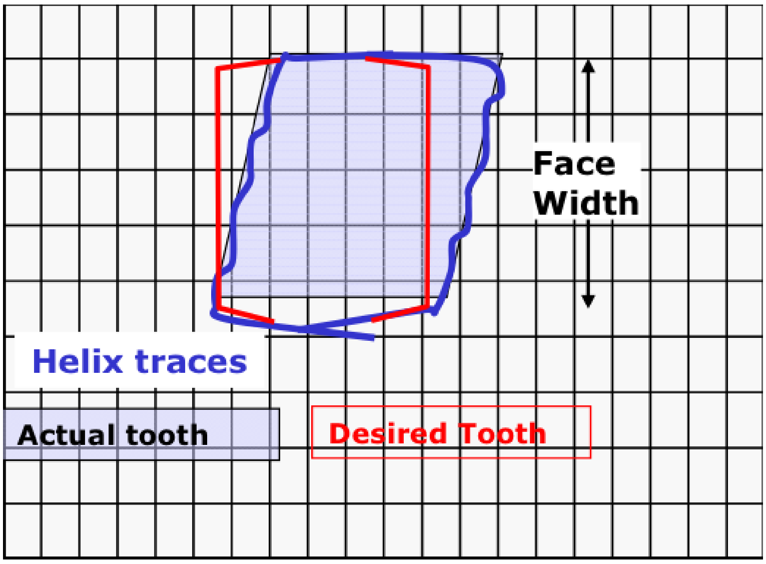

Figure 2.11: Ideal tooth Lead [10]

Four other parameters are used to check the pitch and runnout deviation. They can be defined as follows:

- The single cylindrical pitch "f_p" is the length of the reference circle arc between two successive equal-handed tooth flanks measured at the pitch circle. The reference circle pitch, is the corresponding diameter of the discs when two gear sets are visualized as a pair of smooth contacting discs;
- The total cumulative pitch "F_p" is defined as the difference between the most positive and the most negative pitch values;
- The difference between adjacent pith "f_u" is the difference between the actual dimensions of two successive pitches;
- The pitch line run-out "F_r" combines all tooth eccentricity and it is the radial position difference of all teeth at measuring diameter.

Figure 2.12, Figure 2.13 and Figure 2.14 shows an example of inspection chart. As it was noted above, for profile and lead deviation, the left and the right flank are measured. For each side 6 traces are reported. The traces No. 1b, 9, 18 and 26 refer to the teeth at 90°;

instead the traces "1a" and "1c" refer to the extra traces measured to check the presence of bias error. A scale is shown along the charts' sides; in addition, in the lower part, a table with the measured deviations and inspected parameters is present. Furthermore, in the central part of this table, the maximum allowed tolerances are defined. These tolerances, in the automotive field, range from 7 to 15 μm depending on the parameter analyzed and the type of gear. Generally, tolerances are more strict for pinion gears because they tend to be the main source of noise in an automatic transmission.

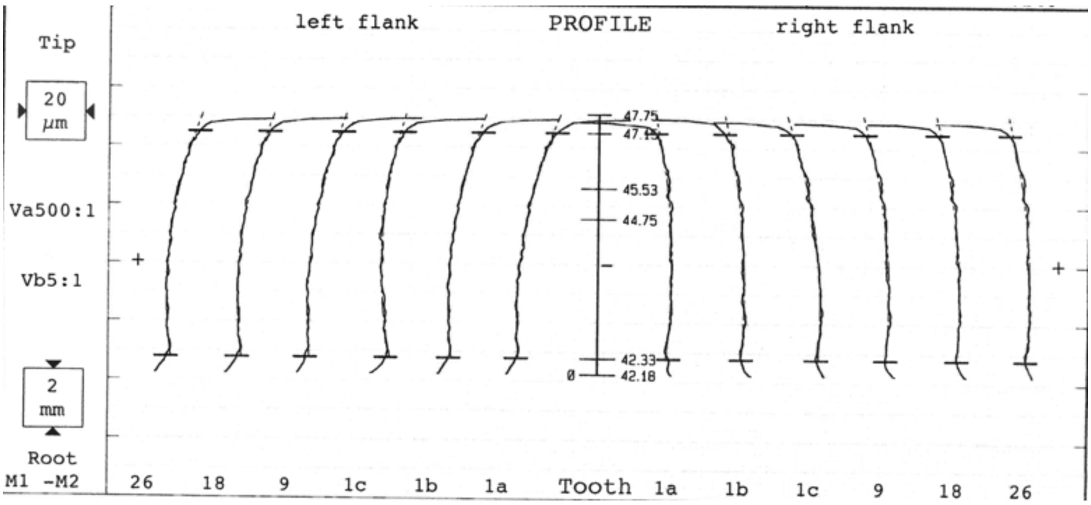

Figure 2.12: Example of Standard Inspection Chart: Profile Deviation

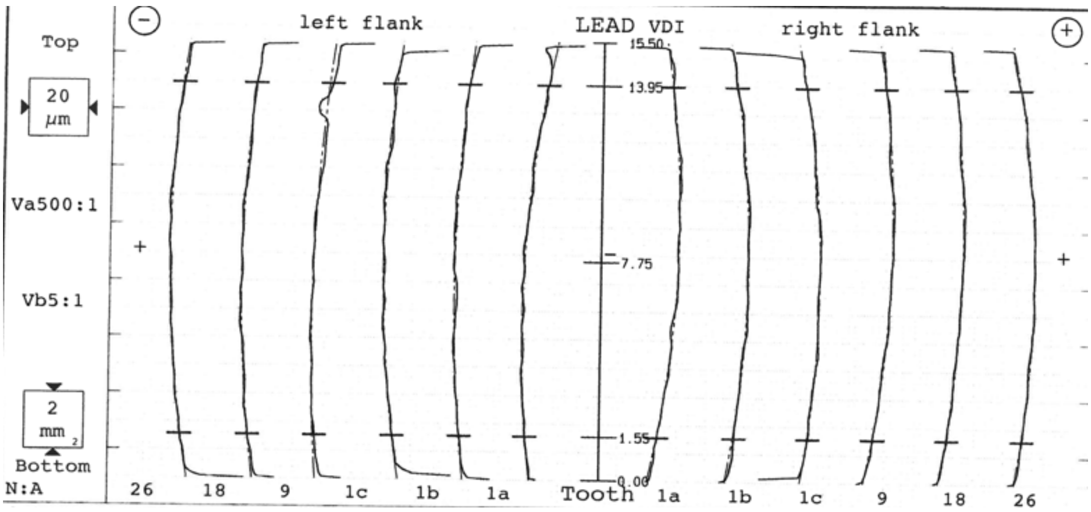

Figure 2.13: Example of Standard Inspection Chart: Profile Deviation

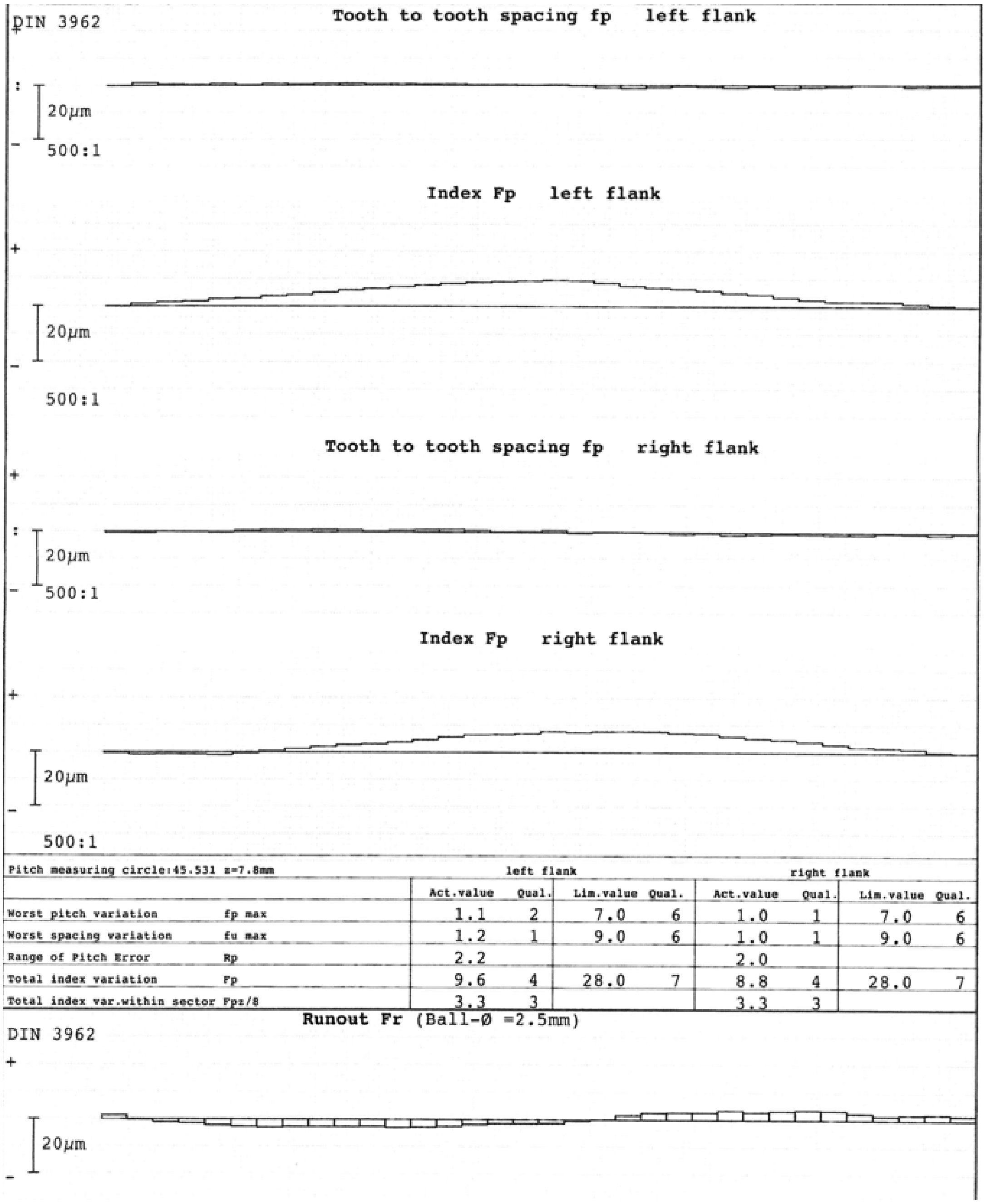

Pitch measuring circle:45.531 z=7.8mm		left flank				right flank			
		Act.value	Qual.	Lim.value	Qual.	Act.value	Qual.	Lim.value	Qual.
Worst pitch variation	fp max	1.1	2	7.0	6	1.0	1	7.0	6
Worst spacing variation	fu max	1.2	1	9.0	6	1.0	1	9.0	6
Range of Pitch Error	Rp	2.2				2.0			
Total index variation	Fp	9.6	4	28.0	7	8.8	4	28.0	7
Total index var.within sector	Fpz/8	3.3	3			3.3	3		

Figure 2.14: Example of Standard Inspection Chart: Pitch and Runnout Deviation

2.2 Gear Manufacturing Process

In order to create a gear, several operations have to be performed. The starting point is a bar of roughly 6 meters in length that it is heated by induction and is cut. These smaller cubes, that will become gears, are subjected to hot forging in order to deform the grain of the original blank until the desired diameter and height are achieved (Figure 2.15). This process is preferred to casting because of the advantages obtained both in terms of cost and strength. Generally, with materials like steel, hot forging is always used in order to avoid the hardening process which poses problems for the subsequent machining operations.

Figure 2.15: Hot Forging Process [15]

The internal diameter is subsequently produced by means of a piercing operation. The final result is shown in Figure 2.16. The material used for gear manufacturing is a Cr-Mo alloy steel with a tensile strength greater than 930 MPa and a hardness that ranges between 260 and 330 HB. The carbon percentage in the steel is between the 0.3 and 0.7.

Figure 2.16: Gear blank after forging and piercing [8]

The starting point to obtain a good gear is a very good blank. How good? For most practices, perpendicularity of bore to clamping faces is less than 12 μm and radial runout of a similar tolerance (Figure 2.17). The metrology department often attributes the fault of a bad gear to the grinding or hobbing process without knowing that most of the errors come from the starting points. This is why it is recommended to improve the quality of the blank in order to achieve the desired quality on the final gear with the minimum cost.

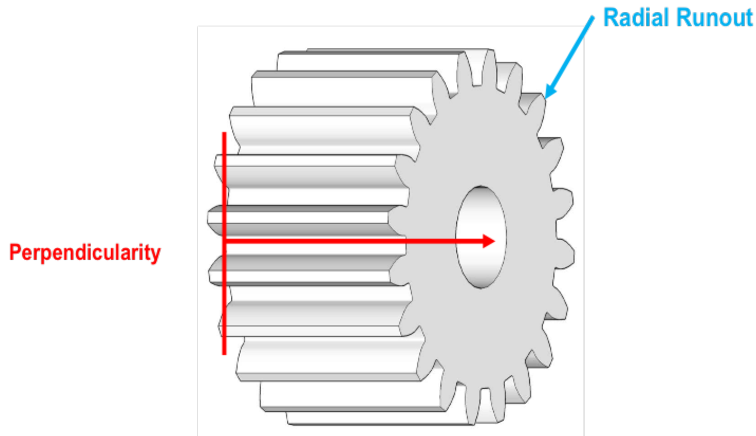

Figure 2.17: Perpendicularity and Runnout of a Gear Blank [8]

2.2.1 Soft Pre-Machining

Gear teeth are created by means of a forming process or soft pre-machining process. For mass production and high precision gears, the form generating process is the most widely used method. In this process, the tooth form is generated by meshing the cutting tool with the gear blank. Hobbing is the widely used material removal process, in which the teeth of the gear are progressively generated by a series of cuts with a hob (Figure 2.18).

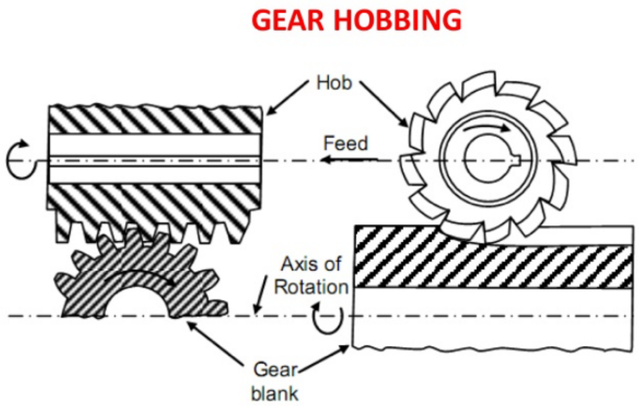

Figure 2.18: Gear Hobbing [8]

The angle between the hob axis and the workpiece axis depends on the type of gear being produced. For spur gears, the hob is angled equal to helix angle of the gear. For the production of helical gears, the angle must be increased by the same amount as the helix angle of the helical gear.

Generally, in order to improve the quality of a gear, two passes are done. The first one, called the rough operation, consists of removing the greatest amount of material from the blank at higher axial feed velocity by using a low hob rotational speed. During the second operation, the axial feed velocity is reduced while the rotational speed is increased. The result is a process that is inexpensive but relatively inaccurate. This operation is applied both for pinion and sun gears and the final result will be a "green" gear. Generally, just 1/3 of gears checked are green gears. This is done in order to be sure of the process quality for the next steps.

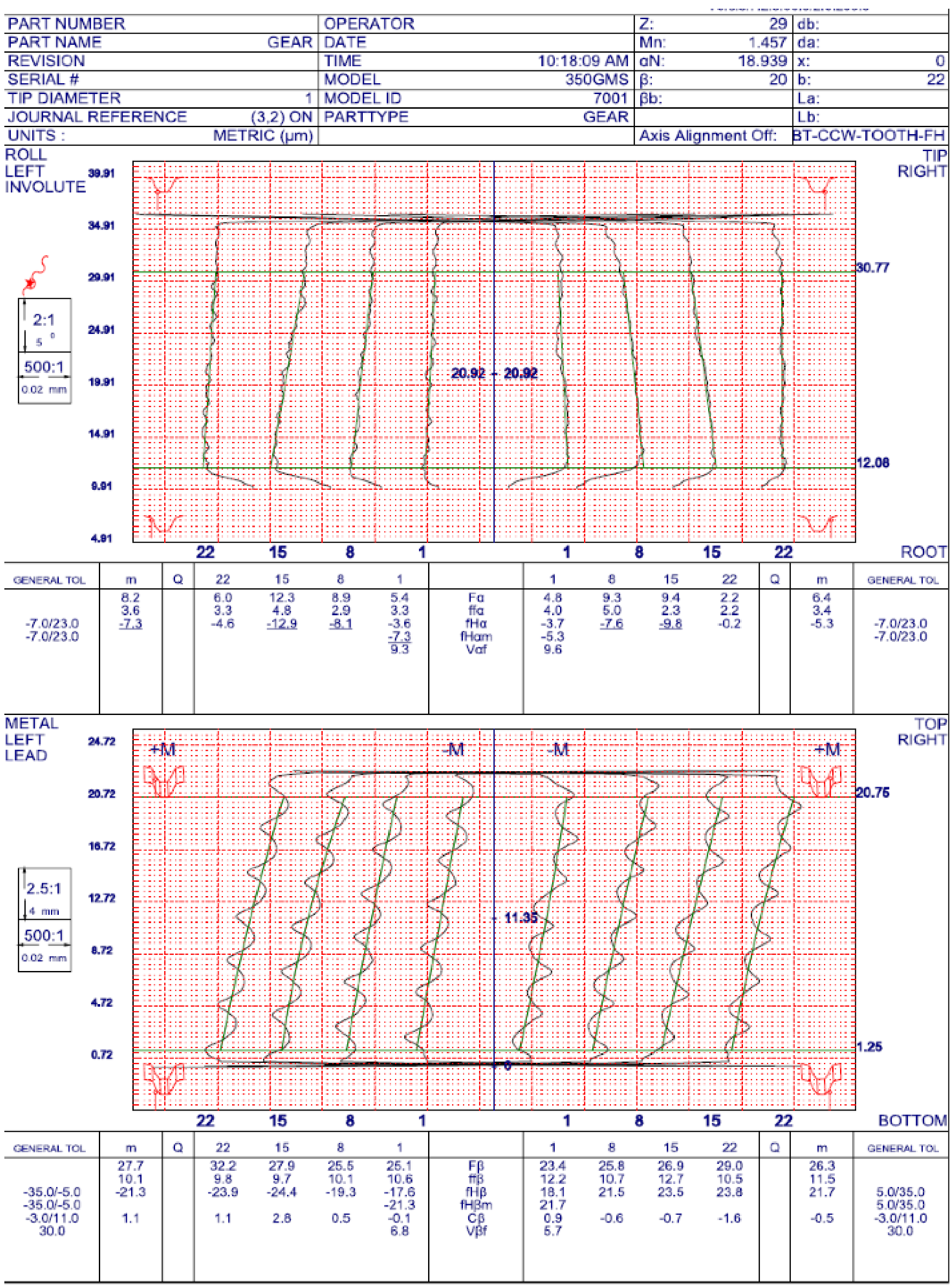

Figure 2.19: Involute inspection after hobbing [8]

Figure 2.19 presents a typical inspection chart of a gear subjected to hobbing. As can

be seen, in the lead trace, different scallops are present. These features are desired because, in the following hard finishing operations, they will be easily removed. Sometimes, slope deviation will be intentionally induced in the lead in order to compensate and prevent distortion that will come out from the heat treatment.
Because of the impossibility of using a hob cutter for internal gears, a broaching operation is used (Figure 2.20).

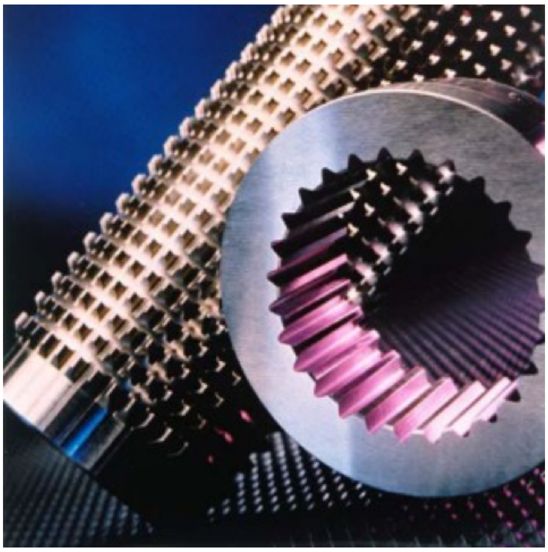

Figure 2.20: Gear broach for Annulus Gear [15]

The broaching consists of generating the gear teeth of an internal gear by an axial relative motion between the broach and the gear fixed in a tool holder. While the holder moves vertically, the broach rotates and removes the material from the gear blank until the final tooth shape is obtained. The cut depth increases progressively when the gear reaches the top part of the broach due to the particular tooth dimensions of this cutting tool. The rotational speed depends on the desired helix angle.
Broaching can provide excellent results in terms of quality and volume production, though it comes with higher manufacturing costs.

2.2.2 Gear Heat Treatment

In order to improve the fatigue strength and wear resistance of gears, heat treatment (HT) processes are used to harden the outer layer of steel while maintaining a soft inner metal core. The metal surface is reinforced by adding a fine layer at the top of the metal alloy. The first step is to perform a carburizing and quenching process. Here, the metal (low carbon steel) is heated in a carbon atmosphere in a such a way as to absorb the carbon and make it harder. The carbon will penetrate in the skin of the low carbon steek and will create an external covering with more carbon than the core. The resulting product will be

much harder. After the carburizing process, a rapid cooling in oil or water is performed (quenching). The scope of the quenching process is to prevent a phase transformation or an undesired thermodynamic reaction. The next step is induction hardening. Induction hardening is a heat treatment performed to harden the surface of steel containing more than 0.35 % carbon. Induction hardening is a form of heat treatment in which a metal part is heated by induction heating and then quenched. The quenched metal undergoes a martensitic transformation, increasing the hardness and brittleness of the part.
The final step will be the tempering process. Tempering is usually performed after hardening in order to reduce some of the excess hardness. It is done by heating the metal to a temperature below the critical point for a certain period of time, then air cooling the material; after that, the material is cooled in air. The exact temperature determines the amount of hardness removed. Figure 2.21. and Figure 2.22 show the typical distortion on lead and profile induced by an heat treatment (HT) process. Figure 2.21 in particular displays a reasonable gear quality before heat treating.

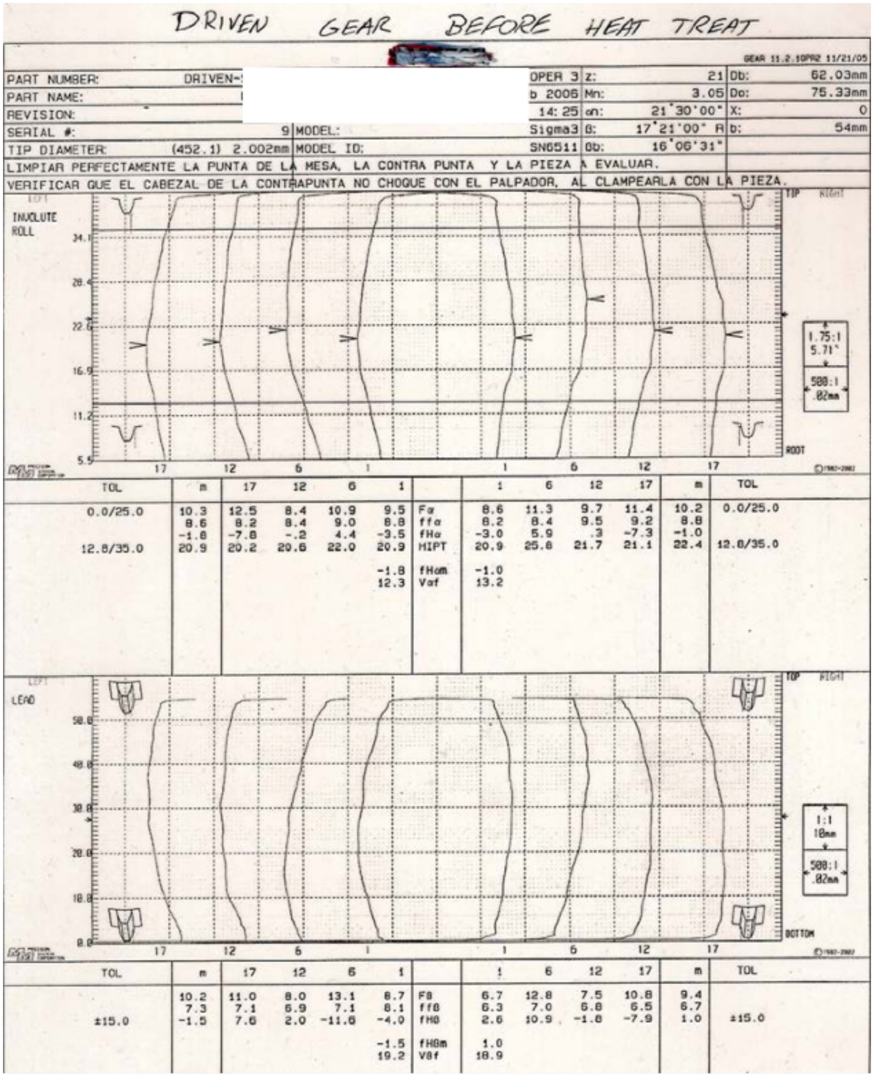

Figure 2.21: Profile and Lead deviation before HT process [8]

By contrast, Figure 2.22 shows the effect of Carburizing on profile and lead deviation. It is noticeable that the consistency remains the same but the profile moves in a negative direction from the approximate pitch diameter, while the lead slope changes significantly.

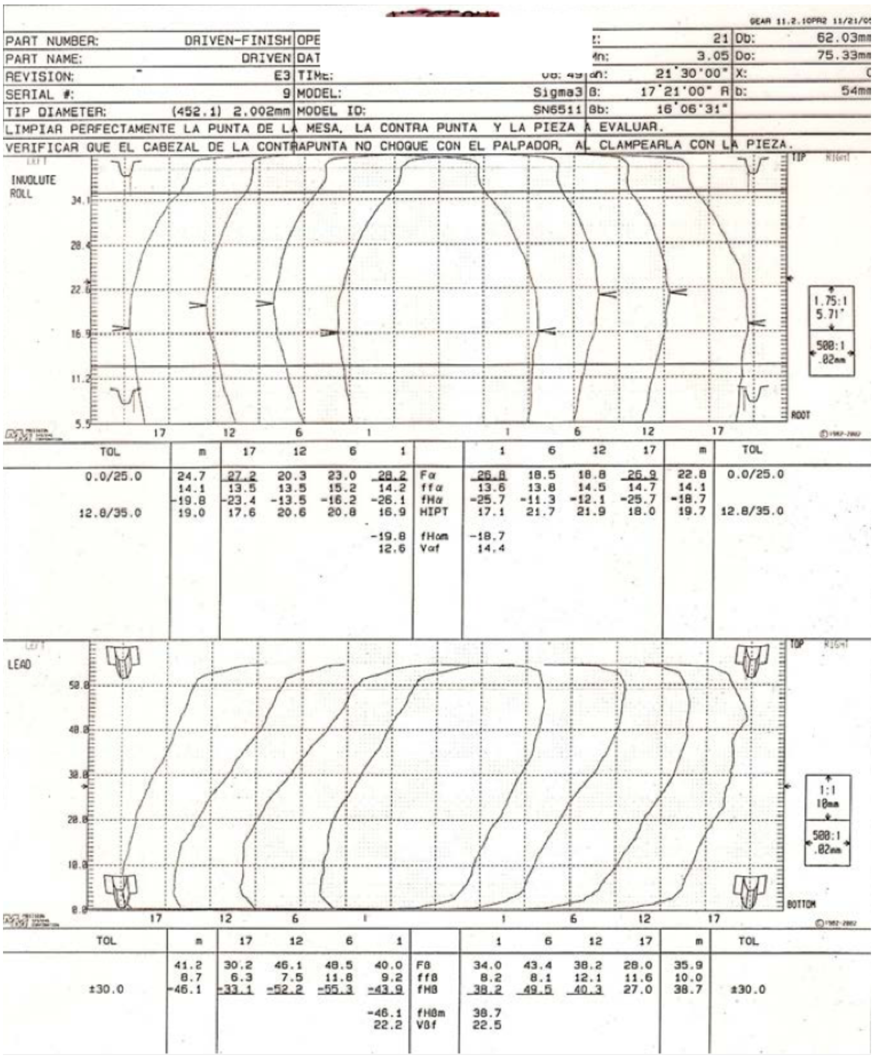

Figure 2.22: Profile and Lead deviation after HT process [8]

Other distortions caused by the HT processes are corrected by hard finishing process such as grinding (Figure 2.23). The goal of hard finishing processes is to remove a very thin layer from the tooth surface and to correct possible error coming from the heat treatment and pre-machining phase. Naturally, because very small corrections are done during the hard finishing operation, every parameter of the previous processes should be the best possible in order to meet cost and quality requirements.

2.2.3 Hard Gear Finishing

Figure 2.23: Gear Grinding process [16]

Gear grinding is a hard finishing manufacturing process used to improve the accuracy and surface roughness of gears by the additional removal of material by means of a grinding wheel (polishing stone) that rotates at very high velocity against the wheel teeth. Each wheel has two grades in order to perform a rough pass first followed by a finish operation at the end. This process is mostly used for pinion gears because it has been discovered that they are the major cause of noise in a planetary gear set.
One of the main problems with grinding wheels is the dressing operation. In fact, if it is not properly done, severe forms of deviations could be present on the gear flank. For this reason, it is performed two times for each wheel, and the first ground gear is always checked. In the case of a bad result, the wheel will be subjected to a second dressing cycle. For sun and annulus gears, just a HT process and a honing process (Figure 2.24) are used. This solution is cheaper compared to a more expensive grinding process and has the ability to modify the gear geometry in order to compensate for the distortions that occur during heat treatment. However, this process achieves a lower overall manufacturing quality.

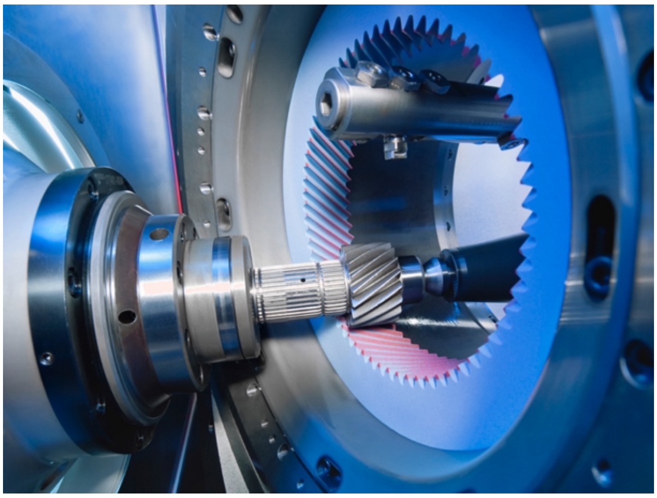

Figure 2.24: Honing processes [17]

Figure 2.25 and Figure 2.26 illustrates the improvements obtained in terms of accuracy on a hobbed and hardened gear by using a grinding process.

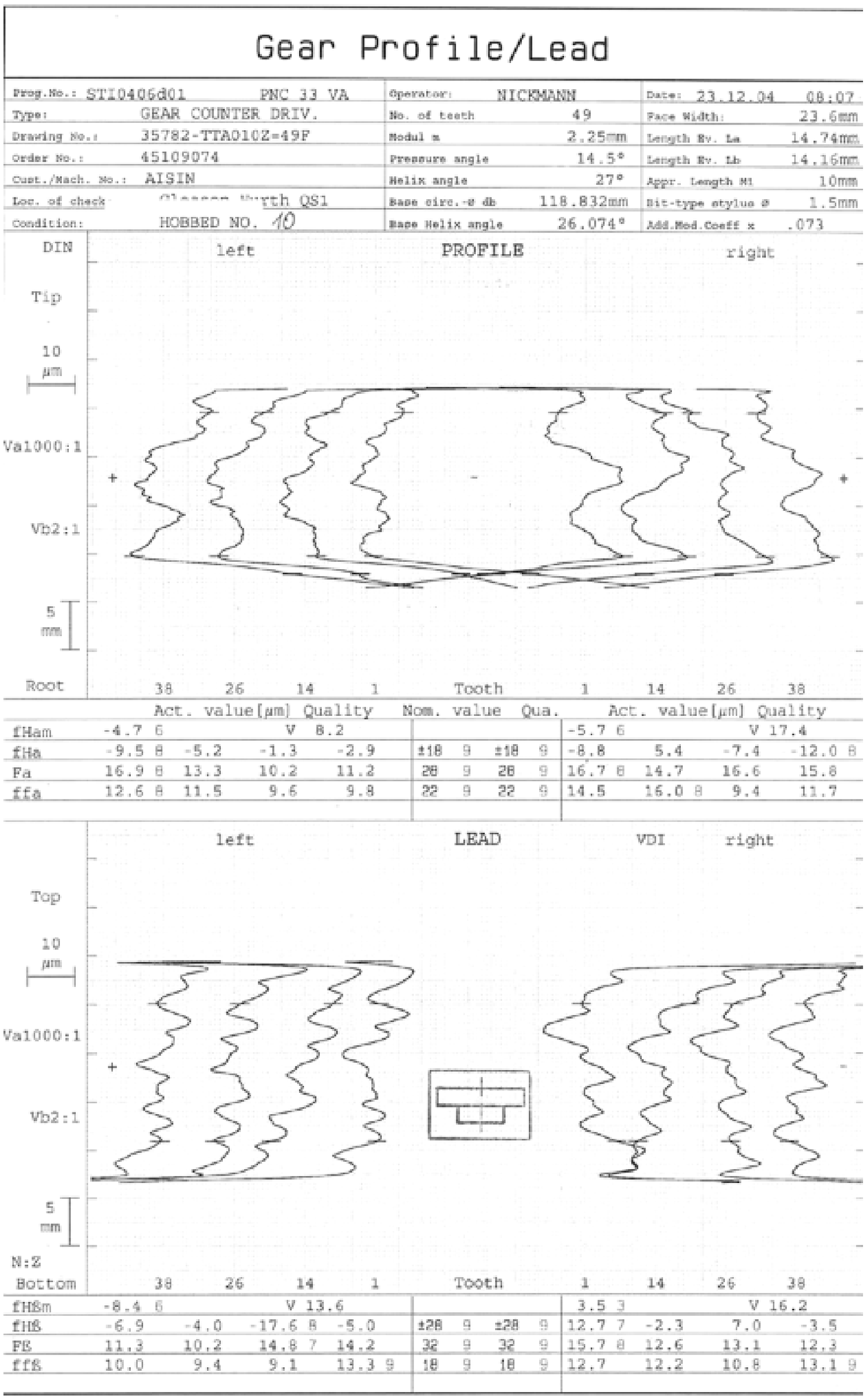

Figure 2.25: Effect of Grinding Process on Profile and Lead Deviation: Hobbed and Hardened Gear [17]

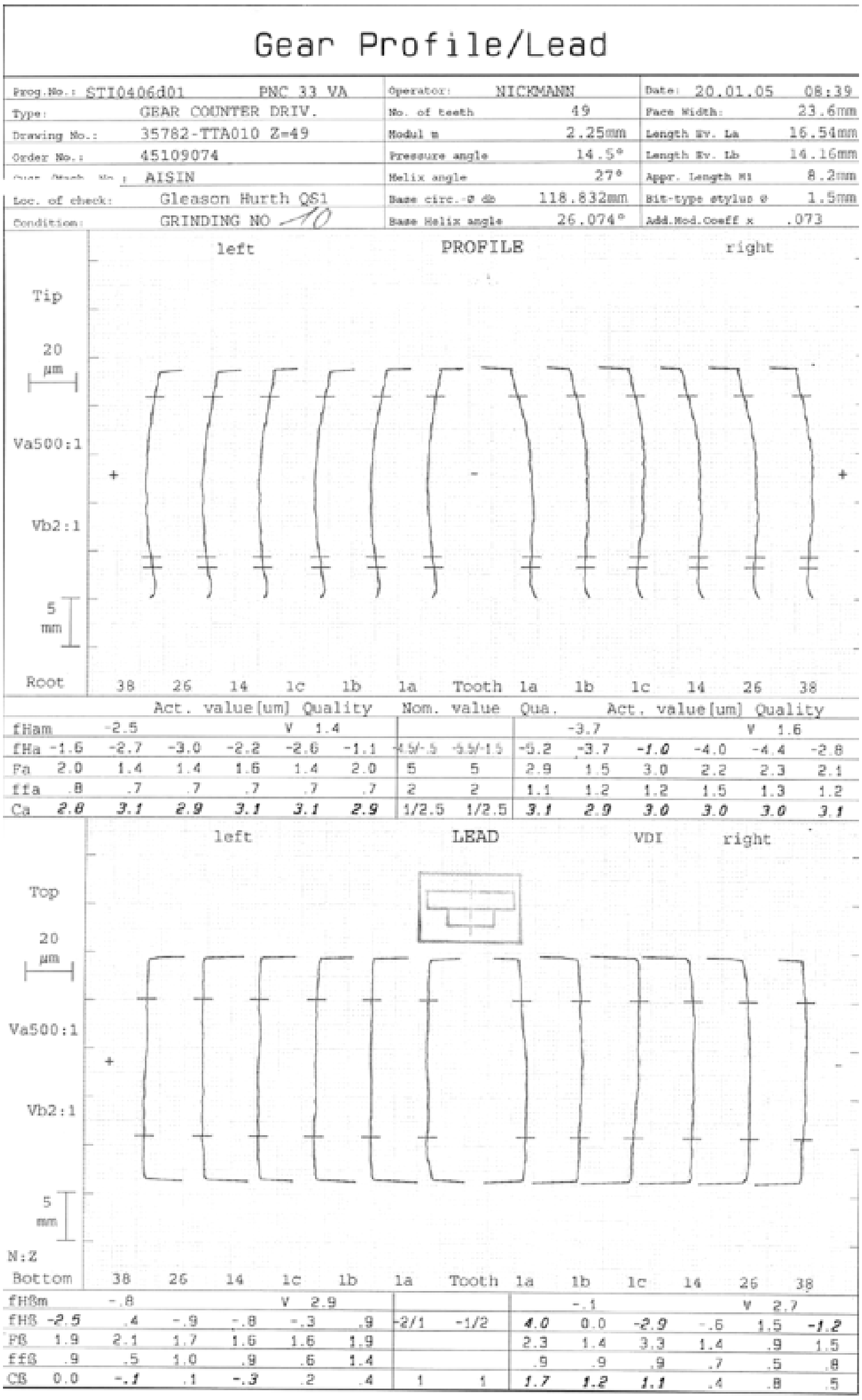

Figure 2.26: Effect of Grinding Process on Profile and Lead Deviation: Ground Gear [17]

As can be seen, any type of scallop or wave generated by the pre-machining has been eliminated. The result is an almost perfect gear where straight traces are measured.

2.3 Contact Gear Metrology

Gears are one of the key components in the automotive field. Gear designers are trying to improve lifetime, power transmission and noise emission because of an increasingly more stringent requirements. A high degree of gear manufacturing accuracy is crucial for achieving that demand. Proper understanding of gear metrology and measurement of gears is essential in order to understand accuracy and quality, manufacturing cost, rejects and scrap, machine control, to determine heat treat distortions and to make the necessary corrections.
Gear metrology organization is summarized in table 2.1 [18].

Table 2.1: Gear Inspection Methods

Functional Inspection	1. Initial set-up 2. Ongoing inspection
Analytical inspection	1. Fine-tuning 2. Production initiation

2.3.1 Functional Inspection Methods

Functional Inspection methods can be divided into:

- Size Inspection
- Runnout Inspection
- Double Flank Inspection

The traditional method of inspecting a gear for correct size is the measurement over pins or balls with a micrometer (Figure 2.27).

Figure 2.27: Measurement over Pins [8]

Pin measurement provides an accurate and convenient method for determining tooth thickness of a gear of any diameter within the capacity of the available micrometers. Size measurement is used to provide the correct backlash when the gear is mounted with its mating gear at operating center distance.

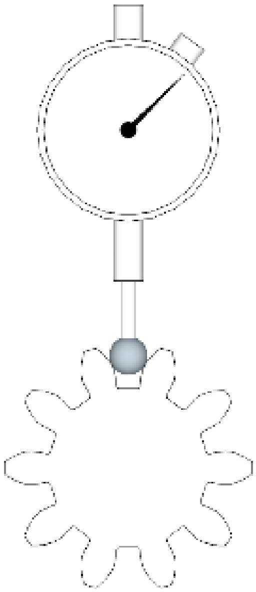

Figure 2.28: Runout Inspection [8]

Runout is the maximum variation of the distance between a surface of revolution and a datum surface, measured perpendicular to that datum surface. Runout of a gear can be measured with a ball placed in successive tooth spaces (Figure 2.28). Its goal is to assure a correct backlash and a minimum variation of rotary motion.

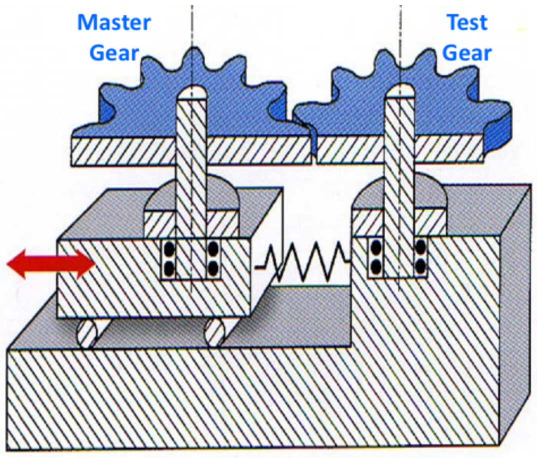

Figure 2.29: Double Flank Inspection [8]

Double Flank (Figure 2.29) is an inspection method in which the work gear is rolled in tight double flank contact with a master gear. No backlash is provided, as the work gear is spring-loaded against the reference gear on the inspection machine. The composite action test done performing an inspection instrument that will allow variation in the center distance during rolling. This variation in center distance will yield a "tooth-to-tooth" and a "total composite" indication that can be read on a simple dial indicator or recorded graphically (Figure 2.30).

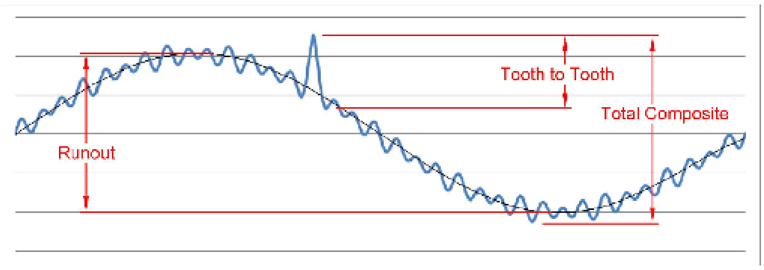

Figure 2.30: Double Flank Inspection: Graphical Result [8]

Double Flank Inspection is a useful shop-friendly tool to determine the general quality of a gear including size, runout, tooth-to-tooth rolling action, and to detect nicks. It is not an appropriate method to determine individual tooth flank errors.
Table 2.2 summarizes the main functional inspection methods and what they are used for:

Table 2.2: Functional Inspection Methods

Size Inspection	1. Tooth thickness measurement
Runnout Inspection	1. Backlash measurement 2. Variation of rotary motion measurement
Double Flank Inspection	1. Tooth-to-tooth measurement 2. Variation of rotary motion measurement 3. Total composite measurement

2.3.2 Analytic Inspection Method

Before the introduction of Coordinate Measuring Machines (CMM) or Gear Measuring Instrument (GMI) technology, gears were measured by manual gauging tools. Therefore, quality control of gears has become more stringent in recent years, as new probing and evaluation methods have been developed. With the introduction of numerically controlled GMI and CMM for the inspection of all kinds of gears including the cutting tools used for their production, the metrology field has seen significant improvement. By using a GMI or CMM, both measuring time and uncertainty have been reduced significantly and more information is available. The measurement is also performed automatically without being influenced by subjective assessment.

2.4 Optical Gear Metrology

The performance of tactile gear metrology has more or less peaked, and significant improvements in terms of accuracy and speed are hardly expected. Consequently, new solutions are needed. Laser line scanners have evolved over the last few years to a point where they have become a valid alternative for tactile inspection of geometrical primitives. Improvements in resolution, optical quality, image processing and data analysis have turned laser line scanning into a sufficiently accurate but much more productive substitute for tactile

measurements, even for feature inspection. The high data rate of optical systems, compared to traditional touch probing, makes this technology extremely suitable for collecting many measurement points required to sample complex (non-prismatic) geometrical shapes. Because optical measurement systems collects much more data in the same or less time and have an higher point density acquisition rate, the representation of the real geometrical feature is improved. However, the measurement of the convex and reflective surface for metallic gears is still a challenge.
The working principle of optical sensors is the triangulation method, also known as similarity between triangles. By knowing the distance between the light source (CLS) and the lens, the distance between the lens and the detector (PSD) and the corners at the top of the two triangles, the distance between the light source and the target can be determined [19].

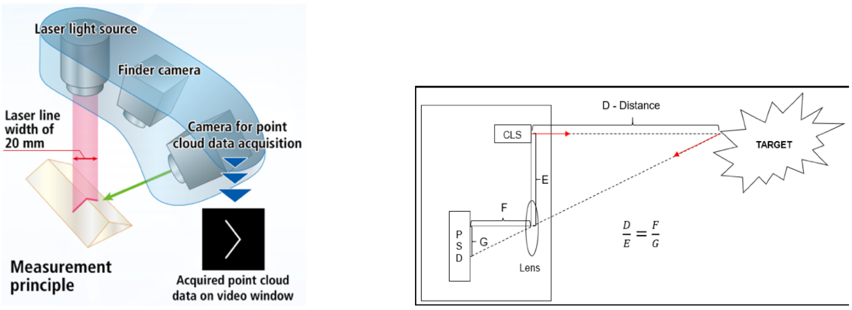

([19])

(a) Triangulation Sensor

(b) Similarity between Triangles

Figure 2.31: Triangulation Working Principle [6]

The device projects a stripe of coherent monochromatic light, coming from the lower source aperture. The laser stripe is projected on the working volume by means of a mirror. The laser light is then deformed by the surface of the scanned object. Meanwhile, each scan line is captured in a single frame image by a CCD camera. The captured image can be reproduced by means of a 3D model on a computer. At this point, quality inspection of the analyzed surface can be performed. The triangulation principle is summarized in Figure 2.31a and Figure 2.31b.
The necessary condition for the laser scanner to function correctly is that some amount of incident light is reflected into the sensor [20]. The amounts of reflected diffuse and specular light depend on the optical properties of the surface and on the angle of incidence of the laser light. Unfortunately, in some cases, some light can also absorbed or penetrate and travel through the material (Figure 2.32).

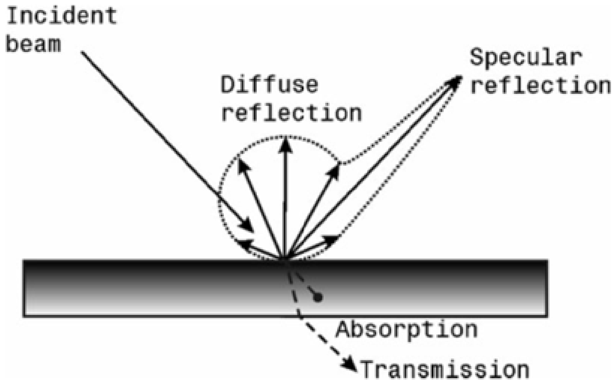

Figure 2.32: Incident laser beam that hits the surface with diffuse and specular reflections [20]

2.4.1 Calibration of laser scanner

The accuracy of laser scanners is influenced by many factors, such as surface quality, surface orientation and scan depth. In their paper, Gestel and CO [21] studied the influence of scan depth as well as in-plane and out-of-plane angles on the accuracy of the laser scanner and made some considerations on the geometries that could be used to calibrate the tool (Figure 2.33).

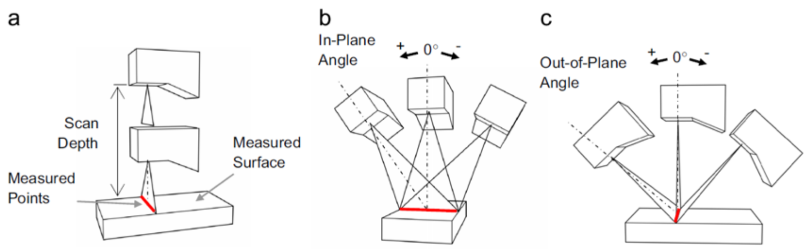

Figure 2.33: Scan depth variation (a), in-plane-angle variation (b) and out-of-plane angle variation (c) [21]

In order to evaluate the scan depth error, the reference plane is scanned at different scan depth levels. Level 1 is the position where the scanner is closest to the reference plane; level 10 is the level where the scanner is furthest away from the reference. Moreover, to have an idea on the repeatability of the results, each measurement has been performed 10 times. The standard deviation was shown to increase with the scanning depth. When the scanner was closer to the plane, the standard deviation of the measured plane was around 15 μm. At level 10, the standard deviation was around 30 µm (Figure 2.34).

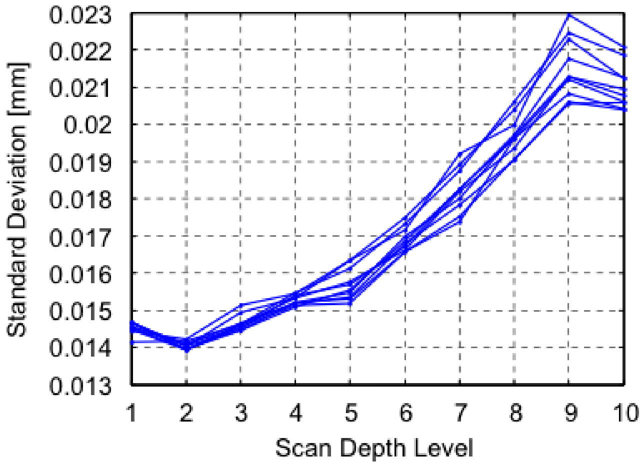

Figure 2.34: Influence of scan depth level on standard deviation [21]

In-plane and out-of-plane angles can also influence the standard deviation of the scanner. To investigate this influence, the reference plane was been scanned while varying these angles (Figure 2.35).

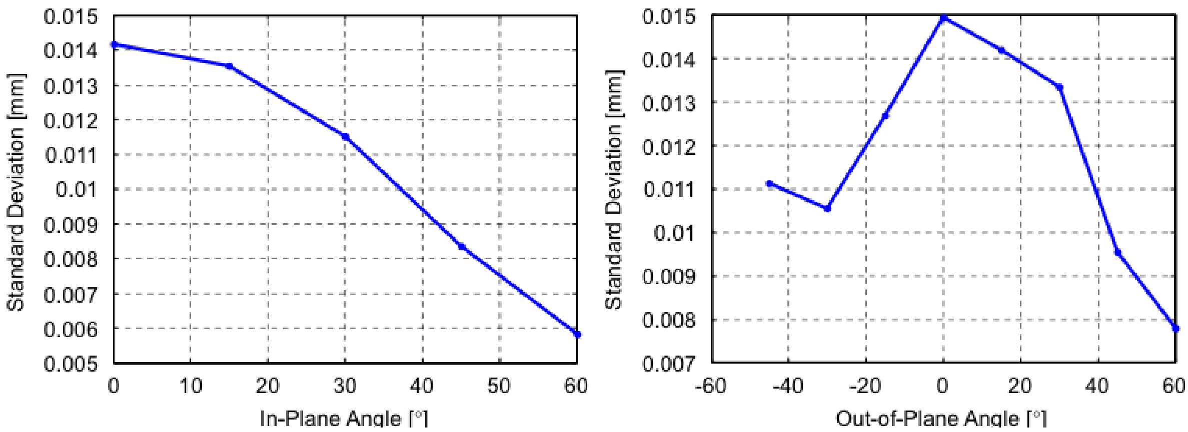

Figure 2.35: Influence of in plane and out plane angle on standard deviation [21]

By observing Figure 2.36, one can see that the calibration operation must be performed after the laser scanner is completely warmed up [21]. In order to evaluate the thermal stability, the scanner was calibrated after warming up for several hours. After switching off the scanner and letting it cool down, the scanner was turned on again. Starting from this moment, the reference plane was scanned every 3 min at level 1, 5 and 10, respectively. This test illustrates that, at the beginning of the test, the difference between the planes, scanned at the lowest and highest position in the range, is about 0.1 mm. This is normal, since the scanner is not warmed up yet. According to the manufacturer's recommendations, the scanner should be warmed up after about 30 min. However, from the results it can be seen that it takes more than 1 hour before level 1, 5 and 10 coincide. [21].

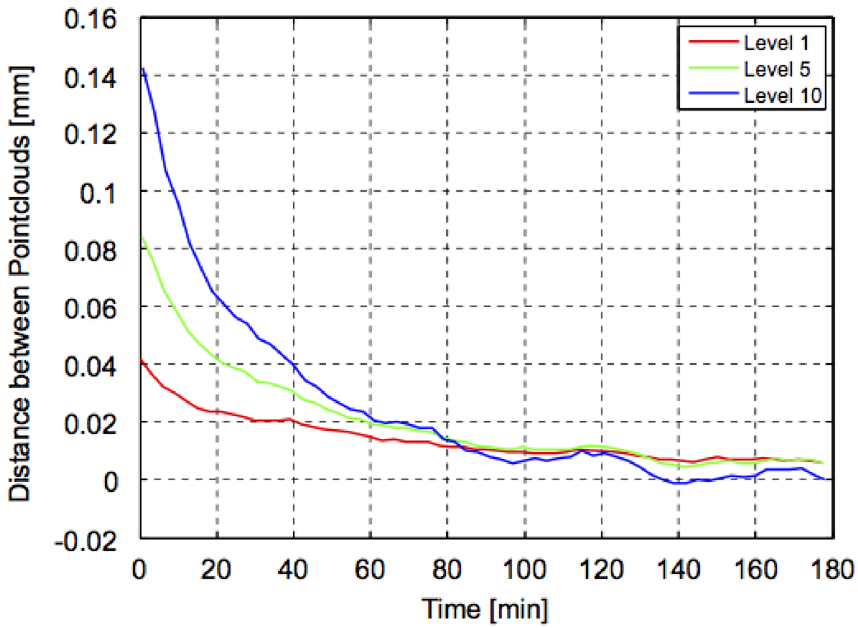

Figure 2.36: Thermal stability influence on the laser scanner: Warm-up Test [21]

2.4.2 Light wavelength and surface color

Because some light can penetrate the material, or can be absorbed into the material or into its surface, it is reasonable to expect that the best measurement results can be obtained with surfaces that have a good diffuse reflection at a proper wavelength. For this reason, Gestel and Co [21] prepared objects of various surface colors: white, red, green and blue. Figure 2.37 shows the results of the spectral analysis. The reflection of white light from a white surface has the highest intensity (line 1). For this reason, all the data sets are normalized with respect to that reflection. The blue line (number 2), green line (number 3) and red line (number 4) represent the spectra of white light reflected from each of those colored surfaces.

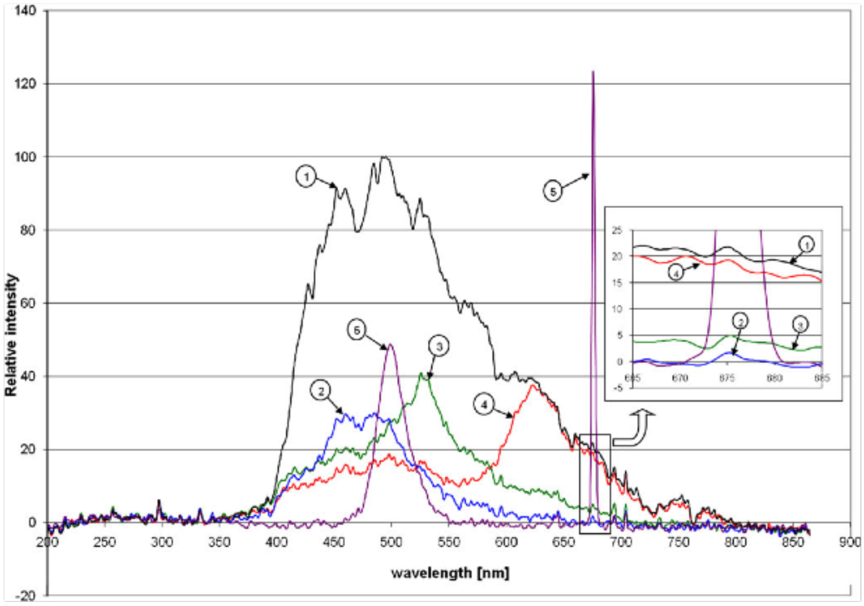

Figure 2.37: Measured spectral response of white light with different coloured surfaces (line 1 white surface, line 2 blue surface, line 3 green surface, line 4 red surface). [21]

The target material is also critical in determining the stability of the measurement [22]. Certain objects or materials such as red-hot metals emit a light at the wavelengths in which red lasers operate. As the target becomes hotter and so emits higher intensity light, the laser measurement fails completely. Blue laser operates at a shorter wavelength, which is far from the red part of the visible spectrum. The blue light is unaffected by the emitted light and it is able to ensure very stable signals. Blue laser sensors are used in the steel processing industry, as well as for automotive brake disc deformation testing and for measuring vibration on exhaust manifolds, but other applications have been discovered. The advantages of triangulation sensors using a blue laser light is not only in the measurement of one-dimensional geometry such as distance, displacement, thickness and vibration, but also in multi-dimensional 2D and 3D inspection such as profile or contour measurements. Furthermore, blue laser sensors have opened up new measurement applications that were not previously possible using red laser sensors. Despite these considerations, for most measurement applications, red laser sensors are still more suitable than blue laser sensors. This is due to a higher intensity and better performance on low reflective surfaces. In addition, suppliers typically offer more variants and options for red laser sensors in terms of sensor performance, measuring ranges and more cost-effective solutions.

2.4.3 Digital vs Analog and CMOS/CCD sensors

The first laser-based displacement sensors based on the laser triangulation principle were introduced in the 1970s in order to overcome the limitations of contact sensors [23]. The first displacement sensors were analog solid-state position sensing detectors (PSDs). Despite the presence of the digital sensors, PSD-based displacement sensors continue to be used today because of their high resolution, high measurement data rates (70 kHz or more) and capability of adjusting laser power in real-time to maintain accuracy for varying surface reflectivity. Analog triangulation sensors do have some limitations, however. In fact they only function when a single laser spot is formed on the imager. This is because, multiple spots coming from reflections or external light, for example, produce inconsistent results. Furthermore, analog displacement sensors provide only an analog output with no ability to process or display the image a to see whether the light is properly focused or if external lights are affecting the measurement.

To overcome PSD limitations, digital imaging-based displacement sensors have been developed. These digital sensors are now widely available with a broad range of specifications and prices. Digital displacement sensors (as well as analog sensors) are data acquisition devices only and in order to analyze data, an external PC or other processing devices are needed. Another advantage of the digital-based sensors is that a video output of the full image can be processed and filtered to remove secondary reflections or other unwanted parts.

In the table 2.3 the differences between analog and digital sensors are summarized.

Table 2.3: Analog vs Digital Sensors

Analog Sensors	1. High Resolution 2. High data rate 3. Capability of adjusting Laser power in real time 4. Provide only an analog output
Digital Sensors	1. Generate digital output 2. Outputs can be processed and filtered 3. Possible reflections can be removed

Digital sensors can work both with CMOS image sensors and CCD sensors [24]. Both CCD (charge-coupled device) and CMOS (complementary metal-oxide semiconductor) image sensors start at the same point: they have to convert light into electrons. The next step is to read the value in the form of accumulated charge. While in the CCD device there is an anolog to digital converter that each analog value into a digital one, in CMOS devices there are several transistors that amplify and move the charge using wires. The CMOS approach is more flexible and each pixel can be read individually. In contrast, because CCD sensors can create high quality images with lots of pixels and excellent light sensitivity and because they have been mass produced and have been around longer, they are the most used. Table 2.4 summarizes these information.

Table 2.4: CCD vs CMOS image sensors

CMOS	1. Every pixel can be read individually 2. Flexible
CCD	1. High quality 2. Excell light sensitivity 3. Cheap

2.4.4 Machine vision based systems for gear measurement

Chodavadiya proposed the use of a machine vision system for the fast and accurate measurement of a spur gear [25]. In this system, a CMOS camera was used in order to capture the image (Figure 2.38).

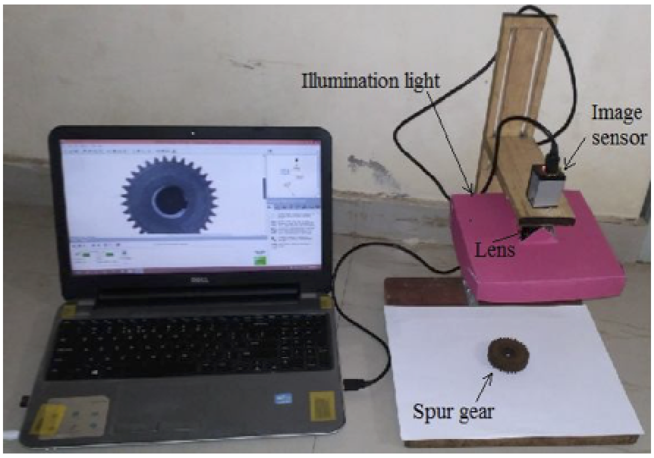

Figure 2.38: Machine vision system [25]

The hardware includes a CMOS sensor and a white LED light as an illumination source. To perform the measurements, the gear is placed on the platform while the camera captures an image and sends the information to a computer. The execution of developed program gives the measurement results. This vision system will be able to compute the pitch circle diameter based on the module and the number of teeth.

To find the outer diameter, a point is generated at the top of the teeth, and by using the intensity transition of this point, the number of teeth are computed (Figure 2.39) . From all these points a circle is formed. The same procedure can be followed both for root and tip circle diameter in order to compute the dedendum and addendum. Once this information is avaiable, the pitch circle can be drawn.

Using these points, teeth thickness on the pitch circle and circular pitch are calculated. The accuracy of the system depends on the size of the gear to be measured. For smaller gears, the accuracy is higher and viceversa. Therefore, this vision system can have information just on the tooth thickness and pitch circle but not on lead and profile deviation.

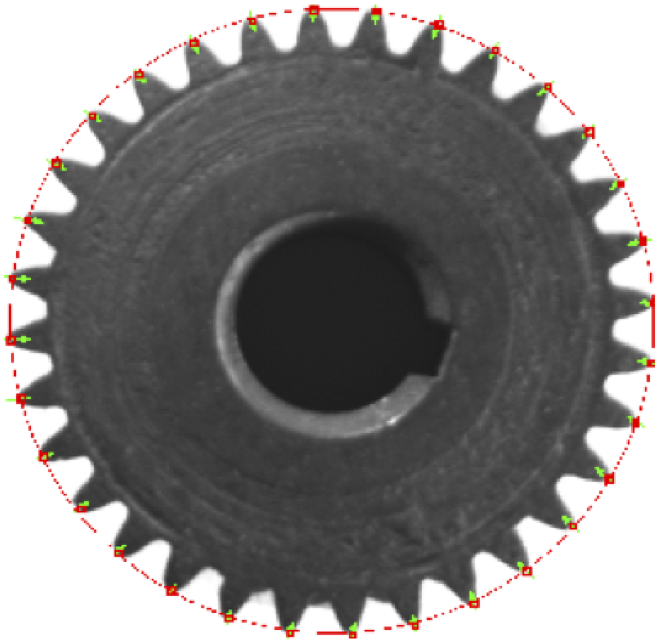

Figure 2.39: Points generation for outer circle [25]

The proposed system was verified by using vernier caliper and gear tooth caliper of 0.02 mm least count. A comparison between the actual and the calculated values of gear parameters was done as well. These differences range from 0.3 mm to 0.15 mm.

2.4.5 Application og a 3D geometric measurement on a large gear

In the research done by Freyberg et al. [26], optical laser scanners have been compared with a tactile measurement method. The measurements were done on a large gear for wind energy application with a diameter of 955 mm and module of 10 mm (Figure 2.40).

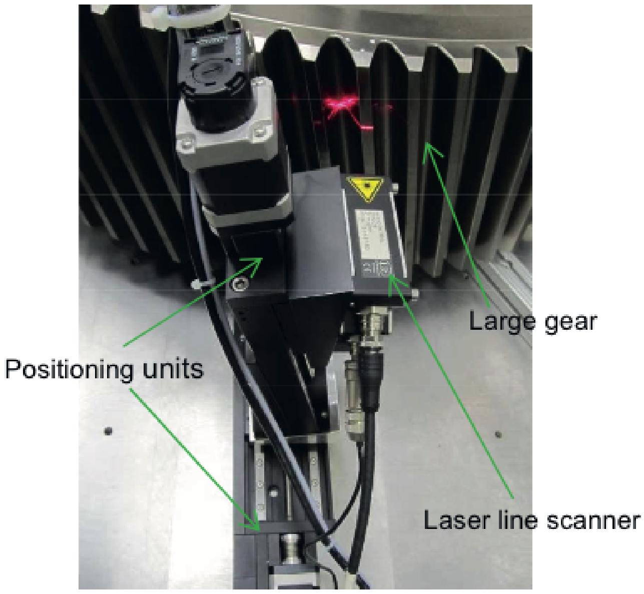

Figure 2.40: Gear and laser scanner configuraton [26]

The laser used shows a depth resolution of 2 μm with 1280 points at a line width of 25 mm, with the lateral resolution amounting to 19.5 μm. The surface was detected by 3500 individual profile lines (acquisition rate of laser up to 2000 lines/s), which corresponds to roughly 4.48 million measurement points. The complete scanning process with the laser line sensor amounted to 2 minutes. In comparison, the measurement time for tactile detection with the same point density would take 190 hours. However, laser line scanners have limited accuracy due to the difficulties of measuring shiny and reflective surfaces. During the data collection, a complete detection of the tooth flank surface was obtained (Figure 2.41).

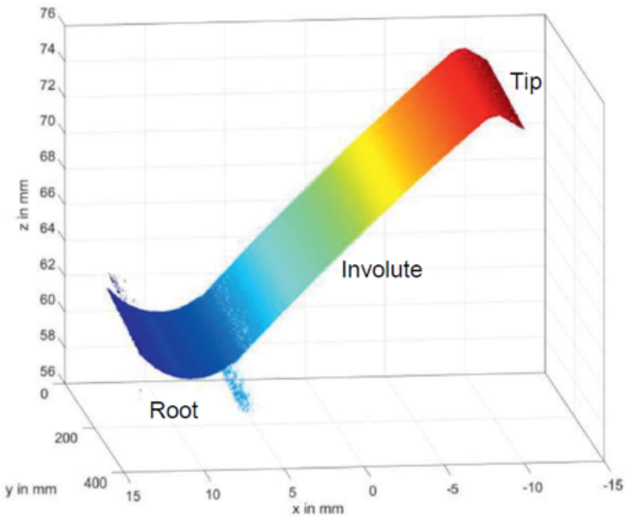

Figure 2.41: 3D surface of a tooth flank [26]

A negligible region, that cannot be detected, is in the transition of the profile line into the root area. The reason is the occurrence of multiple reflections, which disturb the measurement. However, the region is negligible since it is not important for the functional inspection of a gear.
In conclusion, the laser line triangulation sensor studied has a great advantage since a measuring time of <10 ms for one profile line is available with 1280 measuring points which are detected simultaneously.
Other researches has been conduced by Younes et al. [27]. The scope of their research was to use a non-contact system to measure the thickness, pitch and tooth height of a spur gear. The accuracy they achieved was around 5 μm and the measurement time was 1 min. The system, based on optical obscuration, can measure gears with different modules and numbers of teeth. The measured dimensions were correlated with those obtained with other well-established techniques and were found to be in good agreement. In the second part of their research [28] they used a system based on optical triangulation in order to measure the tooth flank. This second system was integrated with the first one, and the measurement of all parameters took less than 1 minute.

2.5 Introduction to Gear vibration sources and Ghost Noise

A low noise level is starting to became of greater importance for the modern gearbox. Because gearbox noise is tonal, its frequency spectrum consists of several sinusoidal components that can be divided into the following effects: [29]

- low harmonics of the shaft speed originating from imbalance or shaft misalignment resulting in low frequency vibration;

- harmonics of the base tooth meshing frequency. They are generated by the time variation of tooth-contact stiffness in the mesh cycle, the inaccuracy of gears in mesh, and non-uniform load and rotational speed;
- ghost (or strange) components due to errors in the teeth of the index wheel of the gear cutting machine, especially gear grinding machines. These ghost components disappear after a running-in;
- components originating from faults in rolling-element bearings which usually emit low levels of noise.

Among these effects, there is interest in tooth meshing frequencies and especially in the ghost frequencies. During the gear manufacturing process, and especially due to cyclic error in the master worm wheel drive in the grinding machine use for the finishing operation, various gear errors such as profile error, pressure angle error, lead error and surface undulation, are generated [30][31]. These errors generate vibrations at meshing and non-meshing frequencies. The meshing frequency is given by the product of the gear rotational speed in Hz and the number of teeth [29]. The vibration at meshing frequency is generated by errors common to all teeth and their amplitude is larger than the vibration at non-meshing frequency.
The problem is that the amplitude of non-meshing frequencies is amplified by resonance effects and becomes larger with respect to the first category, causing severe noise problems. Because these vibrations are hardly detected and not related to nominal geometry deviation, they are also known as "ghost noises", or phantom noises.
What is known until now is that, period waviness or cyclic undulation of the teeth surface generated during the manufacturing process causes “ghost noise”. The diamond grains on the dressing wheel causes undulations on the grinding wheel surface and when grinding the gear, also the gear flank surface will have undulations (waviness). These undulations typically have wavelengths of about 0.5 mm and amplitudes of approximately 4 μm. The frequency of the ghost noise is a non-integer order of mesh frequency. Since the ghost noise comes from a geometrical error, it is not influenced by load [32].

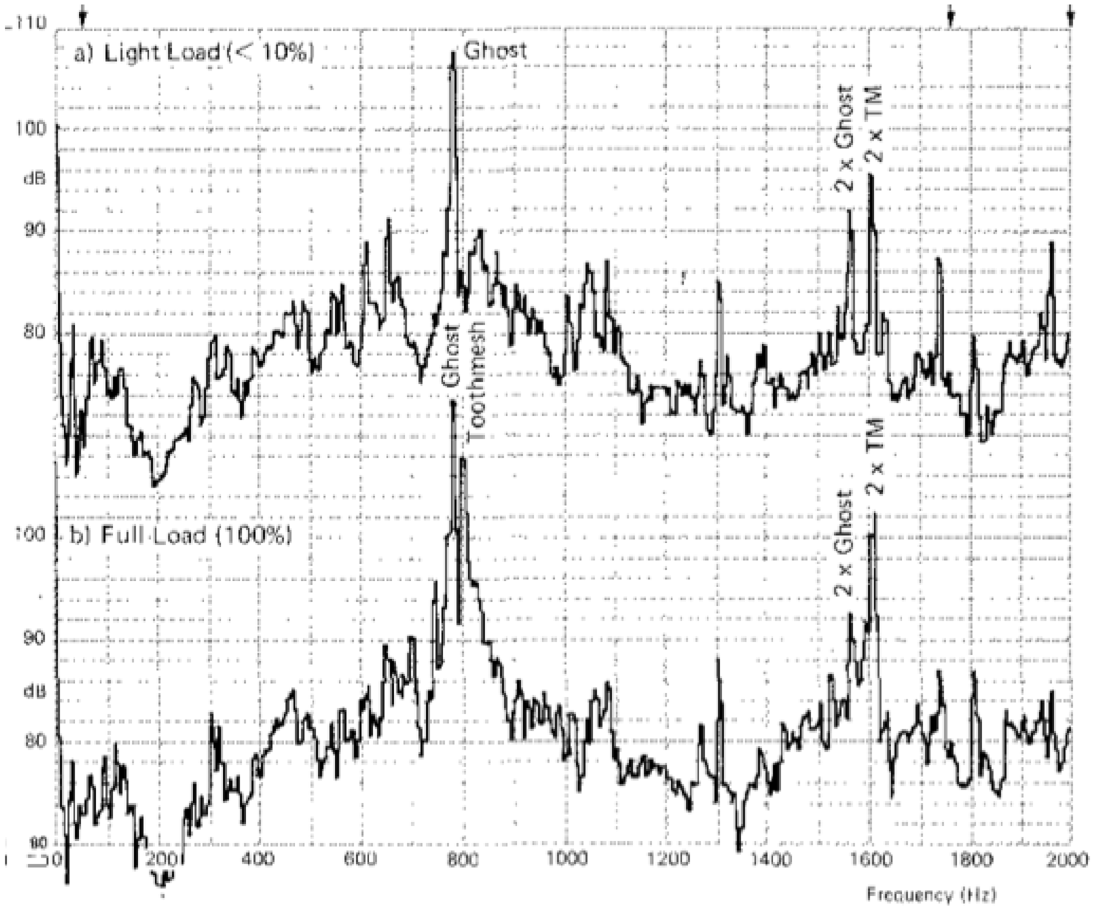

Figure 2.42: Effect of loading on ghost component [32]

From the Figure 2.42, it is possible to see that, going from 10% of full load condition to full load, the ghost component has changed by only 6 dB while, the meshing component, has increased of 21 dB.

2.6 Chapter Summary

The main points that can be derived from the literature survey are:

- Contact metrology has shown limits in the speed of the inspection;
- Non-contact systems, equipped with digital sensors and CCD cameras, can potentially accelerate the data acquisition rate up to 100 times faster than contact machines;
- Problems caused by multiple reflections may occur during the measurement of the gear root;

- Gear grinding can create undulations in the gear profile. These undulations have been indicated as the cause of the Ghost Noise. Furthermore, this strange noise is load independent and its intensity decreases after a running-in phase.

Chapter 3

Evaluation of the Urano HC-N400 Non-Contact Metrology System

Chapter 3 evaluates the performance of the Emera and Urano machines. First, a detailed description of the gear mounting procedure required for tactile measurement systems is provided. The performance ensured by the machine and the procedure needed to obtain them, are shown.
Second, the study of the Urano is laid out using the following points:

- Urano machine description;
- Experimental tests needed to properly characterize the Urano system;
- Analysis of the main inspection charts;
- Agreement between the Emera and the Urano.

3.1 Emera's Contact Metrology System

Gear-based tactile measuring methods dominate today's industrial solution for gear inspection. Today, however, the industry is facing the challenge of micrometer level accuracy required by gear designers and manufacturers.
This technology performs measurements using a touch probe system that is able to perform geometrical measurements. The probe, a high precision switch, is the heart of the system and, when integrated into the machine manufacturing process, can determine workpiece and/or tool sizes and identify part locations. The system utilizes the machine to move the probe along a programmed path. Once the stylus makes contact with the part or tool, a signal is generated which is then transmitted to the machine. The gear measuring instrument (GMI) is then able to store the relevant axis positions and to elaborate the part geometry by means of dedicated probing software. Figure 3.1 shows a GMI machine with a rotary table.

Figure 3.1: Gear Measuring Machine (GMI)

3.1.1 Methodology

Using a contact machine, the gear, mounted on a harbor, is only allowed to rotate. The touching probe, however, can move both vertically and horizontally in a such way as to approach the gear for the beginning of the inspection process. Generally, both for pinion and sun gears, the stylus shown in Figure 3.2 is used. Different dimensions of the head ball are also used in case of "green" gears (gears on which only hobbing maching has been done) or finished gears. For the first type, a 1 mm head ball is mounted on the machine; for the second, the head ball is smaller (0.8 mm). In fact, for "green" gears, too much accuracy is undesirable because of the rougher surface which would output a chart that would be impossible to read. A third type of head ball (0.5 mm) is used for the calibration operation. Prior to the beginning of the measurements, it is absolutely crucial to calibrate the probe in order to have a precise inspection. During this operation, the stylus touches the reference object at different points. This reference tool is an extremely precise, manufactured ball with a known diameter (referred to as a datum ball). The exact dimensions of the ball are the inputs for the measuring software. This operation generally takes 5 minutes and under

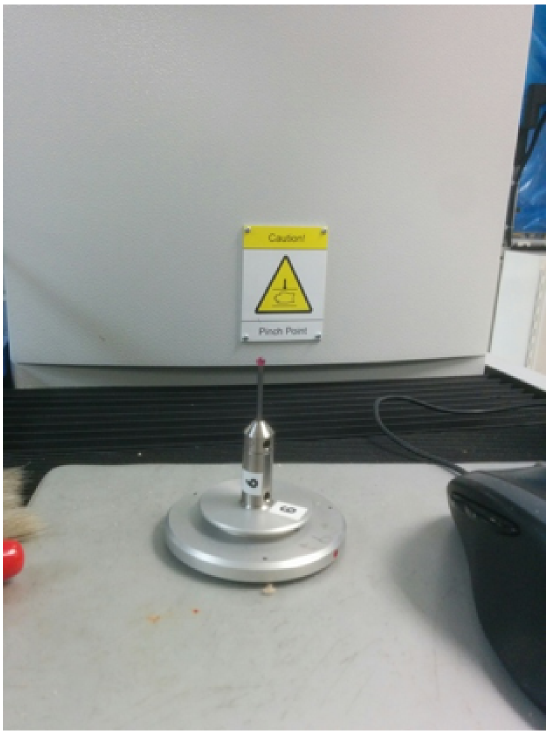

Figure 3.2: Touching Probe used for external Gears

normal circumstances, is done no more than twice per day.
The same probe cannot be used for annulus gears because of the inability of the probe to reach the internal teeth. Consequently a different Stylus shape is used (Figure 3.3).

Figure 3.3: Contact Probe for Internal Gears

In every metrology system, the correct positioning and orientation of the measured part with respect to the measuring tool is essential in order to guarantee a perfect and unequivocal measurement. With a GMI, both pinion and sun gears are fixed relative to the contact probe using a Hydraulic expansion arbor (Figure 3.4).

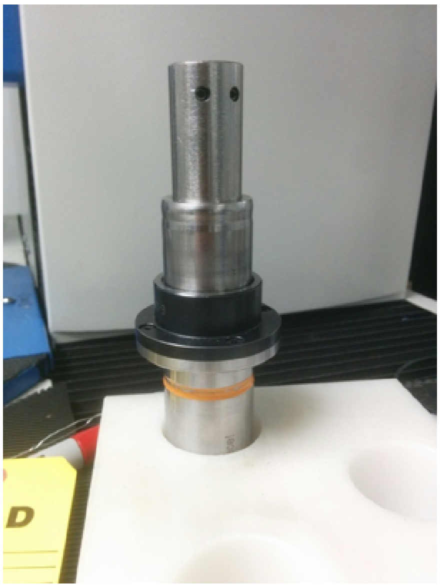

Figure 3.4: Expansion Arbor

The basic concept of an expansion arbor consists of expanding or contracting a steel sleeve within the elastic limits of the material by means of hydraulic pressure. In doing so, the axial center-line of the work-piece is perfectly centered and clamped (Figure 3.5)[33]. Each holding device is composed of a center body with a hydraulic system, a piston and a sleeve. The piston, actuated by a screw, advances in a chamber and causes an increase in the pressure of the hydraulic fluid. Because of this pressure increase, the fluid moves through the ports exerting pressure under the steel sleeve. This sleeve is further compressed radially by the work-piece which results in the work-piece being locked in place. The Arbor is then

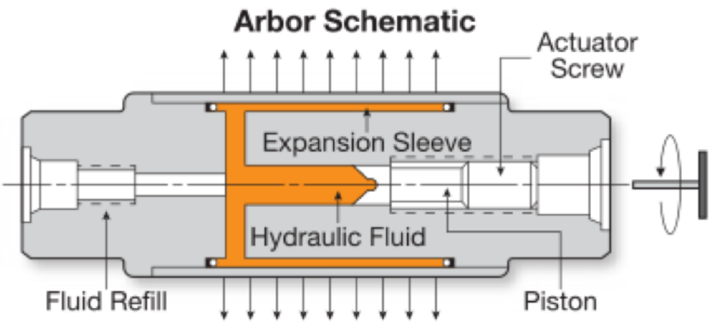

Figure 3.5: Expansion Arbor Working Principle

fixed between an upper and lower center in the inspection machine. In order to be sure of the perfect positioning of the gear and to avoid the possibility of runout problems due to an eccentricity of the center and the arbor, these two components are checked daily. Standard mounting procedures are also used in order to ensure that gears are always mounted in the same direction and there is no confusion between left and right tooth flanks when a chart is read. For the pinion of the second planetary set of an automatic transmission gearbox, a groove is designed on each of the tooth tips. These grooves must be in the lower part of the gear. In the fourth pinion as well as for sun gears, the standard rule is to find the larger boss in the upper part of the gear (Figure 3.7, Appendix G). Figure 3.6 shows a complete mounting set for a Pinion 4.

Figure 3.6: Pinion 4, Mounting Procedure.

Figure 3.7: Gear Mounting, Pinion 4.

A different tool is used to fix the annulus gears: the three jaw chuck. The chuck is a specialized clamp system used to hold objects with radial symmetry. The chuck has three jaws that are arranged in a radially symmetrical pattern and their goal is to hold the tool or the workpiece. The rule for the mounting procedure of an Annulus is that the boss must be in the lower part of the gear. One of the biggest problem with the chuck is that, by tightening the gear, it could cause pressure on the lower boss that will permanently alter the shape of the part.
Once the gear is completely fixed, each measurement must be referred to a precise reference system. For both pinion and sun gears, the datum references are the bottom face and the bore face (internal diameter for a sun gear). For an annulus gears, the datum references are determined by performing an index measurement on 10 teeth and a sweep of the top face defined the part's centreline.

3.1.2 Performance Evaluation of Contact System

Typically, in a high volume gear lab, CMM and GMI machines are used to perform a standard measurement as described in subsection 2.1.3. The time needed for this analysis typically takes around 4-5 minutes for pinion gear, but increases with the number of teeth:

- 7-8 minutes for a sun gear (pitch diameter 103.480 mm, No. of teeth 86)
- 12-13 minutes for an annulus gear (pitch diameter 122.406 mm, No. of teeth 94).

Generally speaking, only about 1% of all gears that are manufactured are checked. When a faulty gear is found, all the gears between the previous good gear and the faulty one are analyzed so that further bad gears are not put on the market.
Sometimes, a full topography of the entire flank of a gear may be needed in the case of a particular noise problem that cannot be identified during a standard inspection. By using contact technology, this kind of inspection will require several hours.
Calibration tests are performed annually on the machine by using a proper gear artifact or a master gear. These tests qualify the tool in terms of accuracy and repeatability [2][3]. According to the standard VD1/VD2 2612 (Appendix D):

- The repeatability is of 0.1 μm;
- The accuracy falls into Group 1 (1 μm).

These values have been obtained by performing a measurement of profile and lead in 3 teeth and by repeating the measurement 3 times. The measured deviations are compared with those of the master gear. The differences between these two values define the machine's accuracy. The repeatability is calculated by determining how much the values obtained in the three repeats differ from each other.
No significant maintenance of the machines is required. Generally, on a daily basis, operators

should monitor whether unusual noise comes from the probes and, if so, should calibrate them. The compressed air supply should be checked on a weekly basis and the fixture components should be cleaned. Other maintenance operations such as the replacement of filters etc. are done two or three times per year.
Regarding the cost related to the maintenance machine, each probe must be changed every two to three years, or sooner if they are broken accidentally by coming into contact with a gear during operation.

3.2 Urano HC-N400 Non-contact metrology System

Urano is the first supplier to have developed a non-contact-sensor optical system with special cylindrical lenses for laser scanner light emitters and an optical system that is able to capture high precision images (Figure 3.8)[6]. The machine, named HC-N400 which stands for high speed non contact laser metrology system, was strongly requested for use by an Asian car manufacturer who is currently using around twenty HC-N400 machines in their gear labs. Other German companies are also investigating the possibility of using this technology.

The laser scanner has an acquisition rate of 120,000 points per second, and a complete

Figure 3.8: Urano HC-N400 [6]

inspection of all tooth surfaces of a gear can be completed in 5 minutes. Apart from a complete 3D image of the surface (Figure 3.9), tooth profiles and lead errors can be displayed in the same way as in a contact inspection. Moreover, information on surface waviness and surface roughness can be obtained. Urano HC-N400 is suitable for the measurement of hypoid gears, bevel gears, helical gears, spur gears, internal gears, splines, turbo compressors, wings and oil seals.

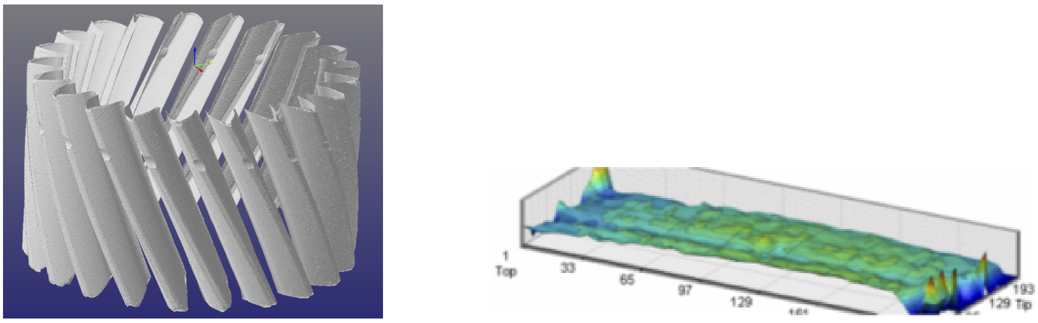

(a) Gear 3D Image (b) Jaw Chuck for Gear Holding

Figure 3.9: Surface Analysis performed by Urano [6]

Of the main suppliers able to integrate a laser sensor to their machine, Urano is the only one also able to perform measurements on internal gears. This is because of a particular laser head (Figure 3.10a) and laser arm that have a nearly unlimited angle of rotation and can guarantee that the laser is able to scan a very wide area covering both the top and side surfaces, and even the bottom surfaces of parts. The gears are held by a Jaw Chuck that is supported by a rotary stage (Figure 3.10b). Urano's laser displacement sensor is a digital

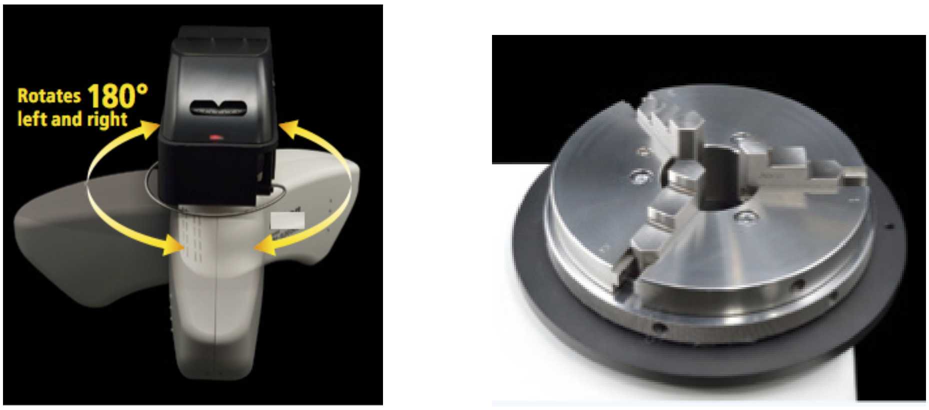

(a) Urano Laser Head (b) Jaw Chuck for Gear Holding

Figure 3.10: Urano Laser and Jaw Chuck [6]

laser. With respect to the analog sensor, the digital one is capable of acquiring data such that it can display the image on a PC, where the image can be processed and filtered in order to remove secondary reflections or other unwanted parts of the image, or to isolate specific regions of interest in the recorded area.
Interest in this innovative metrology machine is very high. As such, it is important to review the Urano's capabilities and to assess the feasibility of introducing the Urano machine in Gear Metrology Labs in which contact machines are currently in use.

3.2.1 Methodology

The scope of the following tests is to review the inspection capability of the Urano Machine and to compare the inspection results on several 9-speed gear types provided by Omega between the Emera (K) and the Urano HC-N400 (N). The following 9-Speed Transmission gears have been provided to Urano for measurements (the number indicates the different planetary set in the transmission (section 2.1.2)):

- Five ground pinion 2 (base circle: 25.83 mm);
- Five ground pinion 4 (base circle: 41.86 mm).

Inspections were performed on the profile, lead, index and runnout of 4 teeth. Furthermore, 3 repeats were performed on three pinion 2 gears, and 3 repeats on three pinion 4 gears, for a repeatability evaluation. All the gears that were analyzed have been through the grinding process and are theoretically ready to be mounted on a transmission. Every "correlation" measurement has been analyzed by using a Bland and Altman plot (Appendix A)[34][35][36]. This statistical tool is able to graphically study the difference between the results obtained by the two machines and to define the agreement interval with a 95 % of confidence level. It is important to note that with the Bland and Altman Plot all the gears per type will be included in the results.
On each gear, 12 lines for the profile and lead deviation (6 for the left flank and 6 for the right flank) were measured. Consequently, 60 numerical values for each profile and lead parameter are available (section 2.1.3). The correlation coefficient will not be indicated because, for the most part, it is inconsistent with the obtained results. Instead, normal distribution tests have been done with positive results. The Bland and Altman axes have not been normalized in order to not loose the effective differences between the two machine's output.

3.2.2 Performance Evaluation of Urano non-contact Contact System

Chart Analysis

As explained in Section 3.1.1 and in Appendix G, for a correct mounting orientation of pinion 2, a groove is designed of the each tooth tip (Figure 3.11).

Figure 3.11: On the pinion 2 grooves for a correct mounting operation on the machine holder.

Generally, for a lead inspection of the first tooth, three traces are analyzed (Figure 3.11 and Subsection 2.1.3).

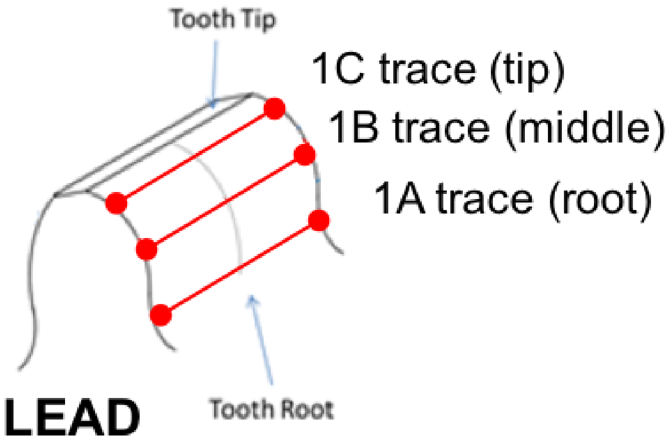

Figure 3.12: Traces evaluated on the first tooth for a lead inspection.

Using contact inspection, no problem was found on trace "1C". Since the laser didn't scan only a line but a cloud of points, the trace "1C" has been affected by these grooves. The result is the presence of spikes in both the left and right flank on each lead trace "1C" (Appendix F and Figure 3.13).

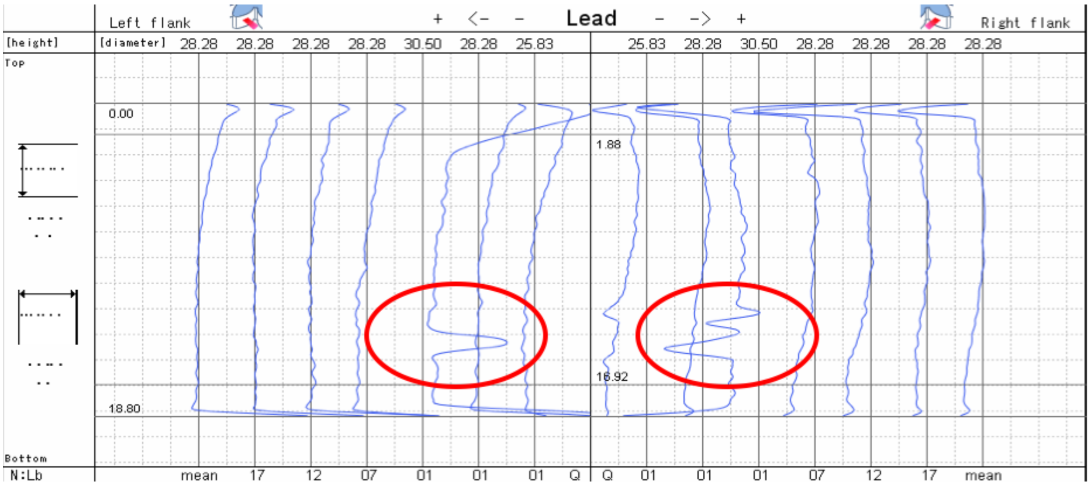

Figure 3.13: Urano lead chart: the presence of grooves causes a spike on the trace 1C

These spikes have a large effect on the lead form deviation measurement ("ffb"). When the Urano moves down the scanned line by just a few millimeters, the spikes disappear. Another huge limitation of the HC-N400 on the measurement of Pinion 2 is noticeable on the root of every tooth. This is because of the fact that the light has been affected by the tip of the closest tooth during the scanning operation. The same problem has been found by using Zygo (Subsection 4.2 and Appendix F). No problems were found during the evaluation of Pinion 4. With this gear type, the deviations measured by Urano tend to be a few microns higher on average. This difference could be attributed both to a higher accuracy of the laser machine and the use of a different filter. Generally, both contact and non-contact metrology machines can use different filters in order to have smoother traces and to avoid losing information due to the presence of waves on the evaluated line. Naturally, by having a smoother line, the measured deviation is lower. By looking at both the Urano and Emera charts, it seems that the latter used a higher filter effect (Figure 3.14a, Figure 3.14b and Appendix C).

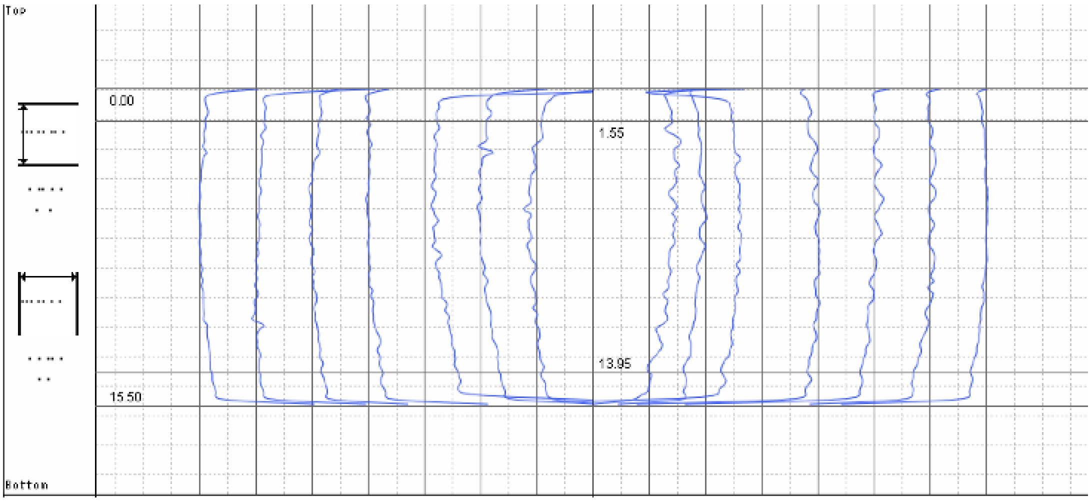

(a) Urano measurement of a Pinion 4

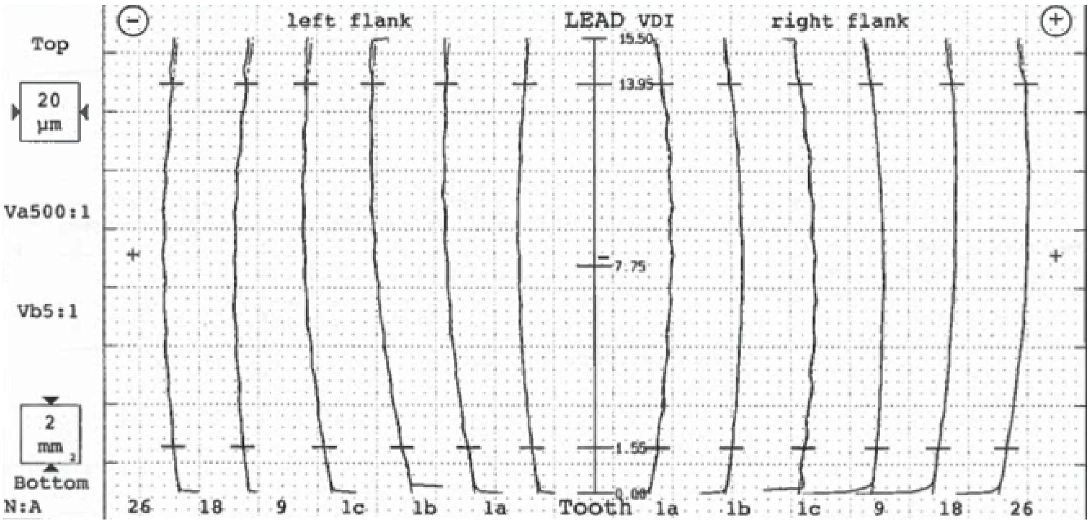

(b) Emera measurement of a Pinion 4

Figure 3.14: Evaluation of the same Pinion 4 done by Urano and Emera: the differebces could be due to the use of a different filter

Data Analysis: Pinion 2

Both profile form and slope deviation measured by the Urano (N) are higher with respect to the ones measured by the Emera (K) (Figure 3.15, Figure 3.16). These differences go up to 14 microns on average in the case of the profile slope deviation (Table 3.1). This is due to the fall-off present in every profile trace. By contrast, the discrepancy in the measurement of crown deviations are smaller (Figure 3.17 and table 3.2).

Furthermore, a precise bias is unable to be defined because the average values between the differences range from 3 up to 15 microns.

Table 3.1: Descriptive Statistics: Profile Slope deviation (μm) on Pinion 2.

Variable	Count	Mean	Standard Deviation	95% LCL of Mean	95% UCL of Mean
N	60	2.67	17.93	-1.96	7.30
K	60	-11.86	18.35	-16.90	-7.12
Difference	60	14.53	11.65	11.52	17.54

Table 3.2: Descriptive Statistics: Crown deviation (μm) on Pinion 2 .

Variable	Count	Mean	Standard Deviation	95% LCL of Mean	95% UCL of Mean
N	60	3.91	2.68	3.22	4.60
K	60	2.86	1.78	2.40	3.32
Difference	60	3.12	0.6	0.25	1.85

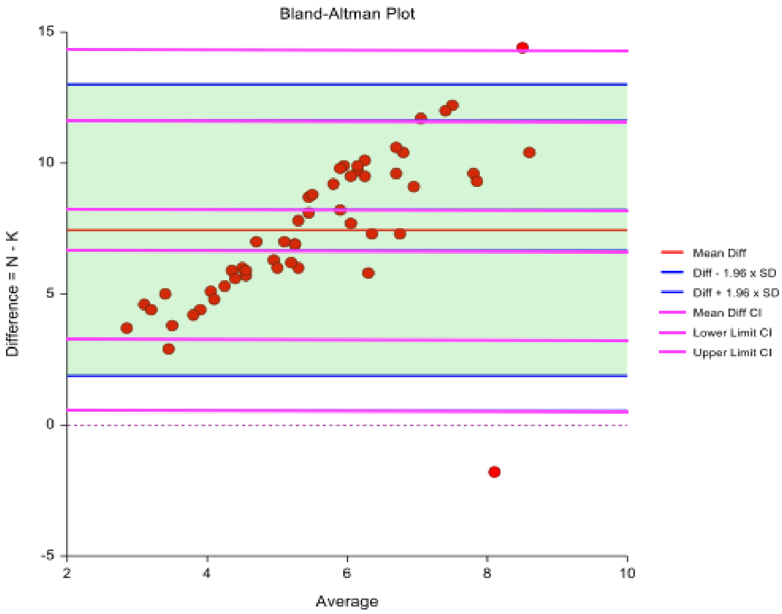

Figure 3.15: Bland and Altman plot: Profile Form Deviation (μm) measured by Urano (N) and Emera (K) on five Pinions 2

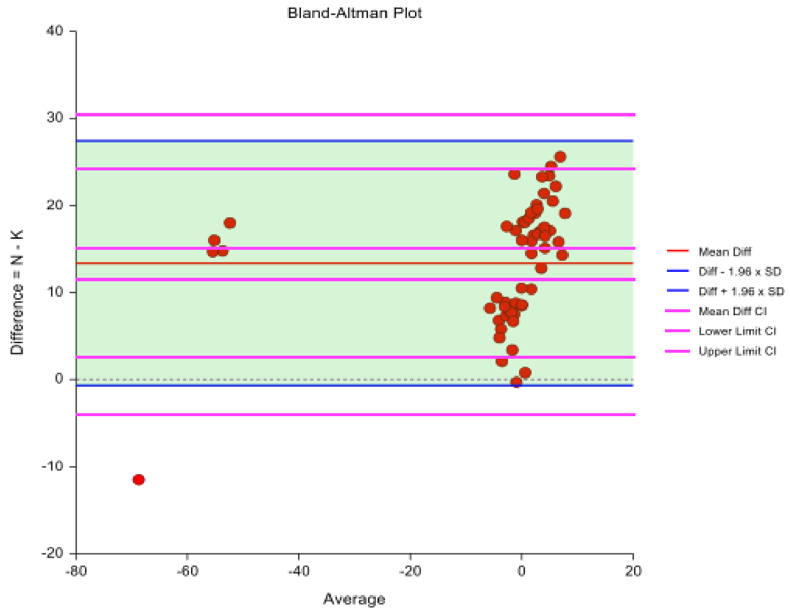

Figure 3.16: Bland and Altman plot: Profile Slope Deviation (μm) measured by Urano (N) and Emera (K) on five Pinions 2

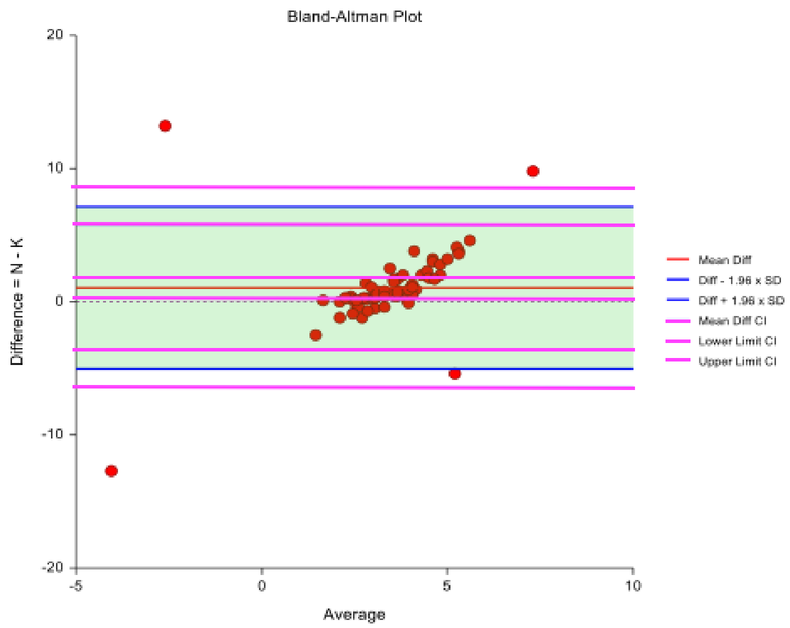

Figure 3.17: Bland and Altman plot: Crown Deviation (μm) measured by Urano (N) and Emera (K) on five Pinions 2

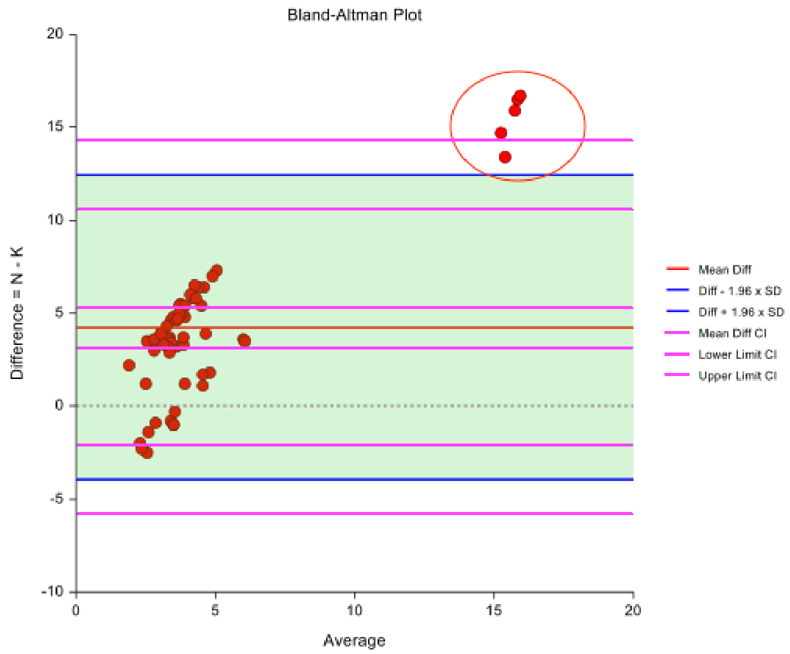

Figure 3.18: Bland and Altman plot: Lead Form Deviation (μm) measured by Urano (N) and Emera (K) on five Pinions 2

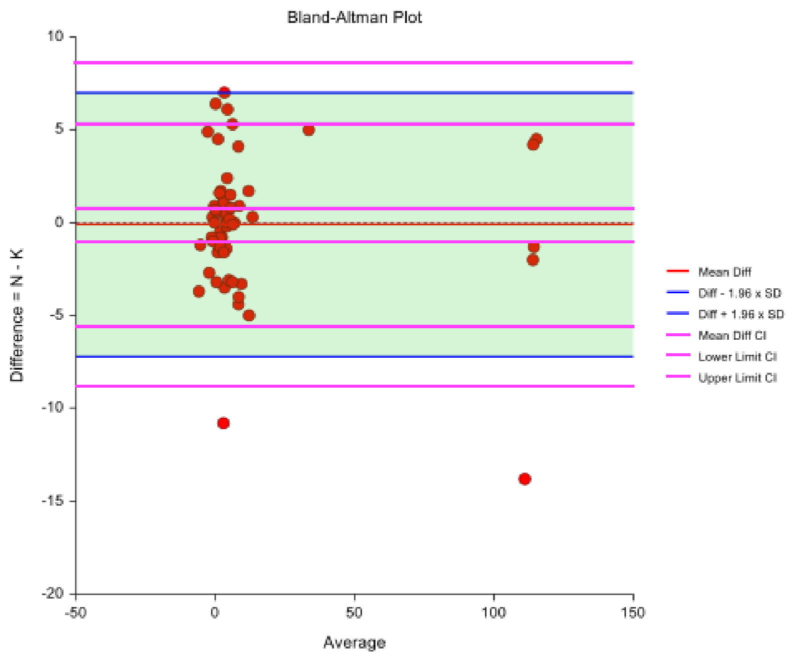

Figure 3.19: Bland and Altman plot: Lead Slope Deviation (μm) measured by Urano (N) and Emera (K) on five Pinions 2

Table 3.3: Descriptive Statistics: Lead form (μm) deviation on Pinion 2 .

Variable	Count	Mean	Standard Deviation	95% LCL of Mean	95% UCL of Mean
N	60	11.67	10.53	8.95	14.39
K	60	2.52	2.44	1.89	3.15
Difference	60	9.50	0.6	6.70	11.62

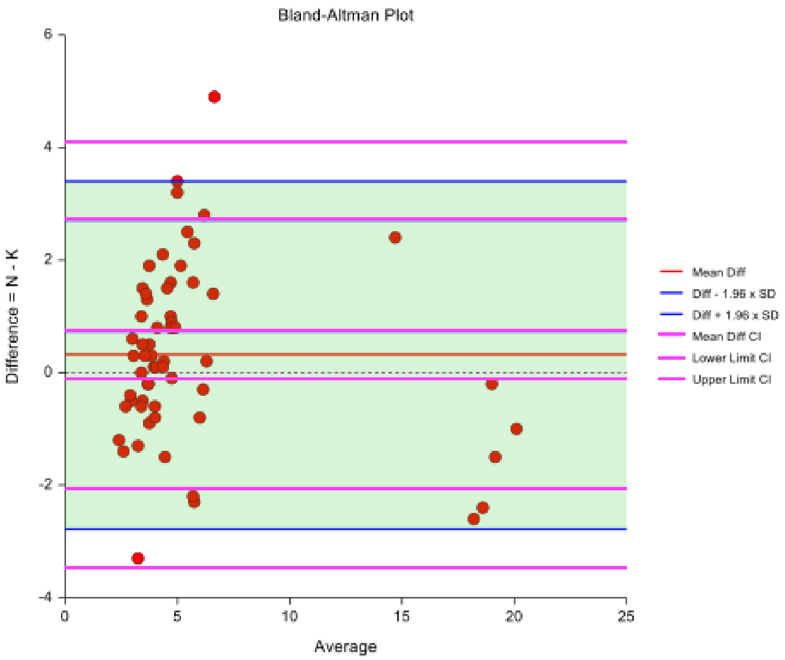

Figure 3.20: Bland and Altman plot: Barelling Deviation (μm) measured by Urano (N) and Emera (K) on five Pinions 2

By evaluating the lead deviation, the large differences between the Urano (N) and the Emera (K) are in the form of the deviation measurements (Figure 3.18 and Table 3.3). It is important to note that the underlined peaks in Figure 3.18 are due to the presence of the grooves along the trace measured by the Urano.
Several repeat measurements (3 repeats on two different gears) have been done both by the Urano and the Emera (Table 3.4 and Table 3.5). The results show a better performance by the contact machine of almost one order in the profile evaluation. Therefore, repeatability on lead measurement of the two machines are comparable.

Table 3.4: Urano (Emera) repeatability in μm: Pinion 2, Profile.

ff α	**fh**α	**C**α
0.3 (0.03)	0.27 (0.03)	0.15 (0.04)

Table 3.5: Urano (Emera) repeatability in μm: Pinion 2, Lead.

ff β	**fh**β	**C**β
0.62 (0.1)	0.35 (0.3)	0.83 (0.1)

Data Analysis: Pinion 4

The agreement between the two machines during the measurement of Pinion 4 was better than the one obtained with the Pinion 2. As explained in subsection 3.2.2, generally, the differences measured in profile and lead form deviation can be due to both a filtering problem and a higher accuracy of the Urano. Numerical values of these differences are reported in the Table 3.6 and 3.7

Just as with pinion 2, a bias in the differences measured by the two machines cannot be defined in the case of pinion 4 either. The Emera measured a higher profile slope deviation, crown deviation, lead slope deviation and barelling deviation (form Figure 3.22 to Figure 3.23, Figure 3.25 and Figure 3.26). The reason for this phenomenon is unknown.

Table 3.6: Descriptive Statistics: Profile form deviation (μm) on Pinion 4.

Variable	Count	Mean	Standard Deviation	95% LCL of Mean	95% UCL of Mean
N	60	4.46	1.29	4.12	4.79
K	60	2.22	0.42	2.11	2.33
Difference	60	2.23	1.27	1.90	2.56

Table 3.7: Descriptive Statistics: Lead form deviation (μm) on Pinion 4.

Variable	Count	Mean	Standard Deviation	95% LCL of Mean	95% UCL of Mean
N	60	5.17	2.18	4.61	5.74
K	60	1.21	0.34	1.12	1.29
Difference	60	3.97	2.18	3.41	4.53

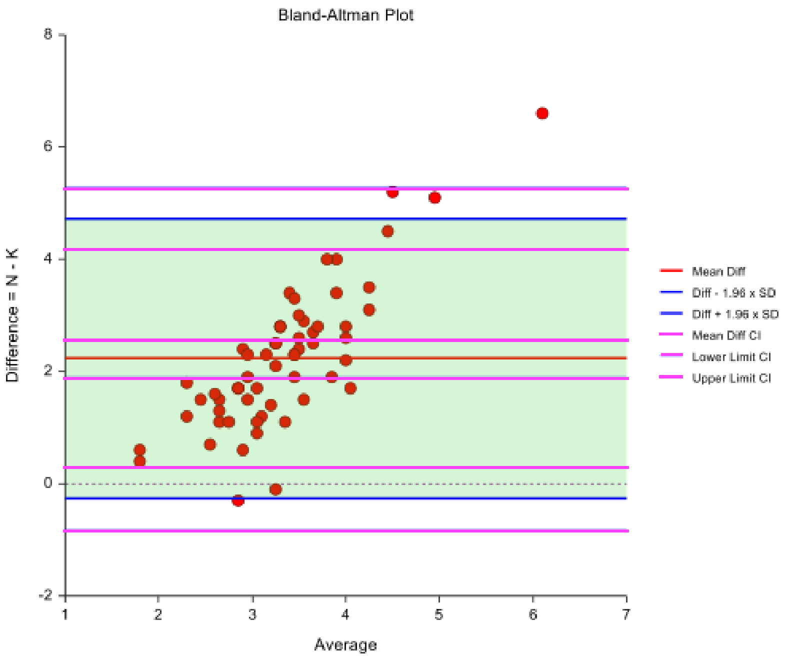

Figure 3.21: Bland and Altman plot: Profile Form Deviation (μm) measured by Urano (N) and Emera (K) on five Pinions 4

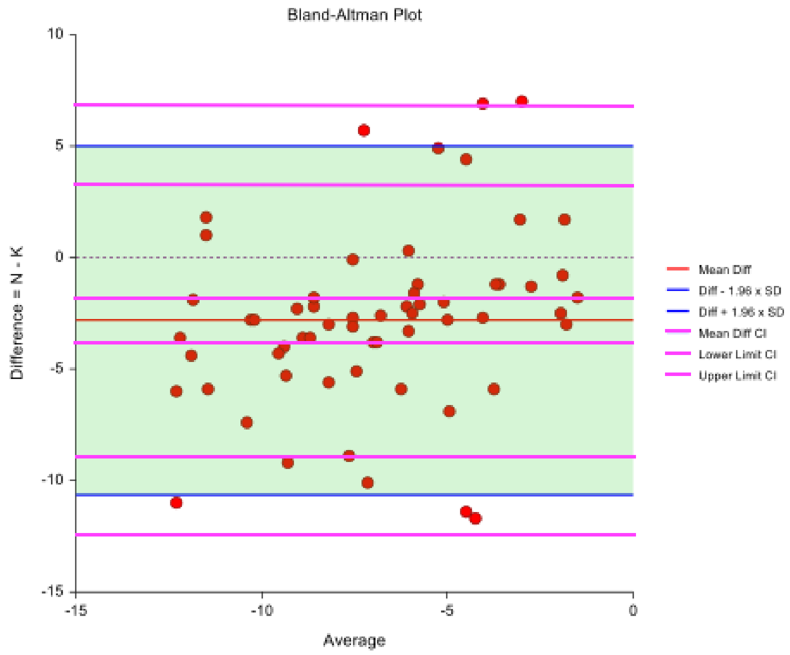

Figure 3.22: Bland and Altman plot: Profile Slope Deviation (μm) measured by Urano (N) and Emera (K) on five Pinions 4

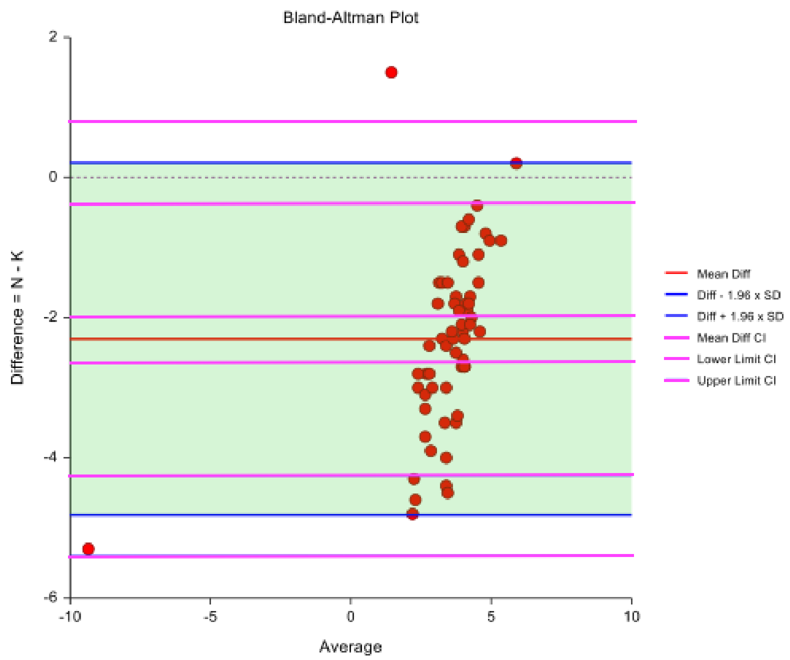

Figure 3.23: Bland and Altman plot: Crown Deviation (μm) measured by Urano (N) and Emera (K) on five Pinions 4

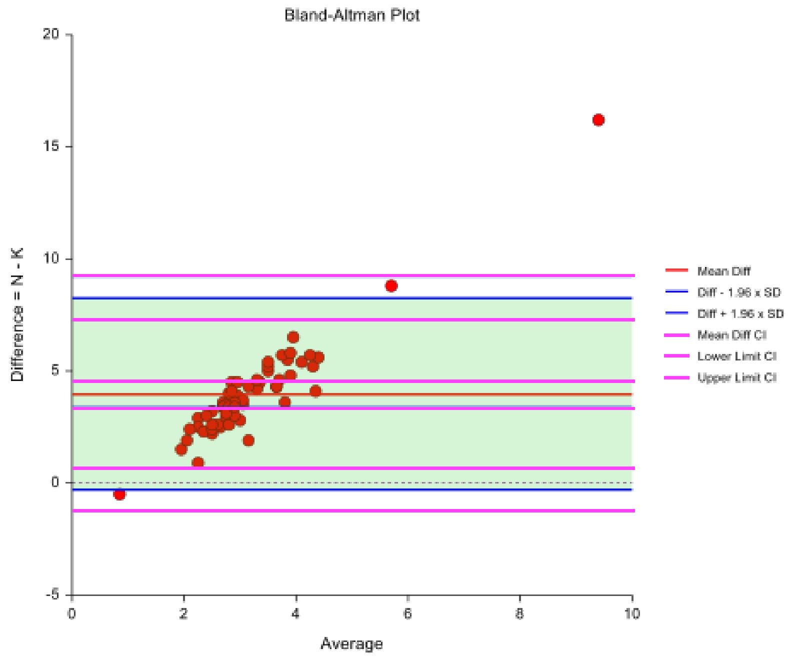

Figure 3.24: Bland and Altman plot: Lead Form Deviation (μm) measured by Urano (N) and Emera (K) on five Pinions 4

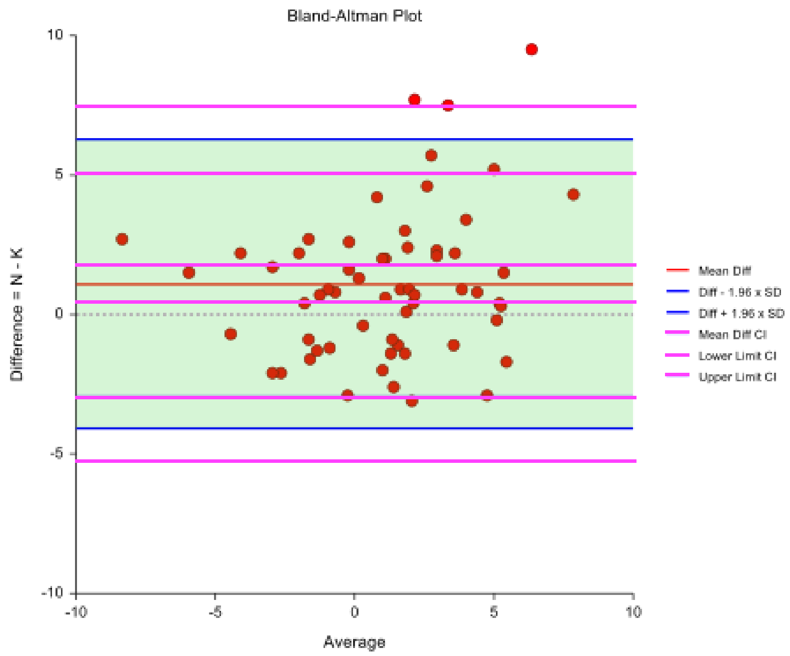

Figure 3.25: Bland and Altman plot: Lead Slope Deviation (μm) measured by Urano (N) and Emera (K) on five Pinions 4

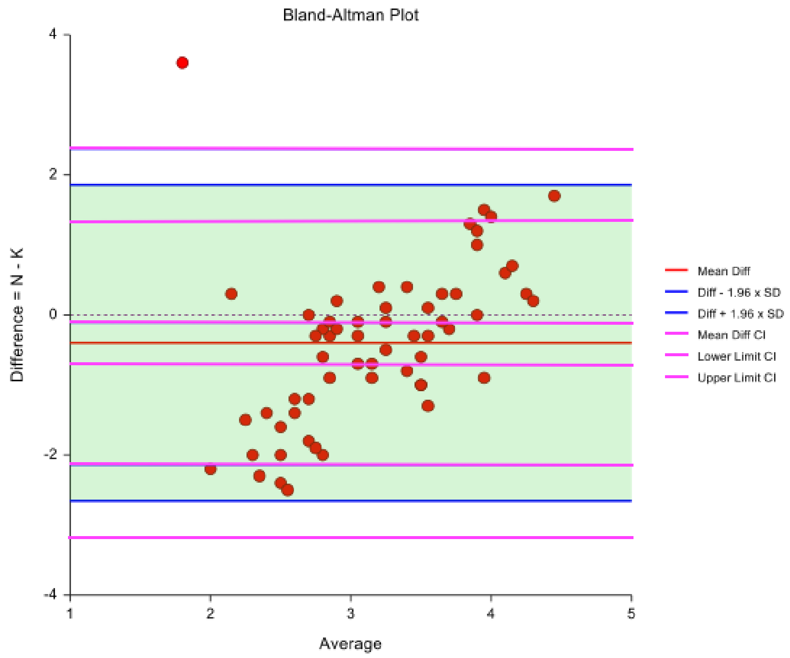

Figure 3.26: Bland and Altman plot: Crown Deviation (μm) measured by Urano (N) and Emera (K) on five Pinions 4

An anomalous point was recorded and is visible in Figure 3.24. This is due to the presence of a single spike recorded on the Urano inspection chart (Figure 3.27). This peak could be due to the presence of dust on the gear.

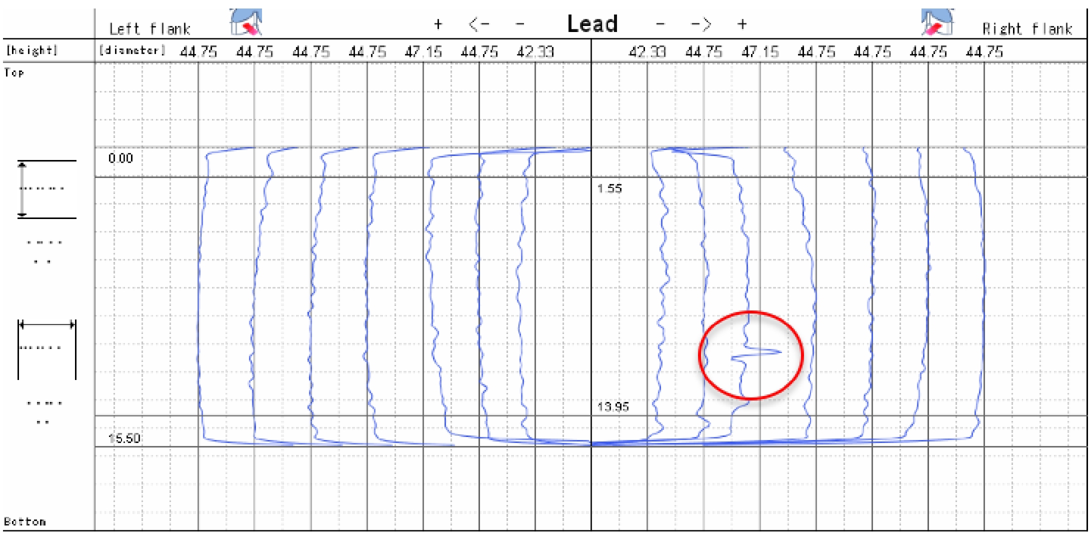

Figure 3.27: Anamalous peak Recorded by Urano during the Lead Evaluation

The same repeatability measurements were also performed on Pinion 4. The Emera was

Table 3.8: Urano (Emera) repeatability in μm: Pinion 4, Profile.

ff α	**fh**α	**C**α
0.17 (0.06)	0.37 (0.07)	0.15 (0.08)

Table 3.9: Urano (Emera) repeatability in μm: Pinion 4, Lead.

ff β	**fh**β	**C**β
0.6 (0.5)	1.2 (0.1)	0.65 (0.25)

able to achieve better results here as well (Table 3.8 and 3.9).

3.3 Chapter summary

The results obtained in the chapter can be summarized as follows:

- Urano has shown fall-off in every profile trace of Pinion 2. This is attributable to the fact that the light is affected by the nearest tooth tip;
- Mainly because of that fall-off, the agreement between the output obtained by the Emera and the Urano on Pinion 2 is low: the HC-N400 machine overestimates the deviation measured in most of the cases. Furthermore, no precise bias can be defined. These differences can range from 3 up to 15μm;
- Results in terms of repeatability have shown the superiority of the Emera, especially in profile measurement;
- The main advantage of a non-contact inspection is in the measurement of large surfaces: in this case, laser systems can be up to 100 times faster than a contact probe. During a standard inspection where individual traces and points are measured, the cycle time of the two solutions is comparable.

Chapter 4

Investigation of the sources of vibration in automatic transmission gearbox: Ghost Noise

The scope of the following chapter is to analyze two gears by means of the interferometer Zygo. One of the two gears has been defined as "worst of worst" (WOW) and has been the cause of a ghost noise problem during a Noise test on a Transmission. The other one, defined as "best of best" (BOB), didn't generate any particular noise problem. Thanks to Zygo, it is possible to look for particular waves on the tooth flank or particular cracks that could be a possible cause of the Ghost Noise. Those deviations present on the "WOW" gear will be compared with the ones present on the "BOB" gear.
The same gears have been also analyzed by analytical inspection machines (Emera and Urano) and there is no indication from them that the "WOW" sample would have generate the ghost noise. Urano was able to find some undulations during the profile deviation measurement on the "WOW" gear. A possible cause of Ghost noise could be attributed to these deviations, but because the tolerance limits have not been exceeded, no more precise indications have been given (Figure 4.1).

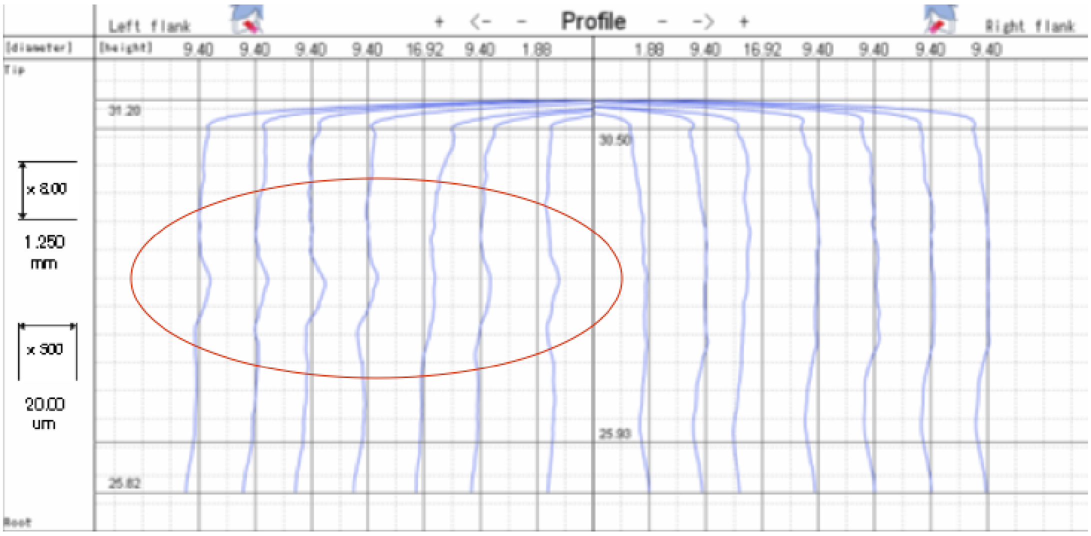

Figure 4.1: Urano measurement performed on the gear with Ghost Noise

Furthermore, a Nital etch test has been done on a third gear. This gear has been analyzed both by Urano and Emera but it has not been subjected to a noise analysis by running the gear on a transmission. The reason for this test is to show the typical overheated distribution on a gear flank after the grinding process. This is because one possible way to detect the aforementioned phantom noise is to look at the grinding burn generated by the hard-finishing processes.
The best of best gear and the worst of worst gear have not been analyzed with Nital Etch test because of the risk of damage to the sample

4.1 Zygo NewView 100: Operating Principle

The NewView 100 (Figure 4.2 and Figure 4.3) is a 3D imaging surface structure analyzer that operates on the interferometry principle. It analyzes the pattern difference of bright and dark lines (fringes) coming from a reference and a sample beam. The light, emitted by a source and then split inside an interferometer, goes to an internal reference surface and to the sample. After reflection, the beams recombine inside the interferometer, undergoing constructive and destructive interference and producing a light and dark fringe pattern. A translation stage and a camera generates a three-dimensional interferogram of the object and this 3D interferogram is translated into a quantitative 3D image by a Frequency Domain Analysis (FDA).
FDA is a mathematical method for processing complex interferograms in terms of phases and spatial frequencies to obtain surface profiles. Here, the Fourier analysis is used to extract a range of phases for each colour or wavelength from the sources spectrum. The particular combination of phases interpreted by FDA uniquely defines the surface height

map.

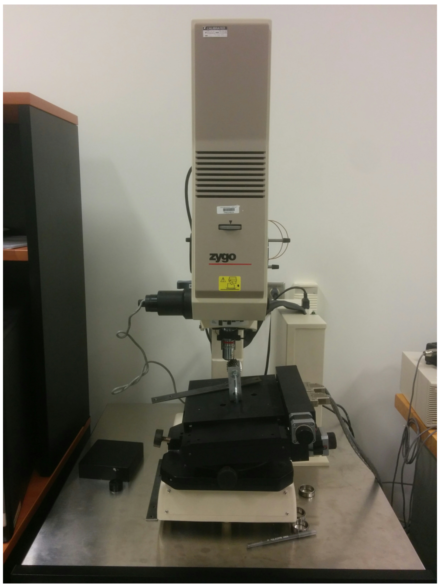

Figure 4.2: Zygo New View 100

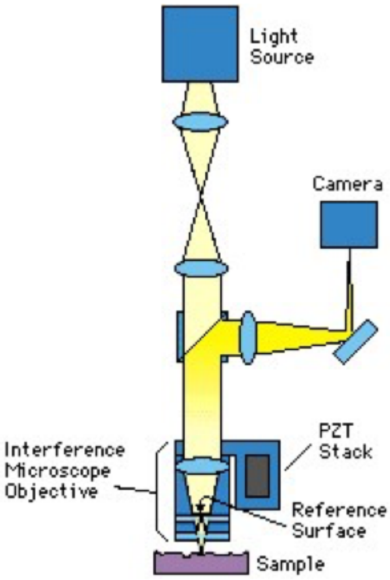

Figure 4.3: Zygo Optical System [37]

4.1.1 FDA working Principle

The following section will provide an overview of Frequency Domain Analysis. The first step of FDA is to determine the relation between intensity "I", and the object distance "L"

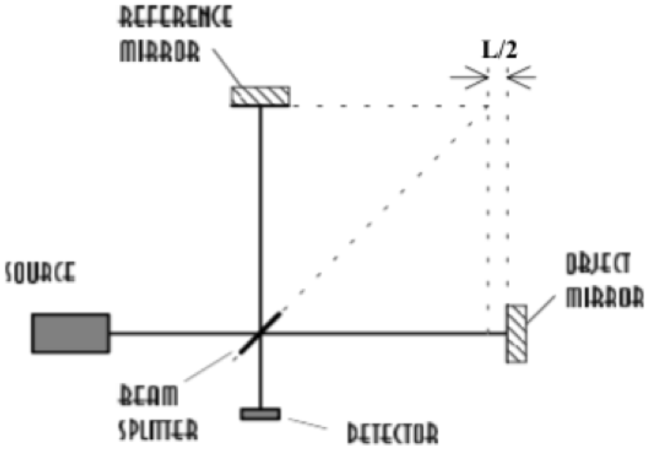

Figure 4.4: Michelson Interferometer [37]

(Equation 4.1 and Figure 4.4):

$$I = \frac{1}{2}(1 + cos(\varphi)) \tag{4.1}$$

The distance L is a function of "φ", the interferometric phase and the phase constant offset "φ_0" which depends on the characteristic of the interferometer and the material properties of the mirrors.

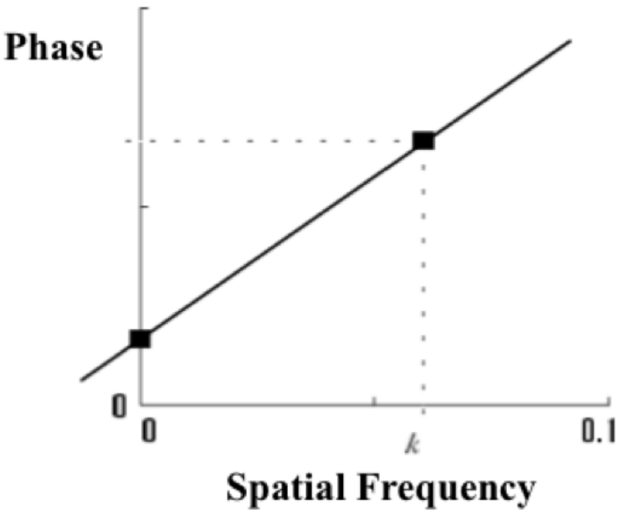

Figure 4.5: Graphical Representation of Single wavelength Interference in the Spatial frequency domain [37]

Because the interferometric phases have a linear relationship with spatial frequency, it is possible to correlate the spatial frequency of the light source "k" and the phase "φ" with a straight line having slope "L" and intercept with the ordinate "φ_0" (Figure 4.5):

$$\varphi = kL + \varphi_0 \tag{4.2}$$

From Equation 4.2, "L" can be deduced knowing "k","φ" and "φ_0". The only problem at this point is how to measure the phase "φ". Generally, this is done by taking a few sample points on the sinusoidal curve of the Light Intensity and transforming the data into the frequency domain by means of a simple algorithm that can be implemented on a computer. "L" will be:

$$L = \frac{\varphi - \varphi_0}{(k)} \tag{4.3}$$

The above is true for FDA with only a single wavelength. However, the NewView 100 FDA analysis works with white light. The white light interferograms tend to be more complex than the single wavelength examples because the whole range of sinusoidal patterns are superimposed onto each other. This is because the white light has a large and continuous range of spatial frequencies and is composed of a continuous band of colours or wavelengths. Despite the complexity of white light, it is still possible to extract phases for the individual spatial frequencies that contribute to the interference effect by means of a Fourier Transform. Once the data has been transformed into the respective frequency domain, the distance "L" can be measured in the same way as before.

4.1.2 Zygo New View 100: Performances and Applications

The Performance of the Zygo New View 100 are:

- Minimum lateral resolution: 0.36 μm to 2.92 μm
- Minimum spatial sampling: 0.22 μm to 8.8 μm
- Vertical resolution: 0.1 nm
- Instrument repeatability: 0.3nm Rq (mean + 2 sigma)
- Maximum vertical step height: 100 μm range
- Data acquisition time: 2.0 μm/sec

The applications in which it is used are:

- 3-Dimensional Images of Surfaces-Flat, Cylindrical, and Spherical
- Surface Roughness Quantification
- Surface Waviness
- Peak-to-valley Measurement

4.2 Methodology

4.2.1 Description of the Gear holder for Interferometric analysis and limitation founded during the measurements

Before introducing the set-up used to perform the measurement of the gears it is appropriate to recall the main gear terminology that will be used in the remaining part of the survey.

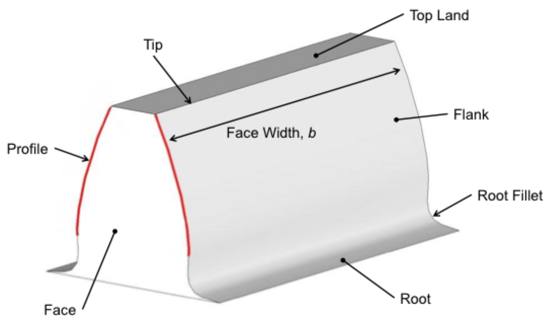

Figure 4.6: Gear Terminology [8]

Figure 4.6 shows the main features of a gear tooth. In addition, during a gear inspection, it is fundamental to determine the tooth numeration and how to distinguish the left from the right flank.

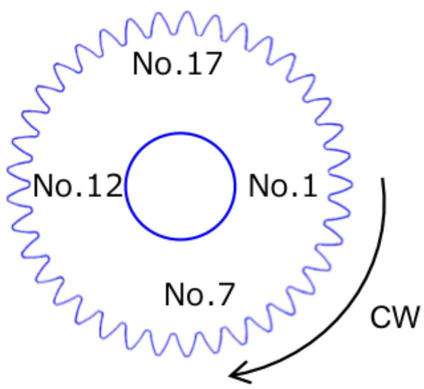

(a) Gear Tooth Number

(b) Top Face Identification

Figure 4.7: Gear Teeth numeration (left) and Top Face Identification (right)

To solve this problem, each gear first has a top face and starting tooth defined. Then, by following a pre-defined rotation, the other tooth numbers are determined (Figure 4.7a). A notch is then etched into the top land of each tooth along one side (Figure 4.7b). This notch is on the opposite side of the top face. The left and right flank are defined by looking down from the top view. Table 4.1 displays the main specification of the gears analyzed.

Table 4.1: Gear Geometric Parameters.

Number of Teeth	Helix Angle	Hand of Helix	Face Width
21	25	Left	18.8

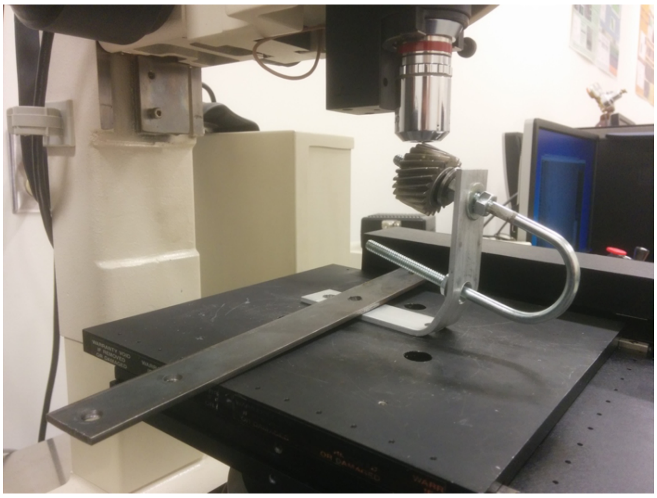

Figure 4.8: Gear Holder

In order to guarantee the perfect orientation of every tooth with respect to the Zygo lens, a particular holder (Figure 4.8) was built at the University of Windsor. The main purpose of this holder is to ensure that, in order to have a fringe generation, the gear flank is as flat as possible with respect to the Zygo Lens. Further, more precise, adjustments of the gear orientation are made possible thanks to a tilting stage. But, during the measurements, because the lens should also be very close to the measured surface and because of the possibility of physical contact between it and the gear, fringe generation was difficult, and sometimes, not feasible at all (Figure 4.9a and 4.9b).

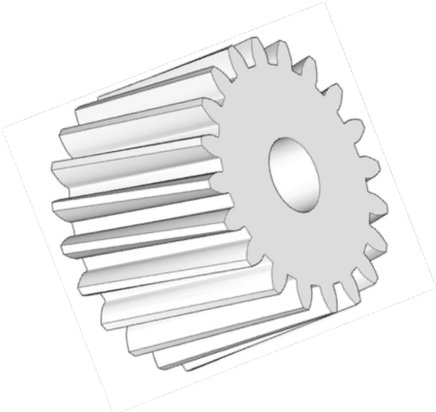

(a) Ideal Orientation of the Helical Gear in order to have the Flank surface as flat as possible [8]

(b) Best trade-off for the gear orientation in order to avoid contact between the Lens and the part, but at the same time mantaining the surface as flat as possible

Figure 4.9: Gear Orientation and Contact of Lens Problem

The measurements are then on both the left and right flank of the gear. The teeth analyzed are chosen at random. Every image captured with Zygo is only 3 mm for each side. Due to an unfeasible number of images needed to scan the entire flank (approximately 60 images for every tooth flank), only critical regions were recorded. Furthermore, due to the impossibility to reach the root (because of the interference of light from the upper tooth), the images refer only to the tips.

4.2.2 Nital Etch Test Introduction and Methodology

If a region of the component is not cooled properly during grinding, overheated areas may be present. Traditional methods for detecting grinding-related damages include visual inspection by nital etching and Barkhausen noise analysis [38]. A Nital etch test is used to locate tempered areas on hardened steel surfaces. The overheated area will appear darker than the surrounding area after the test.
There are several ways to perform the etching process. One procedure was outlined by Alban in his book [39] :

- Clean gear of all grease and oil;
- Place part in a solution of 5% concentrated nitric acid and ethanol for 20 seconds;
- Remove and rinse in clean cold water and dry the sample.

Figure 4.10 shows a typical result obtained after etching the gear.

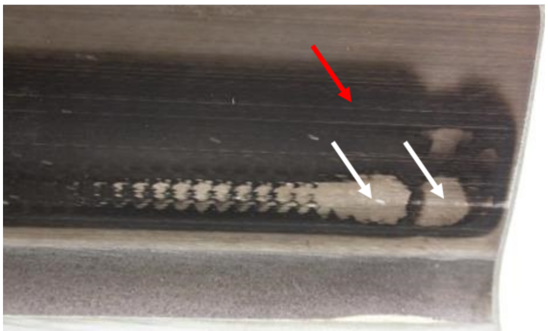

Figure 4.10: Effect of grinding burn after Nital Etching [40]

As it can be seen, dark lines due to grinding burn are shown by the red arrows. Unfortunately, this is a very subjective test [41]. In addition, the test has other disadvantages:

- it can only detect severe grinding damage;
- poor traceability and repeatability.

Table 4.2 reports correlation between the grinding burn, hardness and stress state on a gear react at different temperature ranges.

Table 4.2: Grinding burn vs Temperature .

Temperature (° C)	Hardness	Stress	Nital Etching Response
100-150	Stable	Tension	Nothing
150-300	Decrease	Compression	Grey
350-Austenization Temp.	Decrease	Compression	Dark
Above the Austenization Temp.	Stable	Tension	White

A Nital Etch test was done on one of the samples analyzed by Urano and Emera following the procedure described by Alban [39]. Sample cleaning was done with hexan and acetone

for a total of 20 minutes in an ultrasonic cleaner. The sample was not polished so as to preserve the information of the grinding process.
After being etched, the gear was analyzed both with an optical microscope at magnification x10 and with a scanning electron microscope (SEM) at different magnifications (x30, x50, x100, x500, x1000). The results were compared with those of the gear flanks that were not etched. With the optical microscope, almost all the areas of the tooth were covered during the measurementes. Instead, with the SEM analysis, three lines along profile were consideres as shown in Figure 4.11.
In order to facilitate the entire test (both etching operation and measurement using SEM and a light microscope), one single tooth has been removed from the gear by cutting at very low velicity and with plenty of lubrication in order to avoid undesired stress (Figure 4.11).

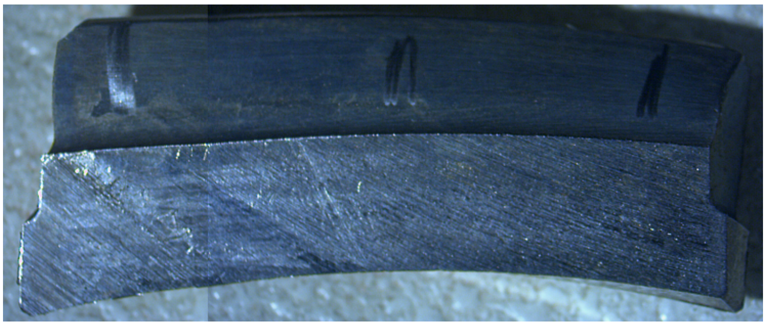

Figure 4.11: Gear flank for Nital Etch Test

4.3 Results

4.3.1 Surface Map and Surface Profile

One of the possible functions of the Zygo New View 100 is to generate a 3D surface map and surface profile of the scanned surface. Both Gear "1" ("BOB") and the Gear "2" ("WOW") were analyzed. As it was already stated during the description of the experimental set-up, the teeth analyzed were randomly chosen. In addition, because of problems with the software application MetroPro used, it was not possible to stitch together the different images. Consequently, this operation was done manually.

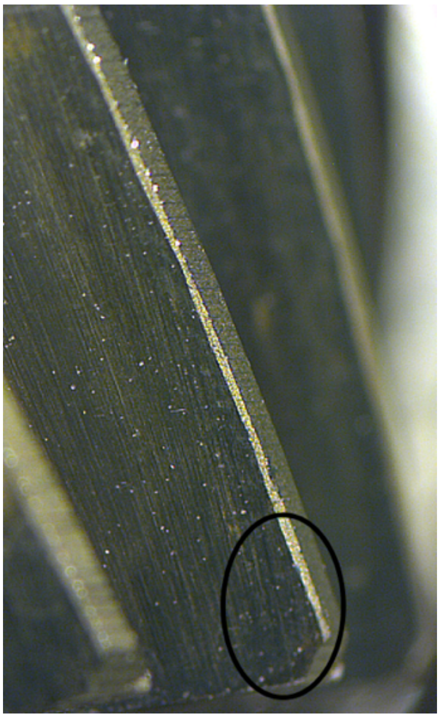

Figure 4.12: Evaluated Region in Gear 1, tooth N. 1 and N. 21

Figure 4.13a and Figure 4.13b, shows the analysis of a limited region of two consecutive teeth; the considered region is indicated in Figure 4.12. As can be seen, they look very similar; other measurements that have not been shown here, were performed, and the same results were found in every tooth.

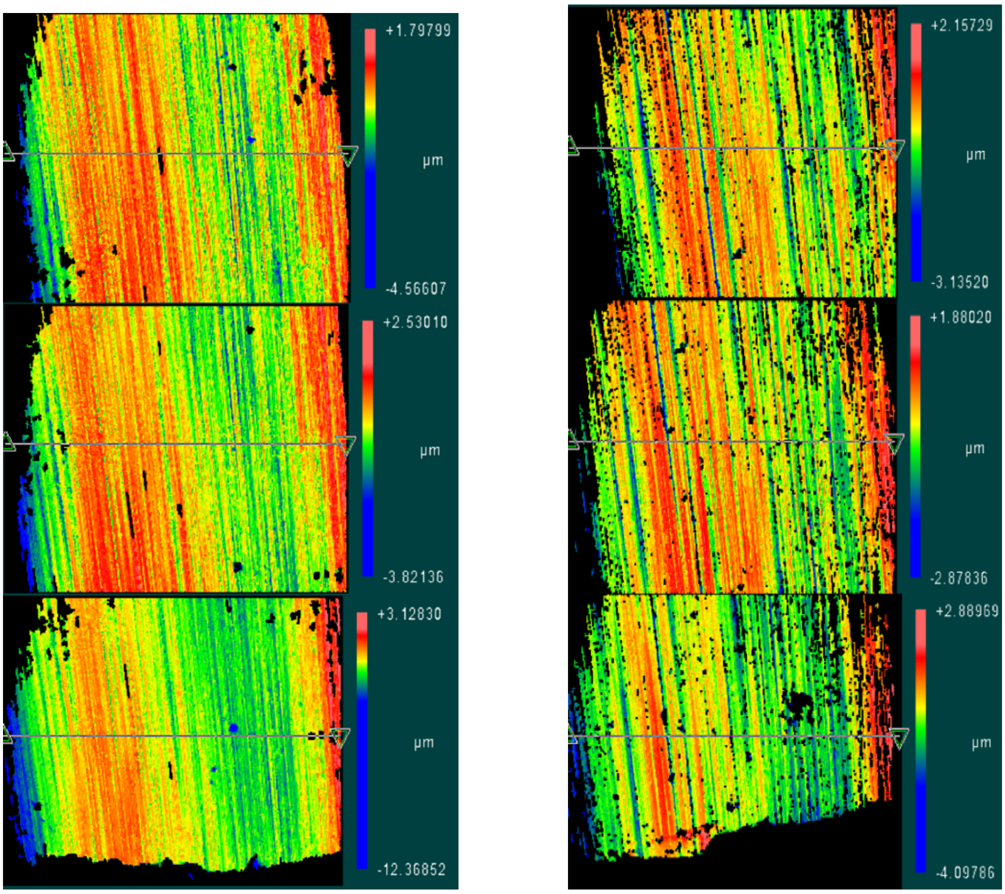

(a) Surface Profile-Gear 1, Tooth N1 (BOB), Right Flank

(b) Surface Profile-Gear 21, Tooth N. 21 (BOB), Right Flank

Figure 4.13: Surface Maps of the Best of Best Gear obtained by using Zygo

Moreover, a wave with an amplitude of few microns is present (Figure 4.14).

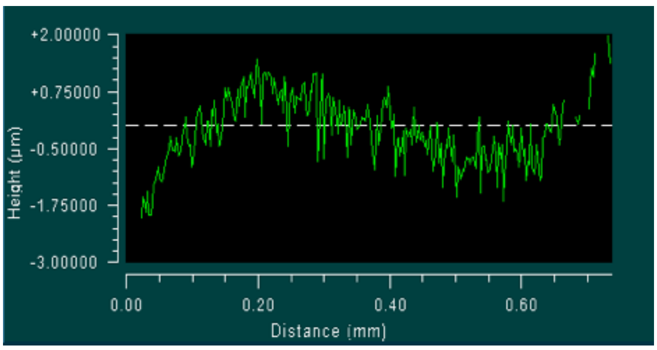

Figure 4.14: Surface Profile Evaluation. The Evaluation is performed at the level of the Bottom line present in the Tooth N. 1

By scanning the flank at the opposite edge, the same wave was present, too. The same does not occur in the central part of the tooth width (Figure 4.15a and Figure 4.15b), or if it is present, its amplitude is smaller (Figure 4.15).

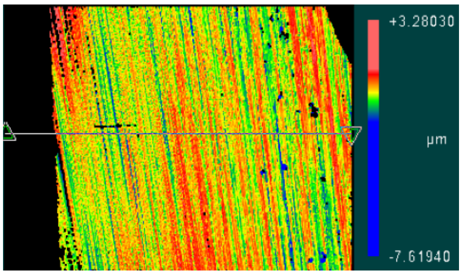

(a) Surface Map of Tooth N. 6, Right Flank

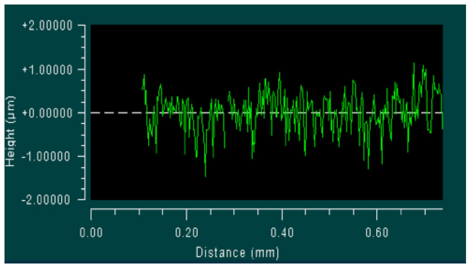

(b) Surface Profile of Tooth N.6, Right Flank

Figure 4.15: Surfaces Map and Surface Profile of the Best of Best Gear obtained by using Zygo

The same characteristic is present on gear "2", too. By performing some measurements on the tooth profile (for both the gear 1 and gear 2), it is noticeable that those waves are extended until the root (Figure 4.16 and 4.17).

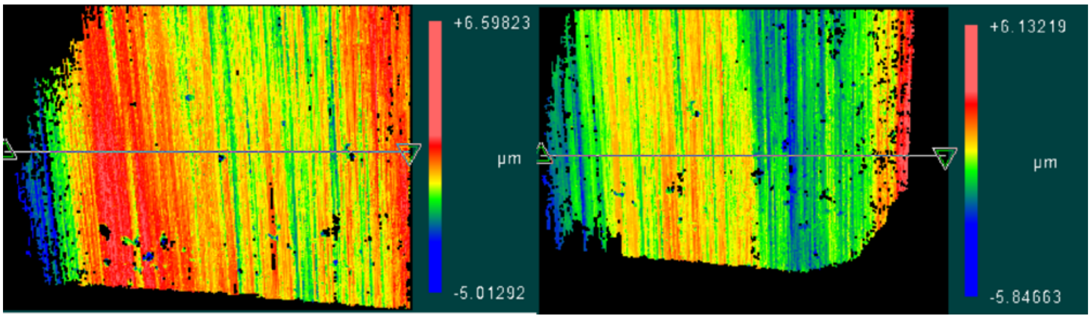

Figure 4.16: Surface Map, Gear 2, Tooth 3, Left Flank

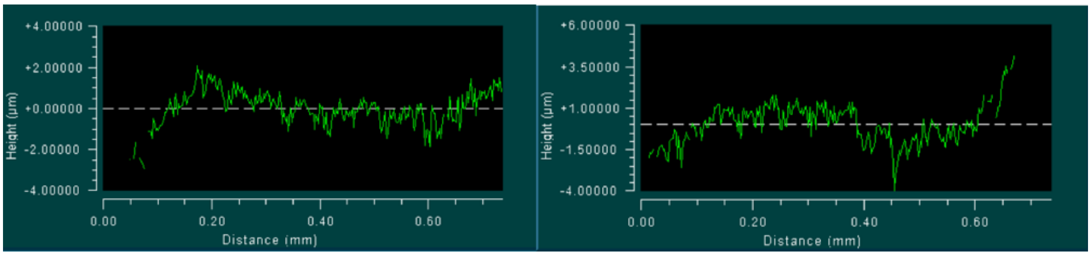

Figure 4.17: Surface Profile, Gear 2, Tooth 3, Left Flank

The same feature is present also on the right flank.
According to the previous observation, the combination of these waves can be one of the root causes of Ghost Noise. To analyze the surface waviness and to compare it with the one of the meshing gear, a more powerful software is needed.

4.3.2 Intensity Map

Analyzing the edge of both gears, through an Intensity Map, revealed some interesting results. In fact, it seems that in the BOB gears, extensive damage is present on the left flank. This damage (Figure 4.18b, Figure 4.18c, Figure 4.19b and Figure 4.19c) was compared with undamaged edges (Figure 4.18a and Figure 4.19a).

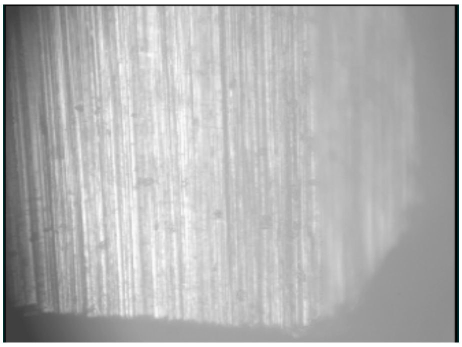

(a) Gear 2, Tooth 2, Left Flank

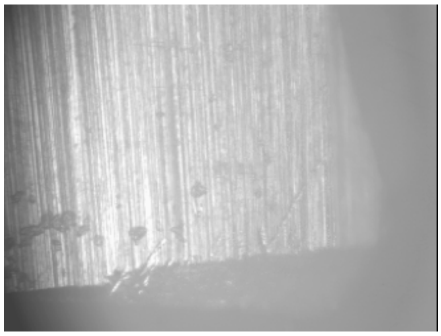

(b) Gear 1, Tooth 2, Left Flank

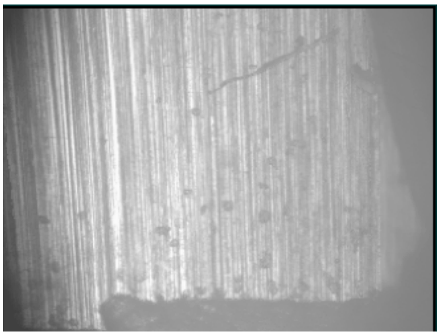

(c) Gear 1, Tooth 1, Left Flank

Figure 4.18: Intensity map of Gear 1 and 2 for the bottom edge

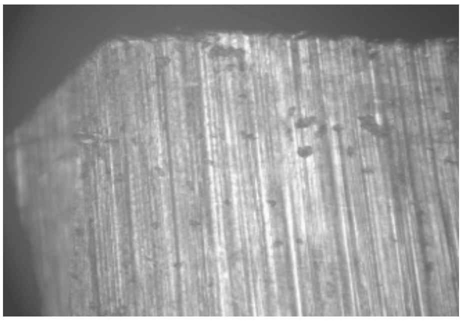

(a) Gear 2, Tooth 14, Left Flank

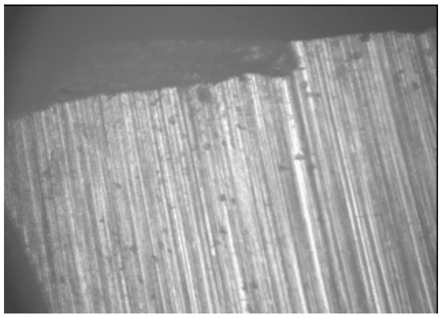

(b) Gear 1, Tooth 2, Left Flank

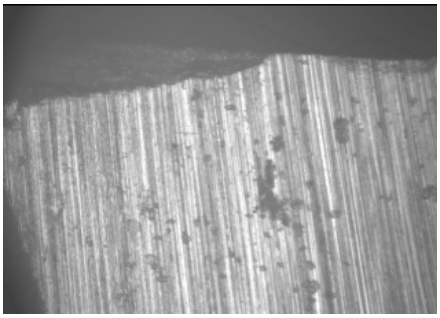

(c) Gear 1, Tooth 4, Left Flank

Figure 4.19: Intensity map of Gear 1 and 2 for the top edge

4.3.3 Nital Etch

Two different flanks of the same gear were observed with an optical microscope at a magnification 10x. The goal was to reveal possible normal overheated regions that occur on a gear flank.

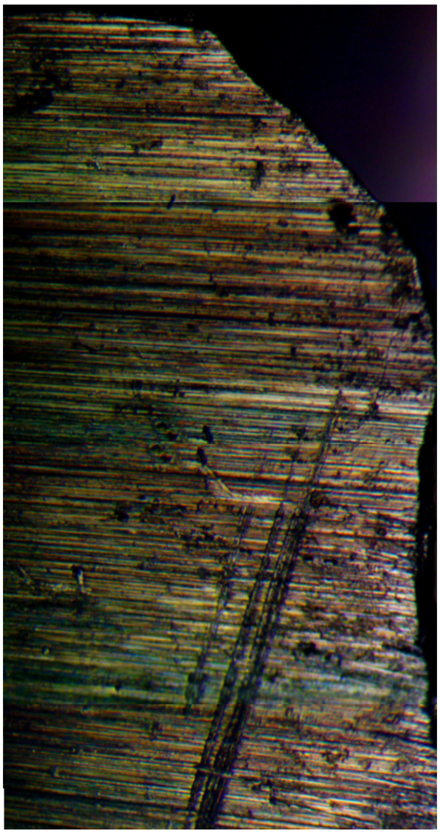

(a) Not Etched

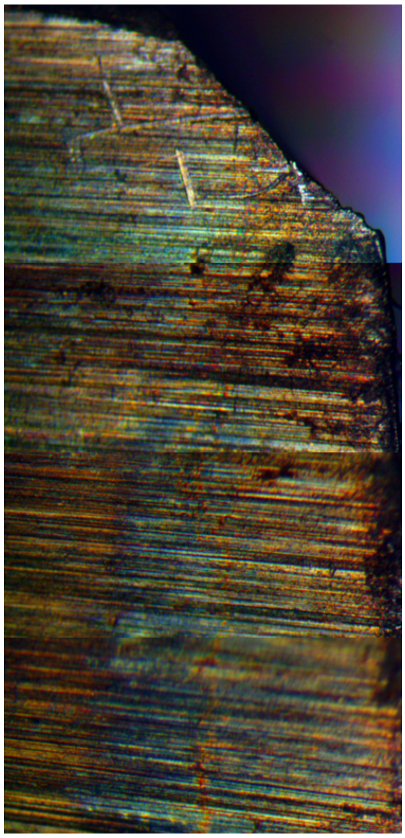

(b) Etched

Figure 4.20: Etched Flank vs. not Etched Flank: light microscope

Figure 4.20a and Figure 4.20b show how the edges of a gear flank, before and after being etched, look like. As it can be seen, the etched edge shows indistinguishable dark regions that may be due to grindind. The same dark spots do not occur in the central part of the flank. According to the literature [42], the reason is attributable to the fact that, during the grinding process, at the tip and edges of a flank, less material is to dissipate the heat is present. This phenomenon can cause a lower heat removal rate that can lead to burns. It cannot be seen in the above photos, but these burns were only found on one edge, and cover an area of only a few square millimeters. The reason for this particular distribution can be due to an imperfect gear positioning during the grinding operation. Further tests were also done on another polished and unpolished flank and the same results were confirmed.
Observations were made with a SEM (Figure 4.21): no significant differences were found.

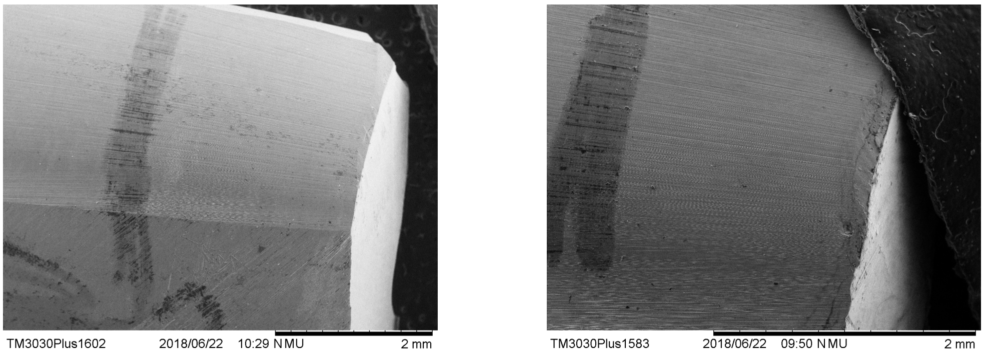

(a) Not Etched (b) Etched

Figure 4.21: Etched Flank vs. not Etched Flank: SEM

By cutting other teeth in a direction perpendicular to the flank, the side of the gear was also studied. The procedure for the sample cleaning and nital etch test was the same except that this sample was also polished. The goal of this test was to study until which depth the grinding process affects the gear underlay.

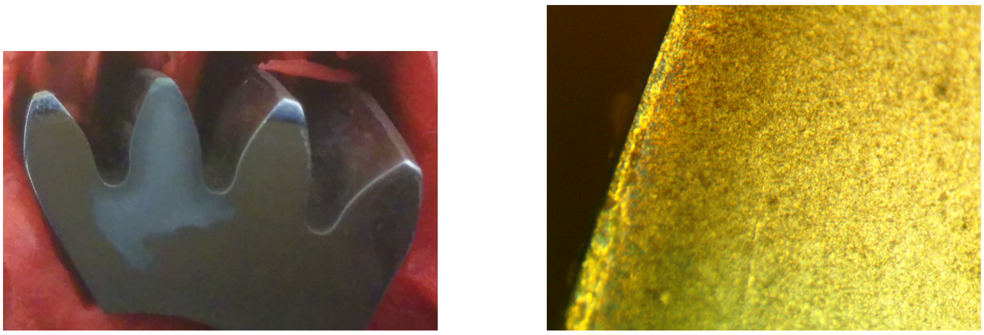

(a) Naked Eye (b) Light Microscope at 10x

Figure 4.22: Etched Cross section

As can been seen from Figure 4.22, only a few microns of the tooth's side appears darker. The result doesn't change if the nitrite solution is applied for a longer period of time.
The scope of the Nital Etch test has been to characterize the damage that a grinding process can create in normal conditions. The results can be used as comparison if the same tests are done on the "WOW" and "BOB" gears.

4.4 Chapter Summary

The main points that can be derived from the investigation of the Ghost Noise are:

- Several difficulties were found during the scanning process of the teeth flank. This is attributable to the complex geometry of the gear analyzed;

- Gear flanks are characterized by waves. The combination of these waves with those of the meshing gear are the cause of the Ghost Noise. More powerful tools to mathematically combine those waves are needed;

- The use of the Barkhausen noise analysis or the Nital etch test is strongly suggested. This could help to identify the potential problem in the grinding process that results in gears with the Ghost Noise.

Chapter 5

Discussion

Chapter 5 considers both the evaluation of the Urano HC-N400 and the Ghost Noise Analysis.
The discussion of the Urano machine has been developed through the consideration of:

- cycle time needed both for the measurement itself and for machine set-up once different gear types are measured;
- environmental conditions needed for the correct functioning of the machine;
- maintenance needed for a precise measurement.

Great importance was given to the level of agreement between the Urano HC-N400 and the Emera as well.
Secondly, further considerations on the ghost noise study were done, as well. The studies revealed the limitations of the Zygo Interferometer and its measurement capabilities. Possible methods of discovering noisy gears early in the inspection process were also discussed.

5.1 Non-contact laser metrology System

The Urano HC-N400 is the first non-contact machine for gear measurement developed for commercial customers. This technology was strongly requested by Toyota and, nowadays, the Urano's goal is to expand their market to other car manufacturers. This machine has great potential in terms of its ability to obtain both a 2D and 3D contour scan as well as to measure waviness and surface finish all in a single machine, but also has great potential in terms of technological innovation.
Omega's main concern is to have in the same gear lab two different machines that could give differing results within the same gear lab. For example, this could cause a problem if one machine finds that a gear is out of tolerance but the other machine finds the opposite. This kind of difference could create of lot of trouble and doubt for the operator. In order to avoid this risk, a lot of weight has been given to agreement tests between the two machines. Other

factors, such as envirormental condition, maintenance for the correct use of the machine, cycle time and time needed to set up the machine in case of gear type change have also been considered.

5.1.1 Cycle Time Estimation

Inspection time for a four tooth, profile, lead and index inspection has been similar to that of the Emera machine:

- Approx. 4 min for Pinion 4 and Pinion 2

The real advantage of the HC-N400 is that in these same four minutes, both 2D (Figure 5.1)and 3D contours (Figure 5.2) of 4 teeth (both the left and right flank) can be obtained. For the surface topography of all teeth, a few minutes more are needed. Compared to contact machines, the ability to obtain a surface topography in just a few seconds rather than several hours represents a considerable advantage.
Contour maps make it possible to look at the entire flank and not just a single line. This is a significant advantage where particular errors or anomalies occur in different parts of the flank.

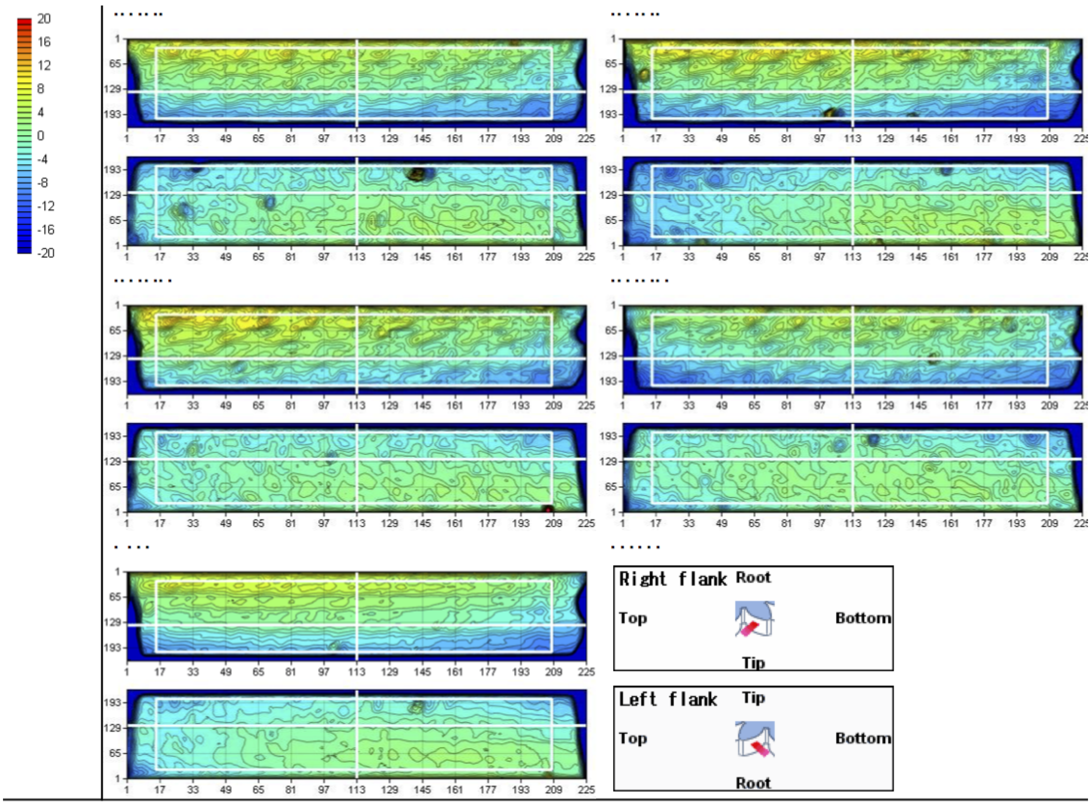

Figure 5.1: Urano 2D contour map

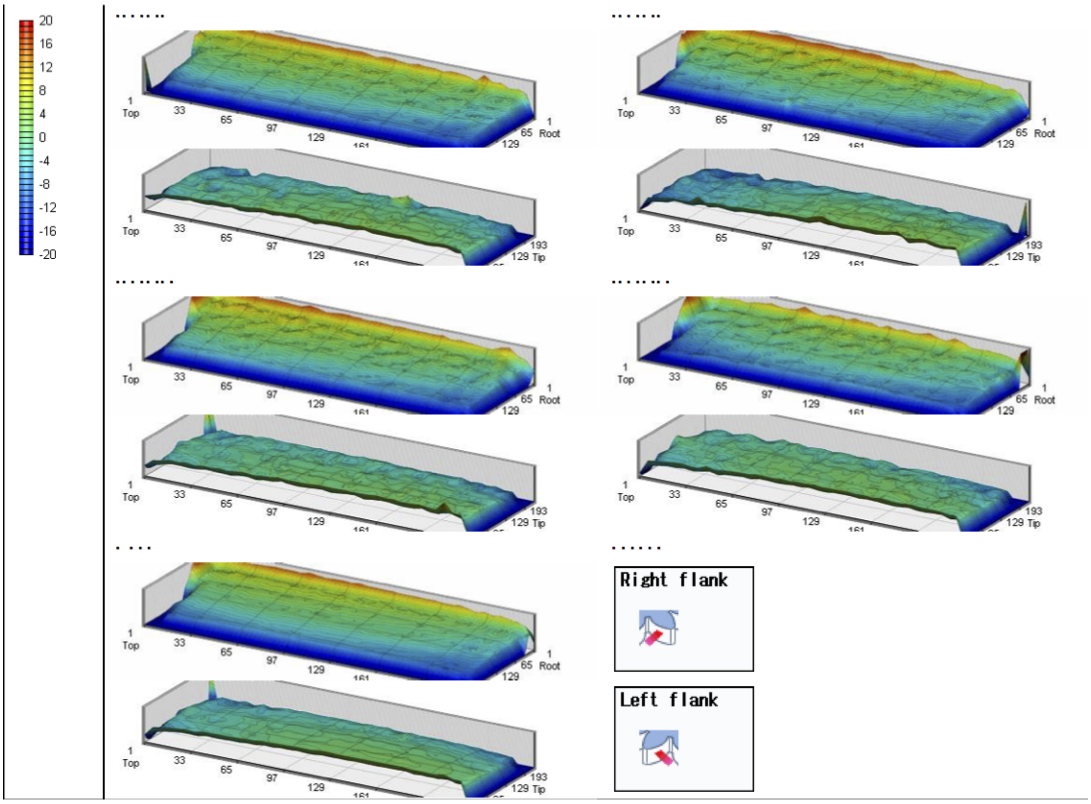

Figure 5.2: Urano 3D contour map

An important question that was raised during the tests was the idle time between the measurement of different kinds of gear. Urano declares that, in order to switch to an existing program to measure a different kind of part, it takes approximately:

- 3 to 8 minutes, according to the different laser positions that should be calibrated.

and the creation of a new inspection program can take around 30-60 mimutes due to the necessity of:

- Manual laser positioning;
- Laser light intensity adjustment;
- Laser Calibration.

Consequently, the Urano HC-N400 is not perfectly suitable for a gear lab where there is a habitual gear type change, but is rather better suited to research and development applications because of the amount of information that can be taken in only few seconds on every flank.

5.1.2 Environmental Requirement

The installation conditions of a measuring device are crucial for ensuring the accuracy and reliability of the measuring results [43]. Major influences include the effect of temperature on the measuring device and on the workpiece undergoing inspection, as well as the effect of vibrations on the device and the cleanliness of the workpiece. As can be seen from Figure 5.3, with a difference in temperature of few degree Celsius, the measurement can differ up to 4 μm.
This is why temperature and vibration control devices are sometimes needed. Unfortunately, because of the presence of these devices, the inspection machines should not be collocated near the shop floor but in apposite gear labs far away from the cutting machines. These long distances will mean wait times for measurement and possible correction to the cutting tools' parameters. Some other suppliers, in order to solve this problem, build machines with temperature compensation software and a vibration pad that can be installed in the shop floor. The first solution was not adopted by Urano, who instead opted for a big chamber in order to ensure a proper temperature during the inspection. This chamber naturally occupies a lot of space and a location on the shop floor is unlikely.

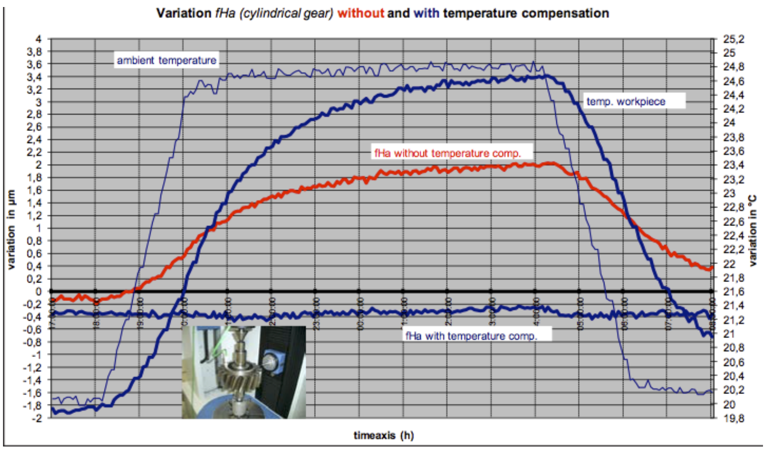

Figure 5.3: Temperature Influence on the deviation measured by a contact inspection machine [43].

Cleanliness has not been a problem for Urano during gear measurement. No particular precaution (such as gloves) were used during the measurement of the gears provided. No other cleaning operations were done either.

5.1.3 Maintenance and Calibration

Urano has declared that the machine should be calibrated once a day or every time it is switched on. For a daily calibration, two different balls are used:

- The first one is used to establish the zero reference position;

- The second one is needed for the calibration of the different angle positions of the laser arm and laser head.

No other particular maintenance operations are required.
Urano has assured very good performance of the laser in terms of repeatability and accuracy for at least 3 years. After that, it should be replaced. The cost is unknown. The laser is typically calibrated according to the JIS B 7440-2 standard (Appendix D). The accuracy of the machine on an inspection of a perfectly known geometry is within 1 μm.
Urano has also declared that only a few days of training are sufficient for a perfect understanding of the machine's use. The duration of this training does not exceed one week. In this time frame, the operators, after a few days, are left alone to use the machine with the supervision of Urano specialists.

5.1.4 Agreement between Urano HC-N400 and Emera

Agreement results were not as good as expected. In some cases, the differences between the two machines was in excess of 5 micrometers, but those differences are not consistent. Consequently, a precise bias was unable to be identified so as to define new tolerances based on the Urano technology.
The worst results were obtained with Pinion 2. The reason for these differences is mostly associated with the presence of some fall-off at the root of every trace measured by Urano. This problem was attributed to the fact that the light coming from the scanner was affected by the presence of the nearest tooth tip. According to Urano, this problem, right now, cannot be solved in the case of very small gears such as Pinion 2. Furthermore, in the 2017, other correlation tests were performed on Sun and Annulus gears (Appendix B). Those gears are "green" parts (Section 2.2.1) and, consequently, do not have a very smooth surface. The agreement obtained by the two machines was not acceptable in this case either. This lack of agreement can be explained by the reflection problem, the higher accuracy of laser machines, and the use of different filters.
In conclusion, the Urano is not suitable for use in the same high volume gear lab as the Emera due to the challenges discussed above, but it is well-suited to research and development purposes.
Table 5.1 and Table 5.2 show which gears are considered good (Accepted) or poor (Rejected) by the Urano and Emera. The criteria for rejection was to reject every gear that had at least one parameter (profile, lead, index and Runout) out of tolerance. As can be seen, the Urano HC-N400 rejects every single gear analyzed, both for Pinions 2 and Pinions 4.

Table 5.1: Acception/Rejection rate of Emera and Urano on Pinios 2

	Emera		**Urano**	
	Accepted	Rejected	Accepted	Rejected
No. 1		X		X
No. 2	X			X
No. 3	X			X
No. 4		X		X
No. 5		X		X

Table 5.2: Acception/Rejection rate of Emera and Urano on Pinios 4

	Emera		**Urano**	
	Accepted	Rejected	Accepted	Rejected
No. 1		X		X
No. 2	X			X
No. 3	X			X
No. 4	X			X
No. 5		X		X

Naturally the possibility of this simply being an extreme case must be considered. In fact, if just one parameter is out of tollerance, the gear is not immediately rejected but further study is done.

5.2 Ghost Noise and Ripple Analysis

In the experimental campaign conducted at the University of Windsor Tribology of Material Research Centre, two gears were analyzed. One has been indicated as a possible source of Ghost Noise (or "Worst of Worst") and the other one as the "Best of Best" gear. The causes of this particular kind of noise are still unknown. What is known is that it is related to geometrical deviation that differs from the nominal deviations, and a standard inspection conducted by means of both contact and laser machines cannot identify any particular cause of this noise.

3D surface images obtained with Zygo did not revealed any particular feature that would differentiate the "Worst of Worst" from the "Best of Best" gear. It must be also noted that several limits were found. First of all, due to the particular geometry of the helical gears, it was difficult, and in some cases impossible, to obtain an image of every point on the gear. In addition, each image covered a very limited area and the stitching operation on the Interferometer was not functioning correctly. Consequently, a complete picture of the entire flank was not available. The possibility that the combination of all possible waves

present along the profile of the different teeth could generate this particular noise must not be excluded.
Cracks were identified on the edges of the left flank of the "Best of Best" gear. But because the Gear is designed in a such way that the load should concentrate mostly on the central part of the flank (Figure 5.4), these particular defects are unlikely to be the cause of noise problem.

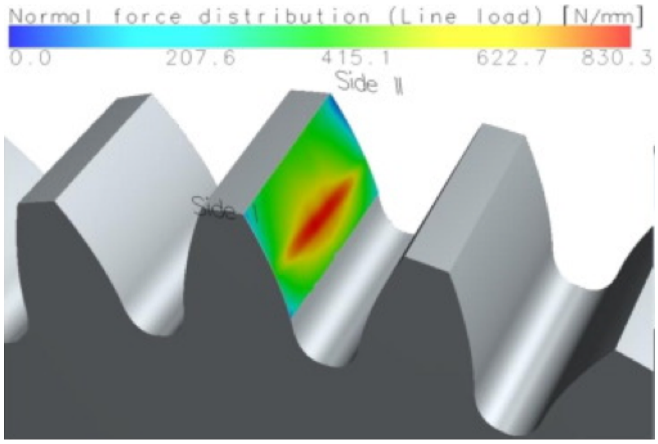

Figure 5.4: Normal Force Distribution on a Crowned Gear Flank [44]

Software capable of studying the different waves present on every gear profile has been developed (Appendix E). By approximating these waves with sine functions and by combining them with the one resulting from the corresponding meshing gear, the causes of particular noises and defects resulting from the manufacturing process can be identified. The ghost noise is one of such noises that has been studied. The software requires a very high degree of accuracy in order to also consider the smallest waves and the analysis of consecutive teeth. Several ghost noise gears were analyzed by this tool and the results are surprising: out of all gears analyzed by this software, all of those that caused the ghost noise were identified.
Further studies were performed by using a Nital Etch test. This analysis was done on a third gear with the goal of showing how grinding burn can be distributed on a flank. In the future, the results obtained, can be compared with the ones from a gear with the ghost noise. The gear tested was analyzed only by the Urano and the Emera but it was not mounted in a transmission gearbox.
It is important to note that the "WOW" and "BOB" gears were not subjected to Nital Etch analysis. This is because, currently, they are the only samples used for studying the problem and, consequently, they cannot be destroyed.
The results obtained by this analysis revealed grinding burns only on one of the edges of the flank. This is because of the less material present in this region that can subtract heat

during the grinding process; this results in overheating. However, no dark spots were found in the region where most of the load is concentrated.
It should also be noted that the same kind of analysis can be done by using Barkhausen Noise Analysis [42]. This kind of test makes it possible to analyze a gear on an objective basis without destroying the sample. In addition, some studies have demonstrated a good correlation between the results obtained with this technology and the Nital Etch test.
Until now, one of the only things known about the Ghost Noise is that one of its main causes can be attributed to anomalies during the grinding process. For this reason, it is strongly suggested to perform similar analyses of this kind on "BOB" and "WOW" gears in the future.
Barkhausen Noise Analysis and the supplier that are able to integrate this test on their machine are introduced in subsection 7.1.

5.3 Chapter Summary

By comparing the Emera and the Urano HC-N400, it was discovered that the cycle time needed for a standard inspection on four teeth, profile, lead and index is very similar. Furthermore, Urano HC-N400 needs more time (3-4 minutes versus 30 seconds) to set up the machine for the measurement of different gear types. The main advantages of the Urano is when a complete 3D image of the gear flanks is needed. In these cases, Urano is up to 100 times faster. No particular problems associated with the environmental conditions and maintenance needed to operate the Urano machine proper were found. The worst results were observed on the agreement between the contact and non-contact machine. The measurements obtained by the Urano are several microns higher and every gear measured was rejected. Furthermore, because no precise bias was found between the different average values measured by the HC-N400 and the Emera, the definition of new acceptance and rejection tolerances could be really complicated, as well.
Thanks to Zygo, undulations on all flanks of the "WOW" and "BOB" gears have been observed. To combine those undulations and to distinguish noisy from good gears, ripple analysis software is needed. Several tests have been done in other research and the software was perfectly able to accomplish this goal. Other possible solutions to detect gears that generate Ghost Noise could be the Nital Etch test or Barkhausen Noise analysis.

Chapter 6

Conclusions and Recommendations for Best Technology

Contact measuring systems are currently the main technology used for gear inspection. Unfortunately, the higher demand in terms of accuracy and velocity of inspection has revealed the limits of this technology and further improvement to it are hardly expected. On the other hand, laser line scanners have been improved over the last few years both in terms of resolution, optical quality and image processing.
The scope of this thesis has been to thoroughly consider the performance guaranteed by some laser systems and evaluate the feasibility of introducing these technologies into an automotive transmission gear lab.
A study on a Ghost Noise problem was done, as well. A gear that presents this noise problem was analyzed at the University of Windsor Tribology of Material Research Centre using an interferometer in order to discern whether some micro cracks at a nanometric level or particular surface waves were present.
In this chapter some conclusions regarding the research on the laser technology and for the Ghost noise problem are discussed.

6.1 Evaluation of the Urano HC-N400 system

During the evaluation of Urano HC-N400, the following conclusions have been drawn:

- Urano HC-N400 is more suitable for research and development purposes. The possibility to obtain a 3D surface in a reasonable time is the main advantage of performing a non contact measurement;
- Urano HC-N400 is not suitable to perform measurement on very small gear (Pinion 2), especially in the profile root where the light of the sensor was affected by the presence of the tip of the nearest tooth. By observing tests done in the 2017 it was found that problems were present on the evaluation of internal gears and non-ground gears, too.

Acceptable agreement in the results was obtained only in the measurement of Pinion 4 where the deviations measured by the Urano were few microns higher than those measured with the Emera;

- Even if no particular problems are present with maintenance and envirormental condition, the possibility exists that operators of the "K" and the "N" could misinterpret the results if the "N" and the "K" are present in the same metrology lab. Indeed, the possibility of the machines providing conflicting results must not be ignored;
- The Emera still represents the best option for Omega high volume gear labs . This is due to its high degree of repeatability, minimal time needed for a new machine set-up for the measurement of different gear types and the ability to measure every kind of gear with a high degree of accuracy;

6.2 Ghost Noise and Ripple Analysis

The research done at the University of Windsor Tribology of Material Research Centre draw the following conclusions:

- Waves were found on both gears. The combination of these waves can be the root cause of ghost noise.
- Ripple Analysis software, that is able to mathematically combine these waves, could be the solution to determine if a particular gear will generate ghost noise or not.
- The presence of small failure has been observed on every left flank edge of the best of best gear. Because of the particular stress distribution on the tooth, these defects are not causes of any noise.

Chapter 7

Future Directions

Over the last few years, many suppliers have been developing new machines capable of performing a non contact inspection. Among these machines, only few are being tested and others, more interesting, have not been studied. Two of these machines declared to perform a profile and index evaluation in less than 1 minutes. These technologies could be very interesting as in-line inspection solution and the possibility to check every single gear coming out from a grinding machine or an hobbing machine could be really possible. The real advantage will be an immediate identification of the defects coming from the manufacturing process and an immediate intervention of the operator on the machine setting without any loss of time.
Among these machines, the new non contact system developed by Ares and Erea seem to be the most interesting for a high volume gear lab. The reason is related to the fact that they are hybrid technology able to integrate in the same machine both a contact inspection and a non contact one. In addition, the possibility of a ripple analysis offered by the first new technology and the Barkhusen Noise Analysis by the second one, could be a real big step in the gear metrology world. For an inline solution, it could be really interesting to test both the Era and Ade because of the throughput these technologies can guarantee.

7.1 Erea

Erea is a multi sensor inspection system that is able to integrate in the same machine different inspection tool:

- Laser scanning head for a non contact inspection
- Tactile probing system for a fast machine set-up and part individuation
- Surface roughness measurement for the measurement of high-frequency, short-wavelength component on a considered surface.
- Barkhausen noise analysis, for detecting grinding burn.

The main benefits of this machine are an increase of the throughput and a reduction of both the cost and floorspace with the use of just one platform. The presence of a touching probe reduces the set-up and the gear individuation time. Once the gear is ready to be inspected, the laser head can be easily substituted to the stylus and a non contact inspection can be performed. The supplier declares an accuracy of the laser scanner that was lower than 1 μm and inspection time for a pinion gear of around 4 minutes. The correlation results between Erea contact machine and the non contact one was in the order of 2-3 μm of difference.
One of the most innovative optional tools offered by the 300GMSL is the Barkhusen noise test. In fact, by using this technology, residual and compressive stresses on gear tooth flanks after grinding can be found [42]. This technique is based on a simple concept involving ferromagnetic materials and a magnetizing field. In fact, the ferromagnetic object, due to the presence of a magnetic field, changes. This change is a result of the microscopic motion of the magnetic domain walls within the material. The motion of this domain wall causes an emission of electrical pulses that can be detected by a coil of conducting wire near the material. By measuring the discrete pulses and their amplitude, information such as inclusions, precipitates, dislocations, grain boundaries and residual stresses can be obtained.

7.2 Era

Era's technology combines double flank inspection (subsection 2.3.1) and non-contact laser system in a single machine. The machine is able to inspect all teeth on a typical helical gear for the index and 4-tooth profile. The cycle times for non-contact index and profile inspection was estimated to be around 10 seconds. Any kind of information regarding the profile and index deviation can be displayed in a standard chart. The machine is not capable of a lead inspection.

7.3 Ade

Ade is a non-contact 3D inspection machine designed for the in-line inspection of gears. This inspection system is used to inspect all the teeth from each gear very quickly. The time needed for data acquisition and data computation is around 5 seconds. All the measurements of the profile, lead, pitch and runout are possible. The accuracy is between 0.2 μm to 1 μm.

7.4 Ares

The Ares is a hybrid machine that combines tactile and non-contact systems. This machine can be integrated with Ripple analysis software. At the moment, this machine is not ready to be tested but must not be excluded from the possibility of the great results achieved by the company.

Bibliography

[1] G Goch. “Gear metrology”. In: *CIRP Annals-Manufacturing Technology* 52.2 (2003), pp. 659–695.

[2] Robert C Frazer and Steven J Wilson. “Implementing ISO 18653–Gears: Evaluation of instruments for Measurement of Individual geras”. In: *Gear Technology* 27.3 (2010), pp. 38–47.

[3] F Härtig and K Kniel. “First International Involute Gear Comparison”. In: *Gear Technol* 31 (2014), pp. 80–84.

[4] Kamlesh Sawant. *https://www.quora.com/What-is-difference-between-accuracy-repeatability-and-precision-in-simple-terms*. 2017.

[5] F Haertig and W Lotze. “3d gear measurement by cmm”. In: *Laser Metrology and Machine Performance V* (2001).

[6] https://www.nikonmetrology.com/en-us/services-support/download-center/technology-articles/tactile-vs-laser-scanning. *Nikon, ’HN-C3030.’*

[7] Monarch Bearing Co. *http://www.monarchbearing.com/equipment-category/gears.aspx*.

[8] C-GGA50 Internal Gleason Training. *Cylindrical Gear School*. 2018.

[9] http://www.fourwheeler.com/how-to/0706or-automatic-transmission-tech/. *Fourwheeler Network*.

[10] Dwight Smith. *Analytical Gear Chart Interpretation*. 2012.

[11] D Gimpert. “Gear Inspection: Troubleshooting Tips”. In: *Gears Solut* February (2007).

[12] D Gimpert. “Guarding against Gear Deviation”. In: *Gears Solut* February (2006).

[13] *AGMA915-1-A02*.

[14] Dennis Gimpert. “A new standard in gear inspection”. In: *Gear Solutions* 10 (2005), pp. 34–38.

[15] Rajmet. *https://www.rajmet.com/index.php/engineering/manufacturingprocess*.

[16] Liebherr. *https://www.liebherr.com/en/hun/products/gear-cutting-technology-automation/gear-cutting-machines/gear-hobbing-and-profile-grinding-machines/gear-hobbing-and-profile-grinding-machines.html*.

[17] Bryan White. *Global Gear Honing Machines Market Emerging Progress 2018-2025.* 2018.

[18] D Gimpert. “An elementary guide to gear inspection”. In: *Gears Solut* June (2005), pp. 32–38.

[19] Joao Antonio Santos Dias Fonseca, Antonio Baptista, Ma Joao Martins, and Joao Paulo N Torres. “Distance Measurement Systems Using Lasers and Their Applications”. In: *Applied Physics Research* 9.4 (2017), p. 33.

[20] Nikola Vukašinović, Drago Bračun, Janez Možina, and Jože Duhovnik. “The influence of incident angle, object colour and distance on CNC laser scanning”. In: *The International Journal of Advanced Manufacturing Technology* 50.1-4 (2010), pp. 265–274.

[21] Nick Van Gestel, Steven Cuypers, Philip Bleys, and Jean-Pierre Kruth. “A performance evaluation test for laser line scanners on CMMs”. In: *Optics and lasers in engineering* 47.3-4 (2009), pp. 336–342.

[22] URL: https://www.micro-epsilon.co.uk/news/2016/UKME272-Comparison-of-blue-and-red-laser/. *A comparison of blue and red laser triangulation sensors.* 30-06-2016.

[23] URL:https://lmi3d.com/company/digital-hub/blog/laser-displacement-sensors-analog-digital/. *Laser displacement sensors – from analog to digital.* Walt Pastorius, 2014-11-6.

[24] URL:https://electronics.howstuffworks.com/cameras-photography/digital/question362.htm/. *What is the difference between CCD and CMOS image sensors in a digital camera?l.*

[25] JaydipChodavadiya. “Machine Vision Based Spur Gear Measurement”. In: *IJSART - Volume 4 Issue 5* (MAY 2018).

[26] Axel von Freyberg, Karsten Lübke, Martina Fuhrmann, Gordon Henske, and Gert Goch. *Laboratory for Large-Scale Gear-Measurements.*

[27] MA Younes, Abdallah M Khalil, and Mohamed Damir. “Automatic measurement of spur-gear dimensions using laser light. Part 1: measurement of tooth thickness and pitch”. In: *Optical engineering* 44.8 (2005), p. 087201.

[28] MA Younes, Abdallah M Khalil, and Mohamed Damir. “Automatic measurement of spur gear dimensions using laser light, part 2: measurement of flank profile”. In: *Optical Engineering* 44.10 (2005), p. 103603.

[29] Jiri Tuma. “Gearbox noise and vibration prediction and control”. In: *International Journal of Acoustics and Vibration* 14.2 (2009), pp. 1–11.

[30] Mats Åkerblom. *Gear Noise and Vibration: A Literature Survey.* 2001.

[31] Chanat Ratanasumawong, Shigeki Matsumura, and Haruo Houjoh. "Inspection of Tooth Surface Geometry by Means of Vibration Measurement". In: *JSME International Journal Series C Mechanical Systems, Machine Elements and Manufacturing* 48.4 (2005), pp. 704–714.

[32] RB Randall. "Cepstrum analysis and gearbox fault-diagnosis". In: *Maintenance Management International* 3.3 (1982), pp. 183–208.

[33] Timothy Zenoski. "A new standard in gear inspectionA Look at Expanding Mandrels for Gear Workholding". In: *Gear Solutions* (April 2017).

[34] J Martin Bland and Douglas G Altman. "Agreement between methods of measurement with multiple observations per individual". In: *Journal of biopharmaceutical statistics* 17.4 (2007), pp. 571–582.

[35] J Martin Bland and Douglas G Altman. "Agreed StatisticsMeasurement Method Comparison". In: *Anesthesiology: The Journal of the American Society of Anesthesiologists* 116.1 (2012), pp. 182–185.

[36] Douglas G Altman and J Martin Bland. "Measurement in medicine: the analysis of method comparison studies". In: *The statistician* (1983), pp. 307–317.

[37] P. de Groot. *R and D Technical Bulletin, Zygo Coporation*. 9/23/93.

[38] Murat Deveci. *Detection Methods of Grinding Damages*.

[39] Lester E Alban. "Systematic analysis of gear failures". In: *ASM International* (1985).

[40] *https://onyxinsight.com/wp-content/uploads/2017/04/*.

[41] B Karpuschewski, O Bleicher, and M Beutner. "Surface integrity inspection on gears using Barkhausen noise analysis". In: *Procedia Engineering* 19 (2011), pp. 162–171.

[42] Jeffrey S Ceurter, Ch Smith, and Roy Ott. "The Barkhausen noise inspection method for detecting grinding damage in gears." In: *Gear Technology* 19.6 (2002), pp. 26–31.

[43] Gunter Mikoleizig. "Gear Inspection in a Shop Floor Environment". In: *GEARTECHNOLOGY* (June 2015).

[44] Yu-Ren Wu et al. "Transmission and load analysis for a crowned helical gear pair with twist-free tooth flanks generated by an external gear honing machine". In: *Mechanism and Machine Theory* 98 (2016), pp. 36–47.

[45] Mitutoyo. *Coordinate Measuring Machines*.

[46] Günther Gravel. "Analysis of ripple on noisy gears". In: *Gear Technol.,(January)* (2013).

Appendix A

Bland and Altman Plot

In a gear lab it is very essential to assess the agreement between two equipments but the statistical approach to determine the level of this agreement is not trivial. Sometimes, correlation and regression studies are used but they just determine the relationship between two or more variables and not their agreement. In 1983 Altman and Bland (B&A) [36][35][34] proposed an alternative analysis that evaluates a bias between the mean differences, and to estimate an agreement interval, within which 95 % of the differences of the second method, compared to the first one, fall. The B&A plot method only defines the intervals of agreement without saying whether those limits are acceptable or not. Acceptable limits must be defined a priori.

A.0.1 Correlation and linear regression

Correlation is a statistical technique that can show whether, and how strongly, pairs of variables are related. The main result of a correlation is called the correlation coefficient (or "r") that ranges from -1.0 to +1.0. "r" gives an idea of the strength of relationship or linear relationship between the variables. The closer the coefficient is to +1.0 or -1.0, the greater the strength of the linear relationship is. Moreover, also the significance of the result should be considered. In fact, if the correlation coefficient is statistically significant with respect to the set limit ($P < 0.05$), it is possible interpret its value. Must be considered that correlation describes linear relationship between two sets of data but not their agreement.

A.0.2 The analysis of differences: Bland and Altman method

Bland and Altman introduced the Bland-Altman (B&A) plot (Figure A.1). This method quantifies agreement between two quantitative measurements by constructing limits of agreement. These statistical limits are calculated by using the mean and the standard deviation ("s") of the differences between two measurements. The resulting graph shows in the Y axis the difference between the two paired measurements (A-B) and in the X axis the average of these measures. We would expect most of the differences to lie between "d

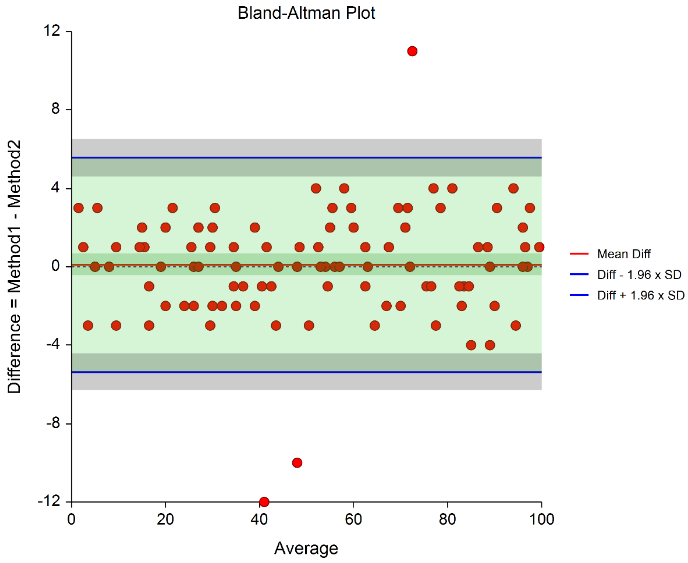

Figure A.1: Bland and Altman Plot Example

-2s" and "d +2s", where "d" is the mean difference, or more precisely, 95% of differences will be between "d-1.96s" and "d +1.96s", if the differences are normally distributed (Gaussian). Normal distribution of the differences must always be verified since in some cases normality cannot be determined simply by observing the histogram plot. If differences are not normally distributed, a logarithmic transformation of original data could be needed. The B&A plot system does not say if the agreement is sufficient or suitable to use a method or the other indifferently. It simply quantifies the bias and a range of agreement, within which 95% of the differences between one measurement and the other are included.

A.0.3 Precision of estimated limits of agreement

The 95% confidence interval (CI) of agreement limits allows to estimate the size of the possible sampling error. It can be measured by using standard error providing that the differences follow a distribution which is approximately normal. Standard error of "d" is "$\sqrt{s^2/n}$" and standard error of "d-2s" and "d +2s" is about "$\sqrt{3s^2/n}$". The result obtained will be just an estimation of the whole population. The estimating precision depends on the sample size. Indeed, the greater the number of samples used for the evaluation of the difference between the methods, the narrower will be the confidence interval, both for the mean difference and for the agreement limits. The 95% Confidence Interval CI of the mean difference illustrates the magnitude of the systematic difference. If the line of equality is not in the interval, there is a significant systematic difference. This will mean that the second method constantly under or over estimates compared to the first one.

Appendix B

Urano Experimental tests: 2017

In 2017, Omega commited Urano the measurement of 2 sun and 2 annulus gears. These samples were not finished parts. The scope of these tests has been always to analyze the performance of the Urano HC-N400 machine. Big differences between Emera and Urano became evident. The reason has been associated both to a different filter use (Appendix C) and reflection problems of the Urano laser scanner. By studying the measurement of the same sun gear, Urano observed a more undulated traces (Figure B.1).

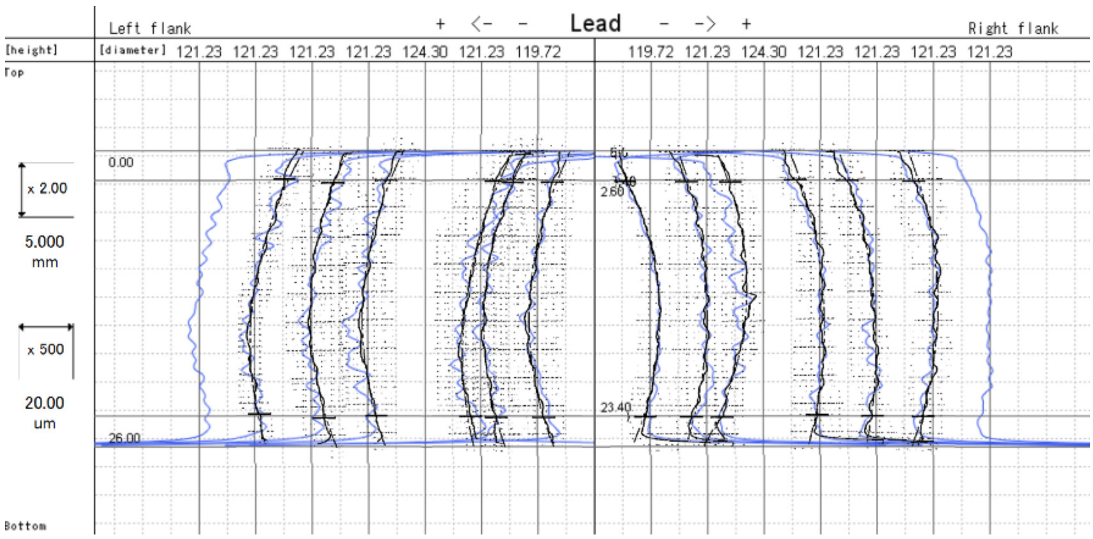

Figure B.1: Lead Deviation on the Sun measured by Urano (blu line) and Emera (black line).

The presence of these undulations means a higher lead form deviation measured by Urano. The result can be shown very well by the Bland and Altman plot (Figure B.2 and Appendix A).

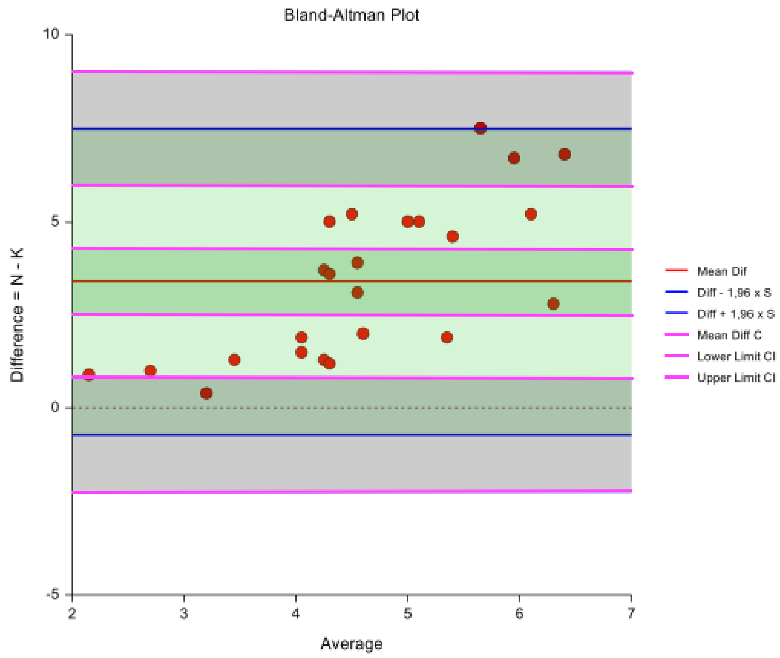

Figure B.2: Bland and Altman Plot: Form Lead Deviation on the Sun measured by Urano and Emera.

Also if acceptance tolerances are not specified for those gears, different results are given by the two machines.
Internal gear measurement is a very big challenge for laser inspection. In fact, it is a very big issue to reach the internal teeth with a laser because of their position and Urano is the only machine that is able to do it. By observing the profile trace, it seems that, in the central part of the profile, the level of agreement is really good and the only differences are due to the different filters applied. Regarding to the numerical values, they seem to not correlate very well. This difference may be due to the fact that Urano had some difficulties to measure both the root and the top of the teeth. In fact, the cut off part occurs way before with respect to the one measured by Emera (Figure B.3).

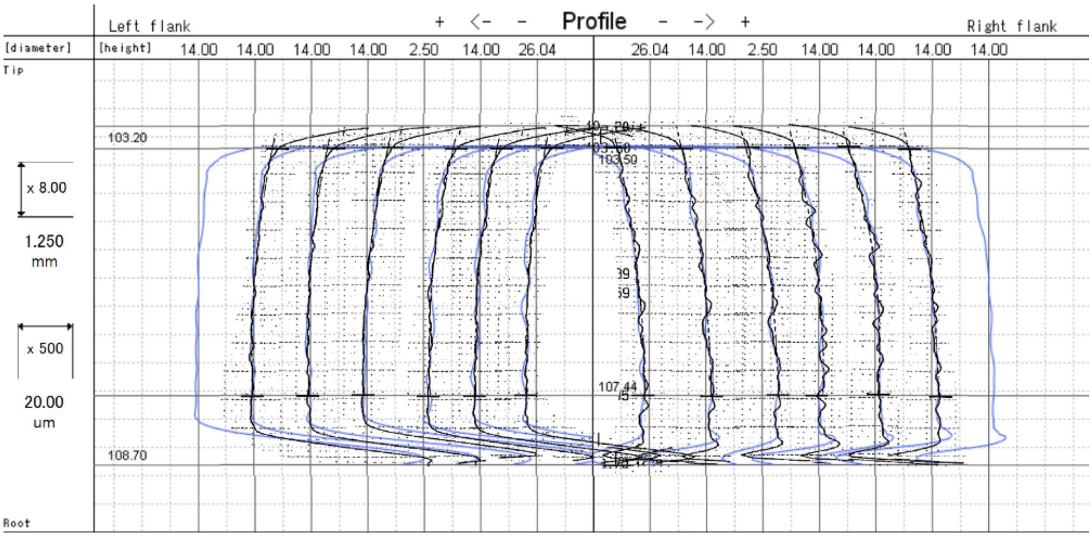

Figure B.3: Profile Deviation on the Annulus measured by Emera (Black line) and Urano (blue line).

Appendix C

Effect of Data Filtering

Figure C.1 and Figure C.2 show the impact that the use of a different filter can have on the measurement of a same gear performed by the same machine. The differences can be greater than 1 micron. Generally, these filters are applied in order to have a smoother trace on the chart and eliminate noise effect of the probe. The side effects is that some information are lost. For a contact machine, the effect of these filters can be both applied by changing the Probe ball size or by manually changing a program set in the computer machine. At the moment, it is not known how a laser machine applies their filters is unknown.

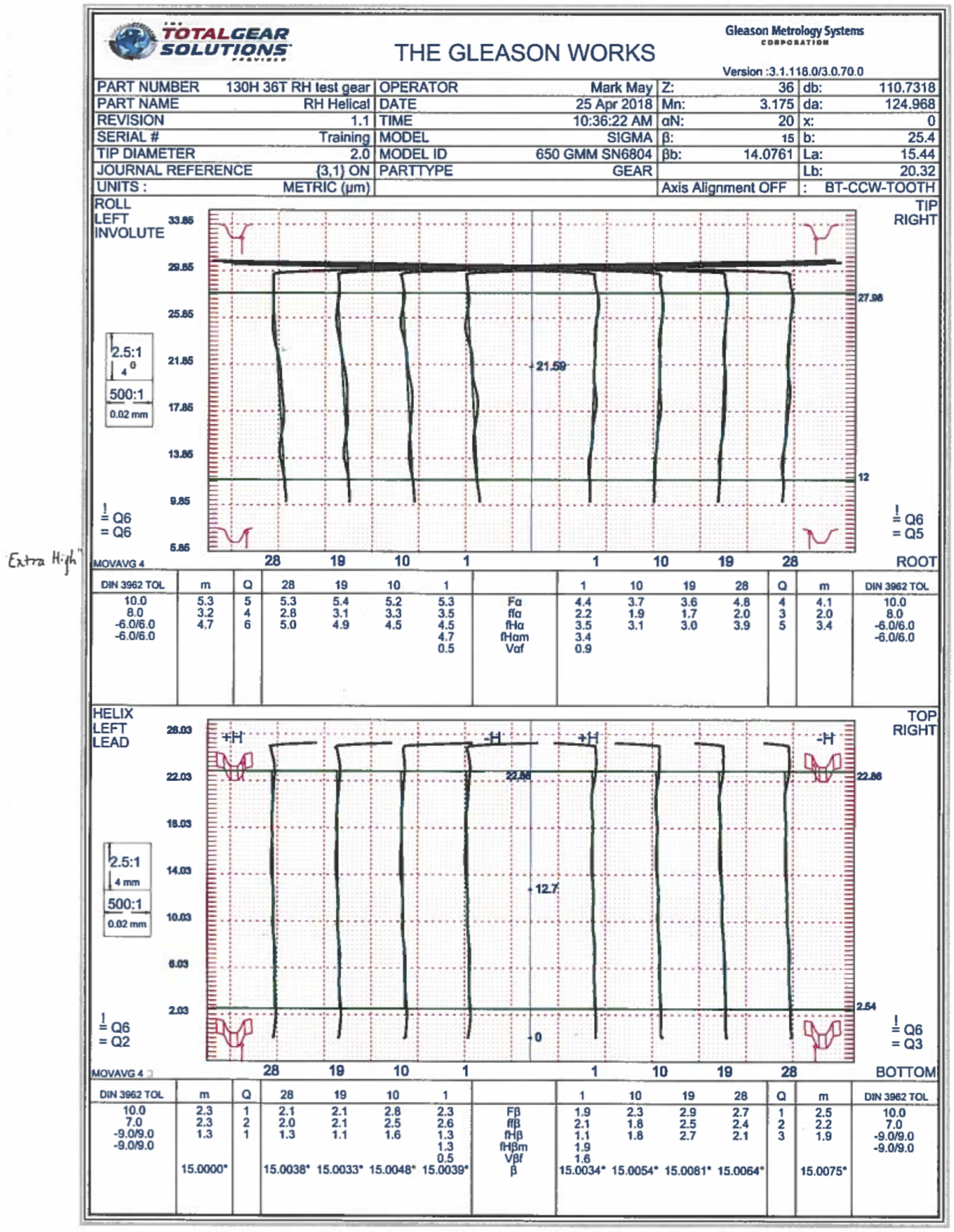

Figure C.1: Application of a high filter during a profile and lead measurement [8].

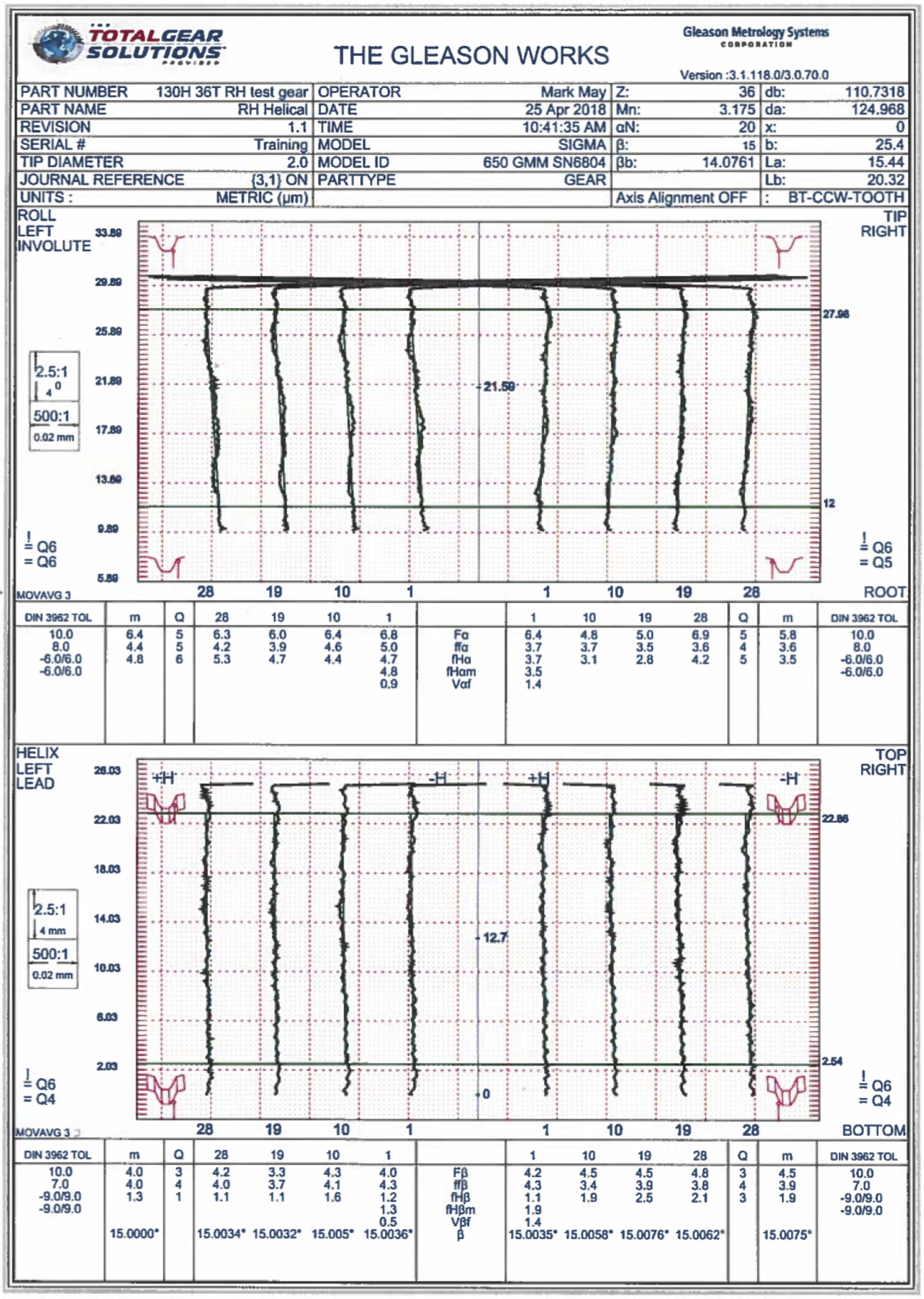

No Filter"

Figure C.2: Application of a low filter during a profile and lead measurement [8].

Appendix D

Machine Certification

before being used in a gear lab, both contact and non contact machine must be certified in order to ensure a proper level of accuracy and repeatability. Generally these tests are done on a geometry of perfectly known dimensions to see how close the measurement detected by the machine is with respect to the one known.
Emera was calibrated by following the standard VDI/VDE 2612. According to this standard, the machine belong to group 1. This means an:

- Accuracy of 1 μm
- Repeatability of 0.1 μm.

The measurement are performed on just two teeth (No. 0 and No. 15th) and they are repeated three times (Figure D.1). The parameter measures are referred to the profile and lead deviation. This kind of calibration is done once time a year.

0 Degree "Left Flank"					
Profile	Test#1	Test#2	Test#3	Average	Variation
fHa	-1.20	-1.00	-1.00	-1.07	0.20
Fa				#DIV/0!	0.00
ffa	1.10	1.00	1.00	1.03	0.10
Lead					
fHB	-1.20	-1.20	-1.30	-1.23	0.10
FB				#DIV/0!	0.00
ffB	0.20	0.20	0.20	0.20	0.00

15 Right Hand Helix "Left Flank"					
Profile	Test#1	Test#2	Test#3	Average	Variation
fHa	-1.50	-1.50	-1.40	-1.47	0.10
Fa				#DIV/0!	0.00
ffa	0.90	0.80	0.90	0.87	0.10
Lead					
fHB	0.20	0.20	0.20	0.20	0.00
FB				#DIV/0!	0.00
ffB	0.30	0.30	0.30	0.30	0.00

15 Left Hand Helix "Left Flank"						Original Master Values			RESULTS		
Profile	Test#1	Test#2	Test#3	Average	Variation	0 Deg.	15R	15L	Dev 0	Dev 15	Dev-15
fHa	0.70	0.80	0.80	0.77	0.10	-0.05	-0.16	1.86	-1.02	-1.31	-1.09
Fa				#DIV/0!	0.00	1.17	1.17	2.82	#DIV/0!	#DIV/0!	#DIV/0!
ffa	1.40	1.40	1.60	1.47	0.20	1.15	1.08	2.1	-0.12	-0.21	-0.63
Lead											
fHB	-1.20	-1.30	-1.50	-1.33	0.30	-0.42	-0.11	-1.35	-0.81	0.31	0.02
FB				#DIV/0!	0.00	1.04	1.19	1.76	#DIV/0!	#DIV/0!	#DIV/0!
ffB	0.50	0.40	0.50	0.47	0.10	0.86	1.1	0.87	-0.66	-0.80	-0.40

0 Degree "Right Flank"					
Profile	Test#1	Test#2	Test#3	Average	Variation
fHa	-0.90			-0.90	0.00
Fa				#DIV/0!	0.00
ffa	0.70			0.70	0.00
Lead					
fHB	-1.10			-1.10	0.00
FB				#DIV/0!	0.00
ffB	0.20			0.20	0.00

15 Right Hand Helix "Right Flank"					
Profile	Test#1	Test#2	Test#3	Average	Variation
fHa	-1.30			-1.30	0.00
Fa				#DIV/0!	0.00
ffa	0.60			0.60	0.00
Lead					
fHB	0.20			0.20	0.00
FB				#DIV/0!	0.00
ffB	0.30			0.30	0.00

15 Left Hand Helix "Right Flank"						Original Master Values			RESULTS		
Profile	Test#1	Test#2	Test#3	Average	Variation	0 Deg.	15R	15L	Dev 0	Dev 15	Dev-15
fHa	0.60			0.60	0.00	-0.05	-0.16	1.86	-0.85	-1.14	-1.26
Fa				#DIV/0!	0.00	1.17	1.17	2.82	#DIV/0!	#DIV/0!	#DIV/0!
ffa	1.40			1.40	0.00	1.15	1.08	2.1	-0.45	-0.48	-0.70
Lead											
fHB	-1.40			-1.40	0.00	-0.42	-0.11	-1.35	-0.68	0.31	-0.05
FB				#DIV/0!	0.00	1.04	1.19	1.76	#DIV/0!	#DIV/0!	#DIV/0!
ffB	0.40			0.40	0.00	0.86	1.1	0.87	-0.66	-0.80	-0.47

Figure D.1: Emera measurement performed on a master gear for the annual calibration

Urano is certified according to the JIS B 7440-2 standard [45]. This standard is used in order to assess a method for evaluating the performance of a coordinate measuring machine. Moreover, in the revised JIS, the standards for scanning measurement and rotary tables have been added to the conventional test. The test procedure consists of performing a series of measurements of five different test lengths in seven directions (35 measurements in total) (FigureD.2). The sequence is repeated twice. The result of the test is expressed according to the following format MPE=A+L/K, where:

- A: Constant (μm) specified by the manufacturer
- K: Dimensionless constant specified by the manufacturer
- L: Measured length (mm)

Naturally, this MPE value should be lower than an upper limit value B specified by the manufacturer. The result obtained by the Urano was MPE 1.6+4L/1000μm.

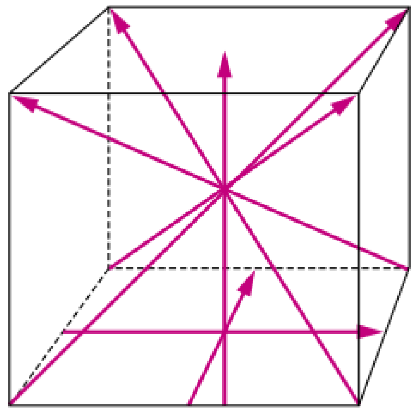

Figure D.2: Test measurement directions defined by the JIS standard [45]

Appendix E

Analysis of Ripple on Noisy Gears

The goal of ripple analysis is to detect particular ripples in an early stage of production that are cause of noise, and not with noise test once the gears are already assembled. To this end, a software for ripple analysis has been developed, making it possible to describe ripples in a deviation curve. In ripple calculation, the most important step is the calculation of the amplitude of the compensating sine wave functions in a selected frequency range. Then, the compensating sine wave with the large frequency is considered the first dominant frequency and it is plotted on the profile as parameter. This dominant sine wave function is then eliminated from the deviation curve and the remaining deviations are re-analyzed. By performing this operation several times, a frequency spectrum of the maximum amplitudes can be obtained. With this type of analysis, each flank is evaluated independently from the others, but it is also interesting to relate different deviation curves in a such a way to resemble the mesh during the rolling process. In fact, by lining up all measuring points of the different teeth and defining them as a function of the rotation angle, a continuous closed measured curve is built (Figure E.1). For the description of periodic signals, compensation sine-wave functions can be used. In fact, respect to a Fast Furies transform, they are able to describe exactly an open curve with overlap and gap. In order to evaluate low frequencies, pitch variations must be taken into account and, to diminish the uncertainty in ripples, more teeth should be measured [46].

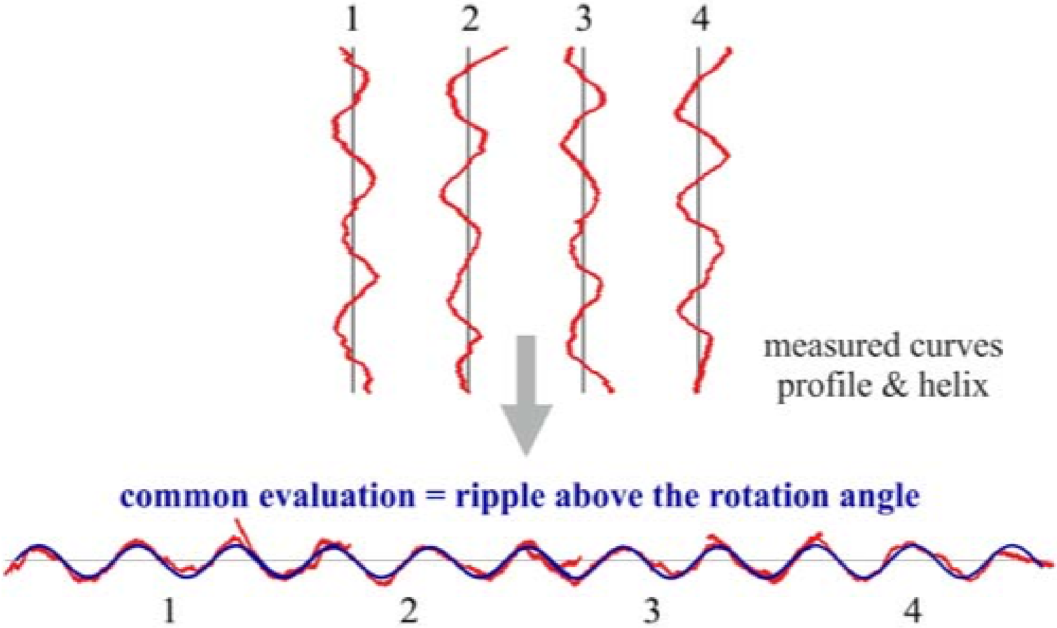

Figure E.1: Method of Ripple Evaluation [46]

E.1 Analysis of Honed Gear

Figure E.2 reports a ripple analysis of an honed gear. Here, profile deviations of left flanks are plotted together as deviation curve for all measured teeth over the angle of rotation. It is possible to see that frequency 1 (one ripple per rotation) represents the runnout deviation caused by the eccentric position of the gear axis. In case of four ripple per rotation, vibration of machine tool or square blank could be present.

E.2 Ghost Frequency and Meshing Frequency

Figure E.3 shows deviation curves of four teeth measured in succession with ghost frequency. The tooth flanks with ripple with varying phase position and the form that change from one tooth to the other could be a good indication of ghost frequency. But for a more reliably analysis, all teeth should be measured. Ripples with mesh frequency and multiples exhibits a constant phase position and very similar form deviations. Moreover, the precision of measuring device must be also considered. In fact, amplitudes of 0.15 micrometres which can cause relevant noise, can be only detected with a resolution of 0.1 micrometres.

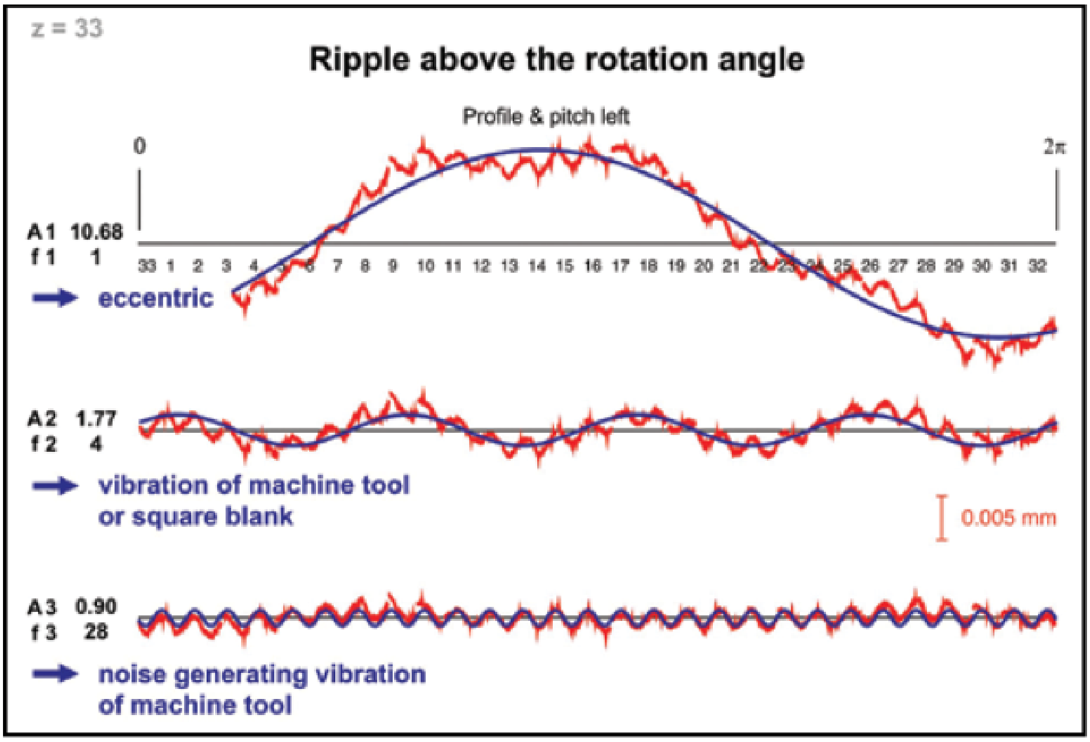

Figure E.2: Deviation curves of common ripples of a honed gear [46]

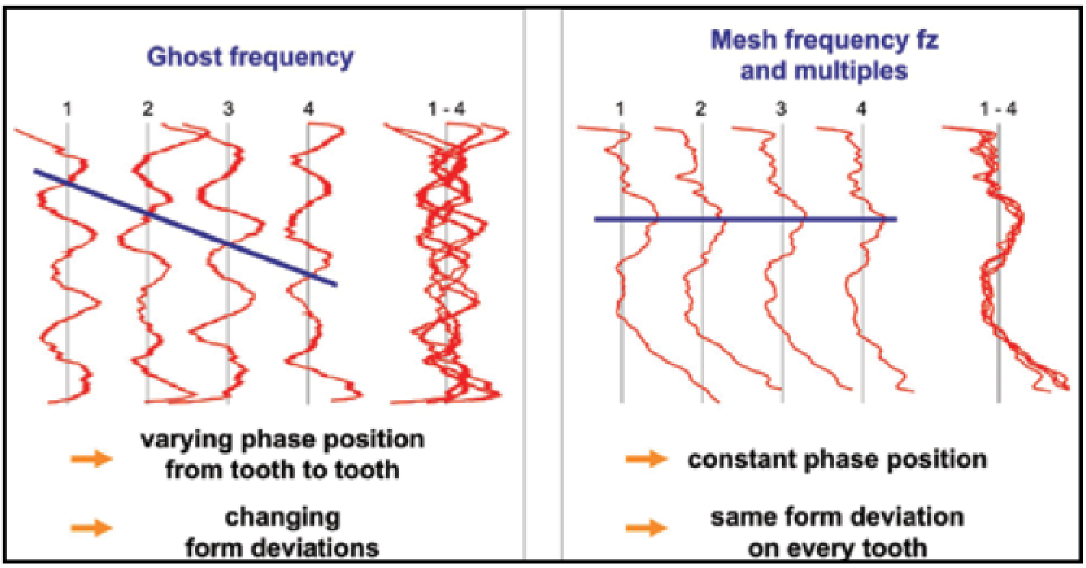

Figure E.3: Ghost and meshing frequency [46]

Appendix F

Emera vs. Urano: Chart Comparison

Figure F.1 represents a chart overlay between the chart obtained by Urano (blue line) and Emera (black line). Here it is very evident the presence of a fall off at the root of the profile trace.

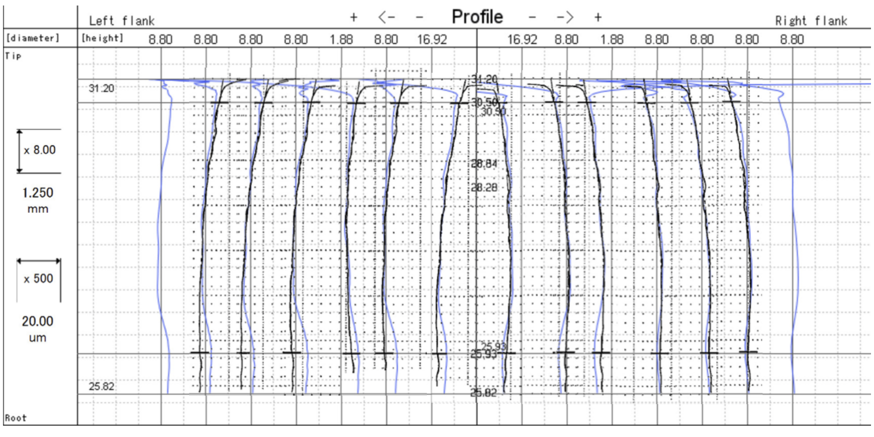

Figure F.1: Chart Overlay: Emera and Urano comparison on profile deviation measurement on Pinion 2

In Figure F.2 it is showed a lead evaluation done by Emera. As it can be seen, no peaks due to the presence of the grove on the Pinion 2 are present such as in the Urano chart (Figure F.3).

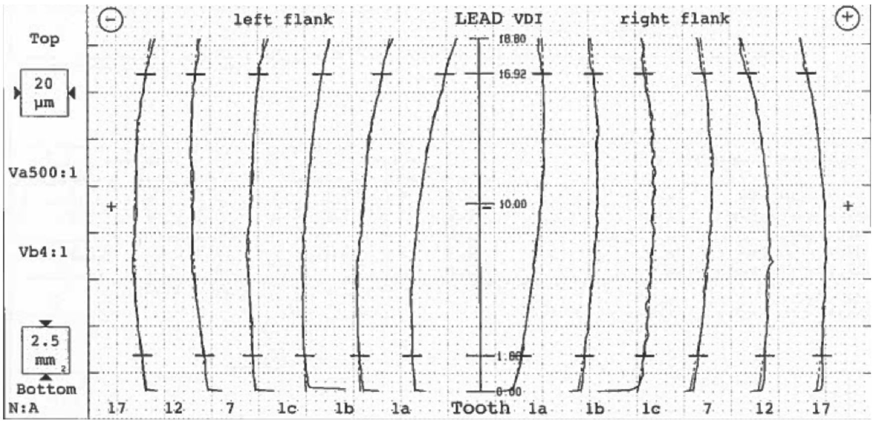

Figure F.2: Emera: Lead deviation measurement on Pinion 2

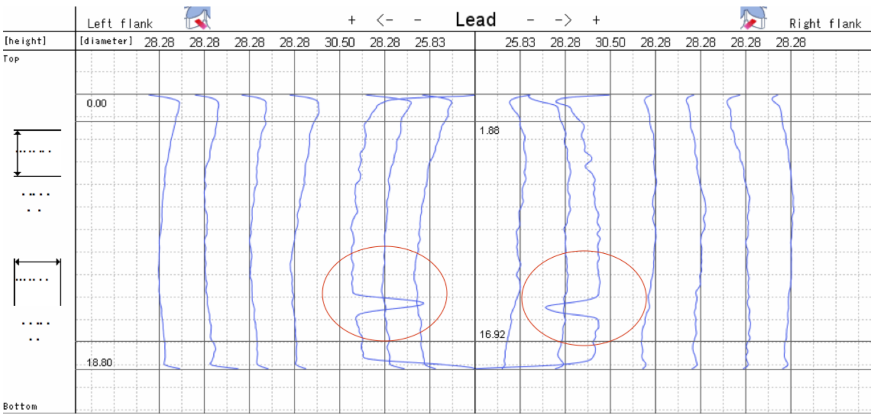

Figure F.3: Urano: Lead deviation measurement on Pinion 2

Appendix G

Gear mounting on Inspection machine and first tooth identification

Every gear lab has a procedure in order to mount a gear in a unique and unequivocal direction. Here, some examples are provided for both Pinion 4 and Pinion 2 (Figure G.1 and Figure G.2). In order to have a correct orientation, the most important features for a pinion 2 are the ID grovees; for the Pinion 4 is the large boss. Regarding the indentification

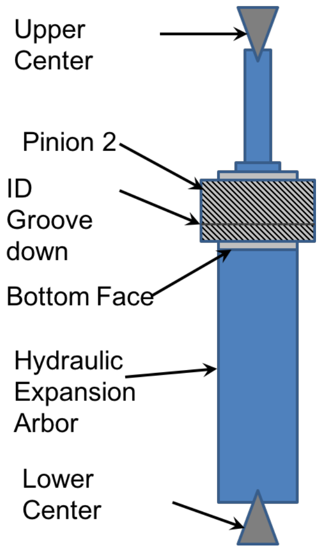

Figure G.1: Gear mounting on an inspection machine: Pinion 2

of the first tooth for external and internal gear, the rules are respectively reported in Figure G.3 and G.4.

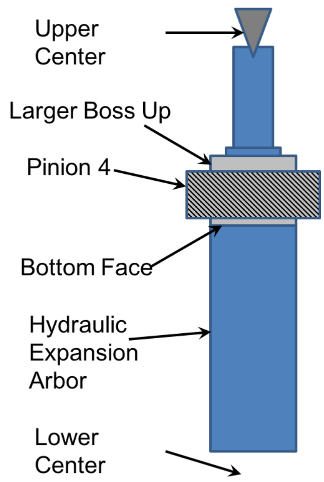

Figure G.2: Gear mounting on an inspection machine: Pinion 4

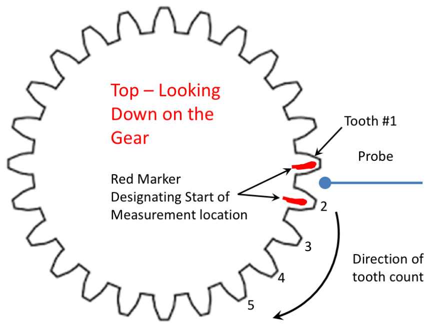

Figure G.3: First tooth identification for external gear

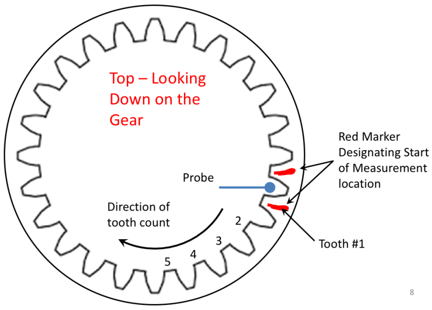

Figure G.4: First tooth identification for internal gear

Vita Auctoris

NAME:	ANTONIO LOGALDO
PLACE OF BIRTH:	MARATEA
YEAR OF BIRTH:	1994
EDUCATION:	Politecnico di Torino, B.Sc., Torino, TO, Italy, 2013 - 2016
	Politecnico di Torino, MASc., Torino, TO, Italy, 2016 - 2018
	University of Windsor, MASc., Windsor, ON, Canada, 2017 - 2018